

JULY 2020

Ph.D. in Civil Engineering

NURULLAH AKBULUT

**HASAN KALYONCU UNIVERSITY
GRADUATE SCHOOL OF
NATURAL & APPLIED SCIENCES**

**USE OF SEWAGE SLUDGE ASH FOR SOIL
IMPROVEMENT**

**Ph.D. THESIS
IN
CIVIL ENGINEERING**

**NURULLAH AKBULUT
JULY 2020**

**USE OF SEWAGE SLUDGE ASH FOR SOIL
IMPROVEMENT**

**Ph.D. Thesis in
Civil Engineering
Hasan Kalyoncu University**

**Supervisor
Prof. Dr. Ali Fırat ÇABALAR**

Nurullah AKBULUT

JULY 2020



© 2020 [Nurullah AKBULUT]



**GRADUATE SCHOOL OF NATURAL &
APPLIED SCIENCES INSTITUTE
PhD ACCEPTANCE AND APPROVAL FROM**

Civil Engineering Department, Civil Engineering PhD (Philosophy of Doctorate) programme student **Nurullah AKBULUT** prepared and submitted the thesis titled “**Use of Sewage Sludge Ash for Soil Improvement**” defended successfully at the VIVA on the date of 01/07/2020 and accepted by the jury as a PhD thesis.

<u>Position</u>	<u>Title, Name and Surname</u> <u>Department/University</u>	<u>Signature</u>
------------------------	--	-------------------------

Supervisor	Prof. Dr. Ali Fırat ÇABALAR Civil Engineering Department University of Gaziantep	
-------------------	--	--

Jury Member	Prof. Dr. Mehmet KARPUZCU Civil Engineering Department Hasan Kalyoncu University	
--------------------	--	--

Jury Member	Prof. Dr. Murat ÖRNEK Civil Engineering Department İskenderun Technical University	
--------------------	--	--

Jury Member	Assoc. Prof. Dr. Nurhan ECEMİŞ ZEREN Civil Engineering Department İzmir Institute of Technology	
--------------------	---	--

Jury Member	Asst. Prof. Dr. Eyyüb KARAKAN Civil Engineering Department Kilis 7 Aralık University	
--------------------	--	--

This thesis is accepted by the jury members selected by the institute management board and approved by the institute management board.

Prof. Dr. M. Fatih HASOĞLU
Director

I hereby declare that all information in this document has been obtained and presented in accordance with academic rules and ethical conduct. I also declare that, as required by these rules and conduct, I have fully cited and referenced all material and results that are not original to this work.

Nurullah AKBULUT

ABSTRACT

USE OF SEWAGE SLUDGE ASH FOR SOIL IMPROVEMENT

AKBULUT, Nurullah

Ph.D. in Civil Engineering

Supervisor: Prof. Dr. Ali Fırat ÇABALAR

July 2020 160 pages

This study presents the application of incinerated sewage sludge ash (SSA) as a soil stabilizing agent. The ash used in this study was obtained from Gaziantep wastewater treatment plant, and had fine particles passing through 0.425 mm sieve. The SSA was mixed with a clay at different percentages (0%, 5%, 10%, 15%, 20%, and %30), and an extensive laboratory study was employed including Atterberg's limits, standard Proctor, unconfined compressive strength (UCS), California bearing ratio (CBR), vane shear, consolidation, fall cone, falling head permeability, and plate load tests. The testing results showed about 30% increment in liquid limit and plasticity index of clay as the SSA percentage increased. A decrease about 2% in maximum dry unit weight for the clay was observed by increasing SSA content up to 30%. An increment about 40% in optimum water content for clay was observed by increasing the SSA percentages up to 30%. The CBR performance of the unsoaked samples was found to be increased up to 6 times greater than the untreated clay, while those of the soaked samples was found to be increased up to 4 times greater than the clean clay. Curing periods have a varying effect on the UCS as well as the CBR testing results. The UCS values was observed to be increased up to 3 times higher than the clean clay samples. In the plate loading tests, the SSA addition increased bearing capacity of clay up to about 75%. The oedometer characteristics of SSA-clay mixtures were controlled mainly by the SSA content. A reinforced circular model box, which has a diameter of 2.0 m and a depth of 1.50 m and a 40 t loading capacity frame, was also constructed to perform plate loading tests in order to investigate bearing capacity of the samples. The results of the plate loading tests showed that the SSA addition increased the bearing capacity, and that the mixtures with SSA had a less settlement than the untreated clay. The laboratory testing results reported in this research showed that the SSA can be used as an alternative soil stabilizing agent.

Keywords: Sewage sludge ash, clay, geotechnical properties.

ÖZET

ARITMA ÇAMURU KÜLÜNÜN ZEMİN İYİLEŞTİRMEDE KULLANIMI

AKBULUT, Nurullah
Doktora Tezi, İnşaat Mühendisliği Bölümü
Tez Yöneticisi: Prof. Dr. Ali Fırat ÇABALAR
Temmuz 2020
160 sayfa

Bu çalışma yakılmış arıtma çamuru küllünün (SSA) zeminlerde stabilize edici katkı maddesi olarak kullanımını sunmaktadır. Çalışmada kullanılan kül, Gaziantep atıksu arıtma tesisinden temin edilmiş olup, 0.425 mm elekten geçebilecek büyüklüğe sahiptir. Farklı yüzdelerde SSA (%0, %5, %10, %15, %20 ve %30) kille karıştırılmış ve kapsamlı bir laboratuvar çalışması yapılmıştır. Arıtma çamuru küllüyle hazırlanmış olan numuneler üzerinde Atterberg kıvam, standart Proktor, tek eksenli basınç dayanımı (UCS), Kaliforniya taşıma oranı (CBR), laboratuvar tipi kanatlı kesici (vane deneyi), konsolidasyon, düşen koni, düşen seviyeli permeabilite, ve plaka yükleme deneyleri yapılmıştır. Deney sonuçları, SSA yüzdesi arttıkça kilin likit limit ve plastisite indeksindeki artışın yaklaşık %30 civarında olduğunu göstermiştir. Arıtma çamuru kül içeriği %5'ten %30'a yükseltildiğinde kil için kuru birim hacim ağırlığın yaklaşık %2 oranında azalma gösterdiği görülmüştür. Kül oranı %30'a kadar yükseltildiğinde kil-kül karışımları için optimum su muhtevasının yaklaşık %40 arttığı görülmüştür. Suda bekletilmemiş CBR numunelerinin performansı katkısız kil numunelerinden 6 kat daha fazla arttığı, suda bekletilmiş numunelerin ise katkısız kile göre 4 kata kadar arttığı görülmüştür. Kür sürelerinin, UCS ve CBR deney sonuçları üzerinde değişen bir etkiye sahip olduğu gözlemlenmiştir. UCS değerlerinin katkısız kil numunelerine göre 3 kat daha fazla arttığı gözlenmiştir. Plaka yükleme deneylerinde, SSA ilavesi kilin taşıma kapasitesini yaklaşık %75'e kadar arttırmıştır. Kül-kil karışımlarının ödometre özellikleri kül içeriğinin karışımdaki miktarı ile kontrol edildiği görülmüştür. Plaka yükleme deneylerinin yapılması ve taşıma kapasitesinin araştırılması için 2.0 m çapında, 1.5 m derinliğinde ve 40 ton yükleme kapasitesine sahip çelik çerçeveli betonarme bir dairesel model kutu inşa edilmiştir. Plaka yükleme deneylerinin sonuçları, SSA ilavesinin taşıma kapasitesini artırdığını ve SSA katkılı numunelerin, katkısız kil numunelerine göre daha az oturmaya sahip olduğu gözlemlenmiştir. Bu çalışmada sunulan laboratuvar deney sonuçları, SSA'nın alternatif bir zemin stabilize edici katkı maddesi olarak kullanılabileceğini göstermiştir.

Anahtar Kelimeler: Arıtma çamuru külü, kil, geoteknik özellikler.



To my beloved family...

ACKNOWLEDGEMENTS

I would like to express my deepest gratitude to my supervisor, Prof. Dr. Ali Fırat abalar, for his unlimited guidance, patience, and support during this research. Without his supervision and advice, this thesis would not have been possible.

I am gratefully thankful to the Board of Trustee vice president Mr. Haluk Kalyoncu, Prof. Dr. Tamer Yılmaz, Dt. Songül Kalyoncu and Mr. Mehmet Okyay for their unlimited support, providing me the required laboratory opportunities and sponsoring this thesis.

I would like to extend my sincere gratitude to Prof. Dr. Mehmet Karpuzcu and Assoc. Prof. Nurhan Ecemiş for their assistance and unlimited guidance during this study.

No research is possible without infrastructure and requisite materials and resource. For this would also like to express my gratitude to all construction team of Hasan Kalyoncu University especially to foreman Yusuf Koin.

I would like to thank my parents, father, and mother sincerely and gratefully, brother and sister for their endless support and encouragement during my study period.

Finally, I would like to thank my wife, Nebile Teke Akbulut for her endless support, without her encouragement, I would not have finished this thesis. Also, I appreciate my little son Yusuf Emir for abiding my ignorance and the patience he showed during my thesis writing.

TABLE OF CONTENTS

	Page
ABSTRACT	iv
ÖZET	v
ACKNOWLEDGEMENTS	vii
TABLE OF CONTENTS	viii
LIST OF TABLES	xi
LIST OF FIGURES	xiii
LIST OF SYMBOLS.....	xix
LIST OF ABBREVIATIONS	xx
CHAPTER 1	1
INTRODUCTION.....	1
1.1 General.....	1
1.2 Statement of the problem.....	2
1.3 Aims and objectives.....	3
1.4 Methodology	3
1.5 Significance of the research.....	4
1.6 Layout of the thesis.....	4
CHAPTER 2.....	6
LITERATURE REVIEW	6
2.1 Sewage sludge ash	8
2.1.1 Sewage sludge production	8
2.1.2 Sewage sludge treatment	9
2.1.3 Sewage sludge incineration	11

2.1.4 Use of sewage sludge ash	13
2.1.5 Environmental assessment.....	14
2.1.6 Sewage sludge ash as a construction material	15
CHAPTER 3.....	78
MATERIALS AND EXPERIMENTAL TECHNIQUES.....	78
3.1 Material properties.....	78
3.1.1 Clay.....	78
3.1.2 Sewage sludge ash.....	81
3.2 Evaluation of index properties.....	88
3.2.1 Particle size analysis.....	88
3.2.2 Specific gravity	88
3.2.3 Hydrometer test	89
3.2.4 Atterberg limits test	90
3.2.5 X-ray fluorescence analysis.....	91
3.3 Geotechnical laboratory testing procedures.....	91
3.3.1. Compaction test	92
3.3.2. Vane shear test.....	92
3.3.3 Fall cone test.....	94
3.3.4 Oedometer test.....	95
3.3.5. Hydraulic conductivity test.....	96
3.3.6 Unconfined compressive strength test.....	97
3.3.7 California bearing ratio test	100
3.5 Model set-up tests	101
3.5.1 Sample preparation	101
3.5.2 Plate load test.....	101
3.5.2 Field California Bearing Ratio Test.....	103
CHAPTER 4.....	105
RESULTS AND DISCUSSION	105

4.1 Compaction testing results.....	105
4.2 Atterberg limits testing results.....	108
4.3 Fall cone testing results	109
4.4 Vane Shear Testing Results	111
4.5 California bearing ratio resting results	113
4.6 Unconfined compression strength testing results	123
4.7 Oedometer testing results	127
4.7.1 Initial void ratio (e_0)	128
4.7.2 Compression index (C_c)	129
4.8 Falling head permeability testing results	130
4.9 Plate load testing results	131
CHAPTER 5.....	137
5.1 Conclusions	137
5.2 Recommendations for future studies	142
REFERENCES	144
CURRICULUM VITAE	155

LIST OF TABLES

	Page
Table 2.1 Contents of mixtures containing sewage sludge as part of the raw feed for cement clinker production (Dhir et al. 2017a)	16
Table 2.2 Effect of SSA content on compressive strength for 28 days concrete (Dhir et al., 2017a).....	21
Table 2.3 The SSA content and curing effect on the development of compressive strength (Dhir et al., 2017a).	21
Table 2.4 Conditions for general ceramic treatment using SSA (Dhir et al., 2017a)	23
Table 2.5 Description of work done with SSA in tiles (Dhir et al., 2017a)	27
Table 2.6 Performance of Water Absorption of Sewer Sludge Ash Tiles (SSA).....	28
Table 2.7 Mix type, design, and heat treatment are for ceramics and glass produced using Sewage Sludge Ash.....	31
Table 2.8 Properties of ceramic and glass produced using sewage sludge ash.....	32
Table 2.9 Sewage sludge effects on the properties of the pressure and dam ratio of the hydraulically related core materials (Sato et al., 2013).....	35
Table 2.10 Sludges of sewage and sludge ash with bitumen content on the flow of bituminous mixtures.....	38
Table 2.11 A series of designs for soil stabilization treatments containing SSA.....	44
Table 2.12 Effect of sludge ash addition on Unconfined Compression Strength (UCS) for Soft Soils.	50
Table 2.13 The percentage of California treated, California Bearing Ratio (CBR) soil treated with sewage sludge ash (SSA) as a stabilizing component.	52
Table 2.14 The work and results arising from the shear resistance properties of soil stabilized with sewage sludge ash (SSA).....	53
Table 3.1 X-Ray Fluorescence (XRF) analysis of clay.....	80
Table 3.2 X-Ray Fluorescence (XRF) analyses of sewage sludge ash.	82
Table 3.3 Sewage sludge statistics per day (Directorate of GASKI, 2018)	86
Table 3.4 Incinerated sewage sludge ash statistics per month (Directorate of GASKI, 2018)	87

Table 3.5	Chemical characterization of GASKI sewage sludge ash.	88
Table 3.6	X-ray fluorescence analysis of SSA and clay.	91
Table 4.1	Standard Proctor results of clay-SSA mixtures.....	107
Table 4.2	Atterberg limits of clay-SSA mixtures.....	108
Table 4.3	Experimental Results of CBR test (MPa)	136
Table 4.4	Effects of SSA on unconfined compressive strength samples.	124
Table 4.5	Hydraulic conductivity values for clay-SSA mixtures.....	131
Table 4.6	Vertical settlements for clay-SSA mixtures in plate load test.....	133

LIST OF FIGURES

	Page
Figure 2.1 Components of the wastewater treatment process. (Ravindra et. al, 2017)	9
Figure 2.2 Sewage sludge treatment and disposal methods. (Werther and Ogada, 1999)	10
Figure 2.3 Use of sewage sludge in Europe (Ravindra et. al, 2017).....	12
Figure 2.4 Stages of typical sludge burning process and key components	12
Figure 2.5 Strength activity index (SAI) results for sewage sludge ash. (Lynn et al., 2015)	18
Figure 2.6 The relationship between the flexural strength and the compressive strength of sludge ash (SSA).....	20
Figure 2.7 The response of the sewage sludge ash process for the treatment of sintering (Lynn et al., 2016).....	24
Figure 2.8 Effects of SSA content on the performance of brick compressive strength	26
Figure 2.9 Effect of SSA content on the performance of tile bending strength.....	29
Figure 2.10 Flexible road structures typical of (a) highways and main roads; and (b) rural roads (Ravindra et. al, 2017)	34
Figure 2.11 Particle size distribution curves for the waste dump produced for the work of highways (Ravindra et. al, 2017).....	35
Figure 2.12 Effect of SSA, with different contents of bitumen on the stability (Ravindra et. al, 2017).....	36
Figure 2.13 The particle size distribution curves of SSA are combined with soil size fractions.....	39
Figure 2.14 The plasticity of ash sludge sewage on the Casagrande scheme.	40
Figure 2.15 Relationships between dry density and moisture content for CBR and both permeability and swelling characteristics.	42
Figure 2.16 Effect of pH stabilizes treatments after (a) 3 treatment hours and (b) 21 treatment days.	45

Figure 2.17 Effect of SSA and additives on soft soil and plasticity with curing time.	46
Figure 2.18 Effect of additive content of stabilizing SSA on soil softness and plasticity properties.	47
Figure 2.19 Effect of additives on optimum moisture content and maximum dry unit weight characteristics. C, Cement. L, lime; SSA, sewage sludge ash.	48
Figure 2.20 Effect of soil stability treatment with SSA on the behavior of soil swell.	54
Figure 2.21 Test box, (a) load-press and consolidation plate (b) side frame and top extensions (Love, 1984).....	59
Figure 2.22 Image of the demining of the dam fund model (Park et al., 2000).....	59
Figure 2.23 Set up preparation for tests presented footing test model (Kumar et al., 2006)	61
Figure 2.24 Set up preparation for tests presented footing test model (Cerato and Lutenegger, 2007)	62
Figure 2.25 Schematic diagram of the test set up (Thallak et al., 2007).....	63
Figure 2.26 A 3D view of the selected pilot setting (Kumar and Bhoi, 2008)	64
Figure 2.27 Model square foot circular (Gupta and Trivedi, 2009).....	64
Figure 2.28 Install the pavement by lime and cement using a circular model box ...	65
Figure 2.29 Schematic of view of the test set up (Nazir and Azzam, 2010).....	66
Figure 2.30 Equipment set up used for conducting model footing tests (Oh and Vanapalli, 2013).....	67
Figure 2.31 The shallow foundation model on the soil supported by the geographic network (Kolay et al., 2013)	68
Figure 2.32 Image of the load test of the plate on the soil with granular layers (Sanjeev et al.,2013).....	69
Figure 2.33 Effect the dimensions of the base and shape using the square model with the frame (Abd elsamee, 2013)	69
Figure 2.34 Set up of testing procedures (Wakil, 2013)	70

Figure 2.35 Schematic view of (a) Test preparation and (b) Shell base model (Azzam and Nasr, 2014)	71
Figure 2.36 A schematic presentation of the test preparation used in the study (Bazne et al., 2014)	72
Figure 2.37 (a) Schematic view of the set-up, (b) photographic view of the set-up (Elsaied et al., 2015).....	73
Figure 2.38 Test Setup: (a) Elevation, (b) Section A-A (Ramadan and Hussien, 2015)	74
Figure 2.39 Test the setup tool (a) the schematic display; (b) photograph (Hegde and Sitharam, 2015).....	75
Figure 2.40 Schematic view of the experimental set up (Sadoglu, 2015).....	76
Figure 2.41 Schematic representation of test preparation and trench planning (Tafreshi et al., 2016).....	77
Figure 3. 1 Grain size distribution of clay.....	79
Figure 3.2 (a) Scanning Electron Microscope and (b) Energy Dispersive X-Ray analysis of clay.....	80
Figure 3.3 Particle size distribution of sewage sludge ash.....	81
Figure 3.4 (a) Scanning Electron Microscope and (b) Energy Dispersive X-Ray analysis of sewage sludge ash.....	82
Figure 3.5 Photo of (a) Gaziantep Wastewater Treatment Plant, (b) Digester tanks in the plant, (c) Digestion plant of the sludge, (d) dried/dewatered sludge and (e) ash occurred after the incineration process of dewatered sludge.....	85
Figure 3.6 Specific gravity test for clay (left) and sewage sludge ash (right side)...	89
Figure 3.7 Hydrometer testing equipments' (left) and hydrometer testing on clay and sewage sludge ash (right).....	90
Figure 3.8 Photos of Casagrande and rolling spaghetti test methods.....	90
Figure 3.9 X-ray fluorescencespectral analysis of (a) clay and (b) SSA.....	91
Figure 3.10 Photo of standard Proctor testing equipment's.....	92

Figure 3.11 Laboratory vane shear device; 1-Vane, 2-Spring, 3-Rotating hand knob, 4-Graded scale, 5-Secondary scale, 6-Raising hand knob, 7-Motorize unit.....	94
Figure 3.12 Photo of fall cone testing apparatus.....	95
Figure 3.13 Photo of oedometer cell components and testing apparatus.....	95
Figure 3.14 Photo of falling head specimens, manometer stand, and water bath.....	97
Figure 3.15 Photo of rammer system components; steel plate, mold, and hammer (Cabalar, 2013).....	98
Figure 3.16 Photo of UCS specimens.....	99
Figure 3.17 Unconfined compression strength testing machine.....	99
Figure 3.18 CBR testing equipment.....	100
Figure 3.19 Photo of CBR mold, compaction hammer, and surcharge load accessories.....	101
Figure 4.1 Plot of standard Proctor results for clay-SSA mixtures.....	106
Figure 4.2 Effect of SSA on optimum moisture content.....	106
Figure 4.3 Effect of SSA on dry unit weight.....	107
Figure 4.4 Effect of water content and SSA on penetration for clay-SSA mixtures.....	109
Figure 4.5 Liquid limit of clay with various SSA content.....	110
Figure 4.6 Effect of SSA on water content by fall cone test.....	111
Figure 4.7 Effect of SSA on water content by laboratory vane shear test.....	112
Figure 4.8 Undrained shear strength of SSA mixtures by FCT and LVT.....	113
Figure 4.9 Stress vs. penetration for soaked samples under 4 days of curing time.....	116
Figure 4.10 Stress vs. penetration for soaked samples under 8 days of curing time.....	117
Figure 4.11 Stress vs. penetration for soaked samples under 16 days of curing time.....	117
Figure 4.12 Stress vs. penetration for soaked samples under 32 days of curing time.....	118

Figure 4.13 Stress vs. penetration for unsoaked samples under 4 days of curing time	118
Figure 4.14 Stress vs. penetration for unsoaked samples under 8 days of curing time	119
Figure 4.15 Stress vs. penetration for unsoaked samples under 16 days of curing time	119
Figure 4.16 Stress vs. penetration for unsoaked samples under 32 days of curing time	120
Figure 4.17 Effect of SSA on CBR values for unsoaked clay-SSA samples.....	120
Figure 4.18 Effect of SSA on CBR values for soaked clay-SSA samples.....	121
Figure 4.19 Plot of stress vs. penetration for clay field CBR samples under 4 days curing.....	121
Figure 4.20 Plot of stress vs. penetration for 10% field CBR samples under 4 days curing.....	122
Figure 4.21 Plot of stress vs. penetration for 20% field CBR samples under 4 days curing.....	122
Figure 4.22 Plot of stress vs. penetration for 30% field CBR samples under 4 days curing.....	123
Figure 4.23 Plot of stress vs. axial strain for 4 days cured samples.....	125
Figure 4.24 Plot of stress vs. axial strain for 8 days cured samples.....	125
Figure 4.25 Plot of stress vs. axial strain for 16 days cured samples.....	126
Figure 4.26 Plot of stress vs. axial strain for 32 days cured samples.....	126
Figure 4.27 Variation of maximum stress with SSA content and curing time.....	127
Figure 4.28 Variation of energy absorption capacity with SSA content and curing time.....	127
Figure 4.29 Variation of void ratio with different oedometer pressures.	128
Figure 4.30 Variation of void ratio with different oedometer pressures.	128
Figure 4.31 Relations between initial void ratio and SSA content.	129
Figure 4.32 Compression index vs. SSA content under different stress changings	130
Figure 4.33 Coefficient of permeability (k) values for clay-SSA mixtures.....	131

Figure 4.34 Pressure-settlement curves for clay in plate load test	133
Figure 4.35 Pressure-settlement curves for 10% SSA in plate load test	134
Figure 4.36 Pressure-settlement curves for 20% SSA in plate load test	134
Figure 4.37 Pressure-settlement curves for 30% SSA in plate load test	135
Figure 4.38 Plot of pressure-average settlement for all mixtures under different applied loads.....	135
Figure 4.39 Time-settlement curves for 200 kN/m ² pressure of clay-SSA mixtures in plate load test.....	136

LIST OF SYMBOLS

B	Pore pressure coefficient
c	cohesion (kPa)
C_c	Coefficient of curvature
C_u	Coefficient of uniformity
D_R	Relative density (%)
D_{10}	Diameter corresponding to 10% passing (mm)
D_{30}	Diameter corresponding to 30% passing (mm)
D_{50}	Diameter corresponding to 50% passing (mm)
E	Young's modulus (MPa)
e	Void ratio
G_s	Specific gravity
σ'	Effective stress (kPa)
γ_{drymax}	Maximum dry unit weight (kN/m^3)
v	Specific volume
σ	Total axial stress (kPa)
ϕ	Angle of internal friction ($^\circ$)
ϕ'	Effective angle of friction ($^\circ$)
w_{opt}	Optimum moisture content (%)

LIST OF ABBREVIATIONS

ASTM	American Society for Testing and Materials
BS	British Standard
CBR	California Bearing Ratio
CD	Consolidated Drained Triaxial Test
CL	Low Plasticity
CH	High Plasticity
CU	Consolidated Undrained Triaxial Test
CLSM	Controlled Low Strength Materials
CNS	Chinese Standard
CPT	Cone Penetration Test
CU	Consolidated Undrained Triaxial Test
ECS	Effective Confining Stress
EDX	Energy Dispersive X-Ray
EPA	Environmental Protection Agency
ESA	Effective Stress Approach
EU	European Union
FCT	Fall Cone Test
FEM	Finite Element Method
FHA	Federal Highway Administration
GASKI	Gaziantep Water and Sewerage Administration
GGBS	Ground Granulated Blast Slag
HSPT	High Strength Plastic Tank

IWSA	Industrial Wastewater Sludge Ash
LL	Liquid Limit
LOI	Loss of Ignition
LSF	Lime Saturation Factor
LVDT	Linear Variable Differential Transformer
LVT	Laboratory Vane Test
MDD	Maximum Dry Density
MDF	Medium-Density Fiberboard
MIBA	Municipal Incinerated Bottom Ash
MPCT	Modern Pollution Control Technology
NCHRP	National Cooperative Highway Research Program
OMC	Optimum Moisture Content
PC	Portland Cement
PI	Plasticity Index
PL	Plastic Limit
SAI	Strength Activity Index
SEM	Scanning Electron Microscope
SS	Sewage Sludge
SSA	Sewage Sludge Ash
TCLP	Toxicity Characteristics Leaching Procedure
TSA	Total Stress Approach
UCS	Unconfined Compression Strength
UFG	Unsaturated Fine-Grained
USCS	Unified Soil Classification System

XRD X-Ray Diffraction

WPSA Water Purification Sludge Ash



CHAPTER 1

INTRODUCTION

1.1 General

The study of soil behavior is critical to civil engineers because every engineering structure such as building, road, railway, bridge, dam, monument, etc. will be rested and founded on a soil layer of structures. The mechanical properties of the soil are significant to carry the loads, under different site conditions; therefore, these properties become an essential factor. When a structure constructed on unstable soil, some ground improvement applications will be needed to avoid settlement and stability problems.

Ground improvement is the temporary or permanent modification of soils to develop their mechanical properties. These modifications control the characteristics of shrinkage and swelling of the soil and enhance the carrying capacity of a sub-layer to support roads and foundations. Ground improvement methods have a long history. The Romans used lime to improve clayey soils (Lindh, 2000). In the 1980s, the leading binding materials have been lime and cement (Åhnberg, 2006). Cement and lime are binding materials that strengthen the soil without the need to add a reactor (Andersson et al., 2006). Cement presents a rapid and high development in strength. The slaking of the lime also contributes to drying and heat evolution, which step up the reaction of the cement. It is reported by different researchers that applying bitumen is also possible to produce a semi-rigid layer of modified soil (Jenkins, 2002).

Researchers are continuously lookout for new materials. Nowadays, new ground improvement methods come out worldwide on using sewage sludge and sludge ash in construction technology. The use of sewage sludge and industrial by-products in construction studied in recent years. The primary aim of this increasing interest in using such waste materials in construction is environmental, economic, and technological reasons. The use of waste materials first removes them, reduces costs, and in several cases, improves the building materials quality.

Sewage sludge ash (SSA) is reported in the literature in different applications. Dried sludge is mixed with clay to generate bricks (Lin and Weng, 2001), Brar et al., 2009). Incinerated sludge in a pulverized form blended with Portland cement has been used to produce mortars (Khanbilvardi and Afshari, 1995), Monzo et al., 1996). Al Sayed et al., 1995) examined the utilization of SSA in asphaltic paving mixes as filler. SSA has also been described as an additive to concrete mixtures (Khanbilvardi and Afshari, 1995), Coutand et al., 2006). Also, it was studied as source material for fabricating glazed tiles (Lin et al., 2005) and lightweight aggregates (Bhatty et al., 1992), Cheeseman, 2003). Moreover, SSA has been presented as a mix with cement to treat the stability of soft subgrades (Chen and Deng-Fong, 2009).

The objective of this thesis is to study Gaziantep wastewater plant sludge ash and its influence on soil consistency, strength, settlement, permeability and bearing capacity parameters. SSA has been obtained from the Gaziantep incineration plant that is produced about 1500 tons/year. Depending on the scientific studies and assessment, the use of SSA, as an admixture for ground improvement was selected for this thesis and described herein:

1.2 Statement of the problem

Population growth indicates that it will generate some massive sewage sludge. Disposal of household sewage sludge will lead to many problems associated with environmental and health hazards. Subsequently, the allocation of sewage sludge should be facilitated to avoid causing severe problems in the entire world. Gaziantep wastewater treatment plant produces high amount of sewage sludge. The estimation of sewage sludge quantities in Gaziantep were around 3920 tons/month (Gaziantep Water and Sewerage Administration). The increasing problem of disposal of sewage sludge in Gaziantep can be eliminated if new waste disposal alternatives other than landfills are found. One of the main challenges in the landfilling system is that this material dissolves over time and is highly related to the management of high-water content and unstable organic matter that cause the production of foul odors and toxic gases. Due to the problems and limitations of sewage sludge disposal options, the process of sewage sludge as a construction material has been studied and studied by different scientific researchers. The unprocessed sewage sludge is used like a filler and blended cement material for concrete and indirectly used as raw material to generate products

like bricks, lightweight aggregate, tiles and paving blocks, and cementitious material (Tay and Show, 1994).

1.3 Aims and objectives

This thesis aims to examine the performance of SSA on some geotechnical properties of consistency, shear strength, compressive strength, compaction, settlement, bearing capacity and permeability of clayey soil. An extensive series of laboratory tests were achieved to investigate the soil improvement due to the addition of 0%, 5%, 10%, 15%, 20%, and 30% SSA by dry weight on a clayey soil. Also, a reinforced concrete circular model footing test equipment with inside dimensions of 2.0 meter diameter and 1.5 meter depth was constructed for the large scale tests. A steel loading frame of 40 tons capacity was designed to conduct the plate load and field California bearing ratio test inside this circular model footing. The circular model set up tests are concerned with the settlement, bearing capacity and stress distribution before, at, and after applying the plate load test of clay-SSA mixtures.

The primary objectives of this research can be summarized as:

- 1- For the purpose of studying geotechnical characteristics (consistency, compaction, shear, and compressive strength, consolidation, permeability, bearing capacity) for clay and clay-SSA mixtures by different testing equipment's (Standard Proctor, vane shear, unconfined compression, fall cone, laboratory and field California bearing ratio, plate load, falling head),
- 2- To determine the effect of the curing time on the engineering properties of the clay-SSA mixtures by unconfined compression strength and California bearing ratio tests,
- 3- To examine the bearing capacity in the model box by plate load test

1.4 Methodology

The following works were set to manage the research objectives:

- 1- Review extensive literature on relevant experimental work, focus on the uses of SSA in project construction especially in geotechnical engineering has been undertaken,

- 2- The critical pieces of information and documents related to Gaziantep wastewater treatment plant have been collected,
- 3- The materials which were used during the experimental work have been prepared. SSA has been collected from the Gaziantep wastewater treatment plant, and the clay has been obtained from the campus of Gaziantep University.
- 4- Required test standards have been read, and sample preparation methods were studied.
- 5- A suitable experimental testing program was developed.
- 6- A circular model footing with a steel reaction frame was constructed to carry out large scale tests.

1.5 Significance of the research

An important growth of sewage sludge and problems of disposing of sewage sludge becomes the attention of many parties. By the successful use of SSA in geotechnics engineering applications, it can reduce or replace the amount of other additive ground improvement materials. This would bring the benefits of

- Reduction of the possibly harmful environmental affects which are develop from its heavy metals content
- Minimization the amount of waste
- Reduction in waste disposal cost
- A sustainable ground improvement

1.6 Layout of the thesis

This thesis deals with the determination of the feasibility of SSA, and its final result on the strength, compressibility, permeability of clayey soil. Gaziantep wastewater treatment plant incinerated sludge was used throughout the study with clay obtained Gaziantep University. The study is consisted of six chapters and planned as follows: Chapter 1 summarizes the general information, contribution, and the aim and objectives of the thesis.

Chapter 2 describes a detailed assessment of the literature review and the beneficial uses of sewage sludge ash. SSA as a construction material was discussed in detail. The chapter also presents studies concerning cement-based, brick, and lightweight

aggregate material production. The chapter summarizes studies related to the sewage sludge uses ash in geotechnical soil stabilization.

Chapter 3 presents the materials and methods that were conducted in the laboratory and field testing stages especially, the methodology of the sample preparation techniques were explained in details. Also in this chapter, the design, construction process, and characterization of the large scale circular concrete foundation test box and steel reaction frame is described.

Chapter 4 presents the findings of the tests and discussions of the data gained from the laboratory and field studies. The strength, compressibility, bearing capacity, permeability, index properties of the stabilization of clayey soil using the SSA are discussed, compared, and interpreted.

Finally, Chapter 5 gives a sum-up of the scientific study, results, and suggestions for further studies.

CHAPTER 2

LITERATURE REVIEW

The population growth leads to increasing the production of sewage sludge from a wastewater treatment plant over the world. A serious environmental problem of sewage sludge is the disposal. The main output of the wastewater plant is the sewage sludge material. The volume of sewage sludge is growing fast over the time and is assumed to rise more due to the metropolization and increase of the population. The removal and use of sewage sludge are done as landfill and agricultural uses. Recent research and studies show that current removal techniques pose ecological topics like water, soil, and air pollution. Among the techniques of removal of sewage sludge, landfill is less expensive because it allows for the cultivation of crops in poor lands, i.e. to use them again. Sludge includes a big percentage of heavy metals and minerals compared with other by-products produced during the process of wastewater operation, and it is demonstrated to contain heavy metals in their chemical formation (Fontes et al., 2004). In addition, the materials that can't be dissolved are also pointed out in sewage sludge material for instance, nutrients, organic matter, pathogens, and minerals. Sewage sludge also includes solvable materials like organic chemicals, minerals, and salts (Yip and Tay, 1990).

Combustion is becoming an alternative and advanced technic of disposal for sewage sludge. Research shows that 550°C is an encouraging situation for sludge combustion. The sewage sludge was dewatered during the filter process from various sewage treatment plants and was auto thermal during combustion at 550°C. Incinerations main purpose was to remove any organic matter of sewage sludge at the temperature above 550°C (Tay, 1987). The main chemical elements of the sewage sludge that occur after passing through a high-temperature of combustion process such as silicon dioxide (SiO₂), calcium oxide (CaO), aluminum oxide (Al₂O₃) are the components of the normal types of cement (Tenza-abril et al., 2011). The combustion procedure decreases the amount of sewage sludge to approximately 10-15% of its original amount. The residue is practically inert and odorless.

At present, waste treatment is one of the highly sensitive challenges in the management of waste worldwide (Uyarra and Gee, 2013). The main targets of the European Union (EU) are to carry out a long-lasting improvement process in the steps of waste administration (Ravindra et al., 2015). Meanwhile, the implementation of community law could decrease or finish the disposal of organic waste in landfills (Lundin et al., 2004). Moreover, through the adoption of suitable improvement techniques, a large volume of material and power can be produced through the waste process. The EU has made a growth in waste management in some countries and as a common structure (Henclik et al., 2014). The EU's goal of reducing the final waste disposal in the future will be 50% higher. To achieve this, a strategy was developed that sets the following step priorities:

- Waste protection and preservation.
- Reducing quantities of waste amount.
- Waste renovation processes through re-use, recycling, and energy generation steps.
- Improvement situations for waste treatment.
- Organization of transport (Fytily and Zabaniotou, 2008).

Recoverable sources can displace a parallel quantity of material that may be required to be generated from original sources (Duic et al., 2013). The EU has compression the issue of the most effective use of waste under "A zero-waste program for Europe". "Zero waste" is a concept to solve the waste problems that appears favorable in future waste administration (Zaman and Lehman, 2013). Conversion to the economy is assumed to be great and essential by means of achieving efficient resource use for economical profits (Quaghebeur et al., 2013).

The goal of the EU economy was to minimize the extrabudgetary sources so that the optimal system works. A crucial benefit of the economy systems is the way to maintain better-quality in outcomes to keep it if possible, for the purpose of reducing and eliminating waste. It retains sources within the economy when the output reaches the end of its helpful life so that it could be reused profitably and thus creates extra value. The conversion to a larger global economy needs a complete changing systematic, innovation in organization, policies, society, techniques, and financing methods. The EU should encourage organizations and individual entrepreneurs to invest in the

establishment and study of a circular economy, and because of the regeneration of the economic system, barriers to mobilizing more private funding for source efficiency should be addressed.

2.1 Sewage sludge ash

Differences in systems of waste administration policies and practices carried world-wide. This thesis focuses on the usage of SSA as a long-lasting building material. An important aspect was to look at the background of the production procedure where it could have a fundamental result on ash characteristics and their usefulness and potential, mechanically, and environmentally, in practical applications like concrete, pavement, ceramic, brick and tile geotechnical applications (padding, soil stabilization, etc.) Familiarity with the production and treatment of sewage sludge is very important and the differences in waste administration strategies and procedures are employed world-wide. These procedures require future modifications for development, with an approach and method of using a material as an energy resource, rather than a waste disposal process. With the recent increased emphasis on sustainable building techniques, the life-cycle assessment should also use SSA products as well as assess the impacts associated with all steps, containing the operation of the original sludge for a possible SSA nomination behavior (Henclik et al.,2014).

2.1.1 Sewage sludge production

Sewage sludge production consists of a wastewater operation process where the collected wastewater is subjected to a sequence of operations to remove and sort dangerous pollutants before the water recycling. Figure 2.1 illustrates the stages include in typical wastewater treatment plants (Ogada, 1999)

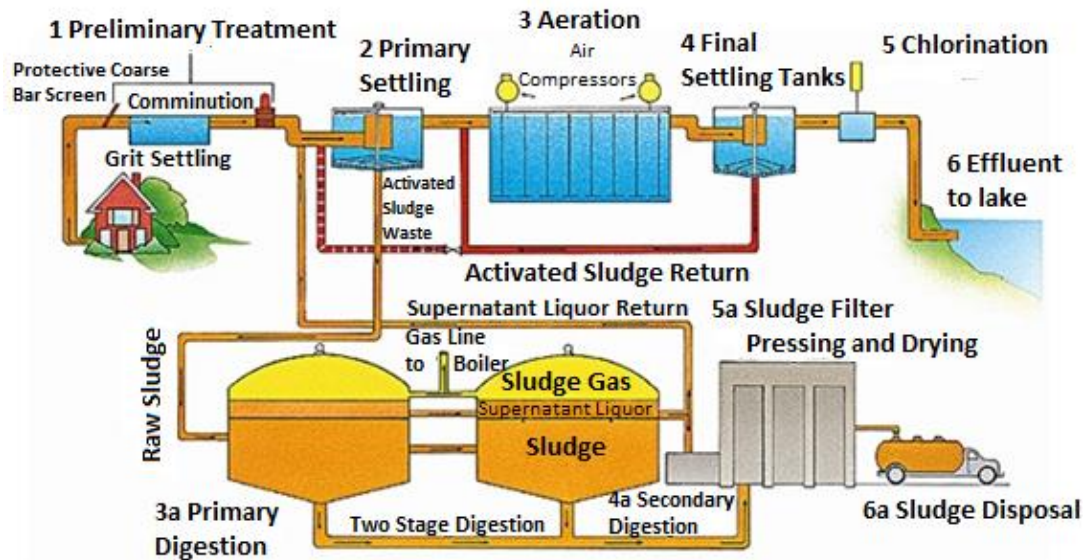


Figure 2.1 Components of the wastewater treatment process. (Ravindra et. al, 2017)

The main steps system involved primary stages, consisting of preliminary, primary, secondary and third step treatment. Details of each processing station may vary in terms of content, consisting of the texture of the incoming wastewater, the sensitivity of the flow sites and the regulations. Primary treatment including an examination to remove the large ingredients, and to remove the gravel. The initial processing phase is often a mechanical process where sludge particles are installed at the bottom of the primary deposition tanks and disposed for deposition and subsequent operation, while the foam layer was also disposed by abrasion. The secondary operation phase uses biological procedure in which bacteria destroy residual organic matter and suspended solids in oxidizing situations. This phase might also contain the treatment of secondary deposits. Triglyceride therapy is an extra phase that might be represent with more stringent needs and might include disinfection, filtration, and disposal of phosphorus and nitrogen. The sludge that is disposed from each stage and which needs subsequent processing before being used in a diversity of issues like agriculture or construction industry or sludge removal is stored in the landfill. (Dhir et al., 2017a; Ravindra et. al, 2017)

2.1.2 Sewage sludge treatment

Sewage sludge from sewage processing needs further treatment before use or disposal. Figure 2.2 presents the selection of the main operation explored in literature. Sewage sludge is not normally subject to all specific procedures, but instead is aimed at

maximizing the value of materials for use as a resource or to modify them in an appropriate form for disposal.

Type of process	Treatment methods
Preliminary operations	Grinding, degritting, blending
Thickening	Gravity thickening Flotation thickening Centrifugal thickening Rotary drum thickening
Stabilization	Lime stabilization Heat treatment Anaerobic digestion Aerobic digestion Composting
Conditioning	Chemical method Heat treatment method
Disinfection	Pasteurization
Dewatering	Vacuum filter Centrifuge Sludge drying beds
Heat drying	Flash dryer Slow dryer Rotary dryer
Thermal reduction	Multiple-hearth incinerator Fluidized bed incinerator
Ultimate disposal	Land application Distribution and marketing Landfill Lagooning

Figure 2.2 Sewage sludge treatment and disposal methods. (Werther and Ogada, 1999)

2.1.2.1 Thickening

The first treatment process results in a crucial reduction of water amount and thus the quantity and volume of sludge must be handled according to specifications and requirements. Werther and Ogada (1999) indicated a decrease around 50% in volume after sludge thickness from 3% up to 6% of total dry solids. Almost 10% of the solid content could be obtained using this operation, with gravity thickness and flotation thickness being two possible technics.

2.1.2.2 Stabilization

The possible renovation of biogas might be an additional profit for the treatment of anaerobic fermentation and as an effect of the installation of sewage sludge using biological methods, containing air fermentation, anaerobic fermentation, and chemical technics, also containing lime and chlorine fixing, organic and harmful microorganisms (Werther and Ogada, 1999).

2.1.2.3 Conditioning

Sludge preconditioning is an extra operation that could use to enhance water flow and pumping characteristics by neutralizing charge and sludge particles to promote water reduction and draining. This could be implemented using chemical additives, heat operation or snow, ice melting and thawing (Werther and Ogada, 1999).

2.1.2.4 Dewatering and drying

Sewage drains and drying are used by both mechanical and thermal methods to reduce moisture content within the sludge, thereby reducing sludge volume resulting in more suitable material for the purpose of transport, end-use or other treatments such as incineration (Werther and Ogada, 1999).

2.1.2.5 Thermal treatment

Heat treatment techniques such as incineration, carbonation, and pyrolysis could be used to decrease the sludge size of the management and as a means of restoring energy. With particular emphasis on ash handling from sludge burning, the combustion procedure was reviewed in Section 2.2.3 (Werther and Ogada, 1999).

2.1.3 Sewage sludge incineration

This is a procedure including the burning of waste, which might also involve the renovation of energy from the resulting heat. This step brings a significant decrease, up to 90%, in the volume of waste, in this condition with sewage sludge, output the remaining SSA. The operation is having high premier regulation expenses due to structural needs and combustion is getting a significant waste operation alternative world-wide and is financially more desirable when conducting in large-scale

treatments in spite of the slightly negative impression of users, as shown in Figure 2.3. In fact, waste incineration is expected to continue to rise as restrictions on landfill and related costs increase (Werther and Ogada, 1999).

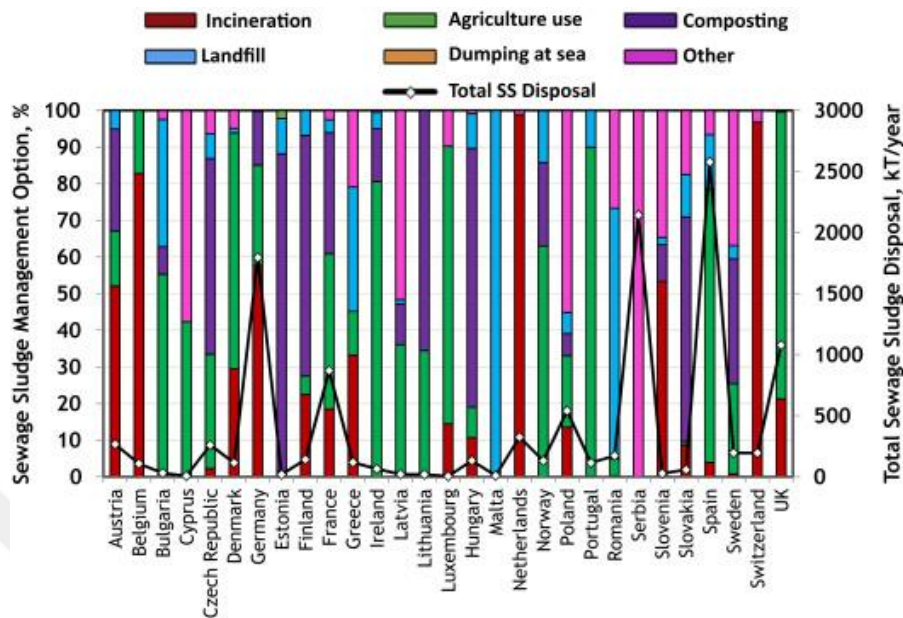


Figure 2.3 Use of sewage sludge in Europe (Ravindra et. al, 2017)

The combustion procedure has taken place over the past years and has been producing significantly related materials, including the burning of sewage sludge. Figure 2.4 illustrates the general step of the model sludge incineration method and In terms of process, it could be separated into four main parts: the pre-treatment phase of the sludge and then the combustion stage, followed by the stage of energy recovery and finally the stage of cleaning systems.

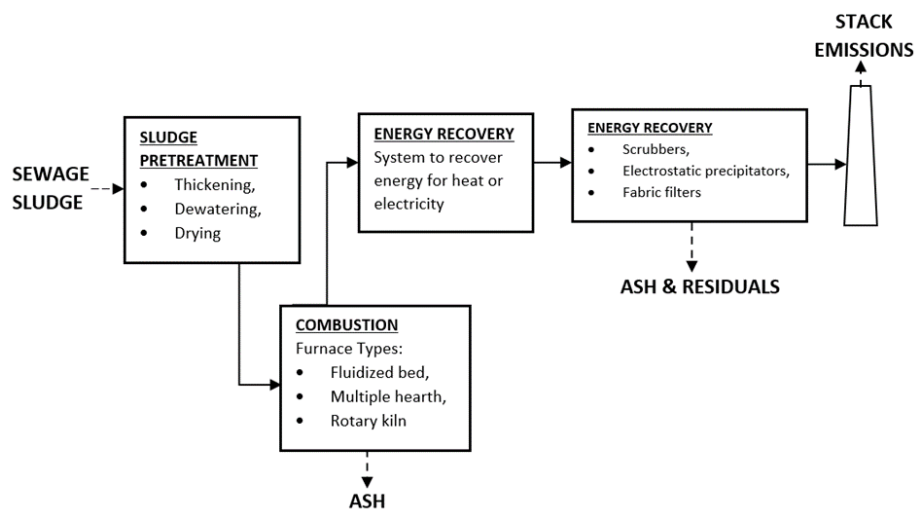


Figure 2.4 Stages of typical sludge burning process and key components (Ravindra et. al, 2017).

- a) **Sludge pretreatment:** Sewage sludge is usually exposed to thickening or drying operations, as expressed and given in section 2.2.2, for the purpose of raising the total solids content to > 25% and the thermal value to prepare the material ready for burning (Ravindra et. al, 2017).
- b) **Combustion:** Sewage sludge is flow into the kiln with pressurized air for incineration. Kilns that used contain fluid kilns or multiple or rotary ovens. The first alternative is the main known option for sludge burn because it is easy to manage, without mechanical shift parts, which reduces corrosion in machinery, and it provides more flexibleness with available cyclic treatment. While warming, at a degree of heat usually between 850°C up to 950°C, organic and volatile chemical elements were burned as gases and transported from the furnace chamber to the fine particulate matter of the particulate matter. In some plants, the bottom ash residues are collected (Ravindra et. al, 2017).
- c) **Energy recovery:** Hot gases go out of the oven through a system to restore energy, where energy could be renovated in terms of electricity or heat. The heat or electricity could be utilized to incinerate the air or to dry the drain systems (Ravindra et. al, 2017).
- d) **Cleaning system:** The resulting flue gases are released during sludge burning through controlled cleaning steps. Ashes, dust, and dangerous gases are usually removed by washing units, while electrostatic precipitators and textile filters, especially when released with municipal solid waste, are used to effect compliance (Ravindra et. al, 2017).

2.1.4 Use of sewage sludge ash

Referring to the raw materials in the production of concrete clinker, SSA can be incorporated into limited contents within the components of the material, up to about 5%, without prejudice to the strength or behavior of modified cement. SSA contents up to 11% result in the formation of tricalcium silicate (C₃S) and adversely affect the properties of the initial setting and early strength (Dhir et al., 2017a).

The SSA pretreatment process, as part of the integrated approach to the extraction of phosphorus and its derivatives for use in the agriculture sector by fertilizer for plants, is a potential complement, allowing the use of higher SSA contents (Dhir et al., 2017a).

As a binding element of concrete and mortar, the direct substitution of cement with SSA resulted in a decrease of workability and strength. Testing results indicate that permeability properties are not significantly affected by SSA. SSA showed a positive result on corrosion resistance caused by chloride in amounts of less than 20%. No expansion induced by sulfate could be seen with SSA. On the other hand, heavy metals in SSA were successfully packaged inside the concrete and concrete matrix. Structure and high porosity of SSA seems to rise the need of water. Strength and density mostly decreased when using SSA, although it sometimes showed positive filling results. The material appears more suitable for use in low content (up to 20%) since the effects on the above characteristics can be controlled at this level (Lin and Lin, 2004, 2005, 2006, Lin et al., 2005, 2009; Lam et al., 2010).

Lightweight specification was achieved after granulation and flocculation at temperatures between 1060 and 1080°C, the strength was 3 to 5 MPa. The usage of these lightweight SSA aggregates inside the concrete have a good impact on the SSA pellets. SSA seems to provide similar strengths or greater intensity to certain commercial lightweight mixtures. The level of water absorption of concrete containing SSA aggregates were similar as those of the commercial useable mixtures (Lin and Lin, 2004, 2005, 2006, Lin et al., 2005, 2009; Lam et al., 2010).

2.1.5 Environmental assessment

The possible application of SSA as a construction product is depending on the confidence that the substance does not lead to harm the environment. There is a benefit of this material and has a clear environmental effect related with the usage of SSA; preserving natural sources, decreasing carbon emissions and the number of substances that can be moved to the landfill (Dhir et al., 2017a; Ravindra et al., 2017).

Research's on the environmental effects related with the usage of SSA are obtainable in the following productions: as a raw material in clinker, light aggregates, natural mortars, concrete mixtures, and low strength materials. (Dhir et al., 2017a; Ravindra et al., 2017).

Whereas the heavy metal amount in the SSA mixture controls the fractured parts, which were tested according to the toxicity characteristics of leaching procedure, had been often lower than measurable limits, for the similar level of the control mixtures.

And, within organizational minimum levels (Lin and Lin, 2004, 2005, 2006, Lin et al., 2005, 2009; Lam et al., 2010). Environmental Protection Agency (EPA) leaching tests showed that the reported solid wastes had concentrations of heavy metals under the observed limits (Bhatty et al., 1992). The leaching test indicates that the pollutants are efficiently included within the outer surface of the solid layer that is developed in the overall production process.

2.1.6 Sewage sludge ash as a construction material

2.1.6.1 Cement-concrete related applications

Concrete are one of the most used building materials in the world because of their hardness, durability, and compression strength. However, their production process leads to a high carbon footprint, largely because of cement clinker manufacture. Global focus on sustainability, including conservation of natural resources, has caused different considerations for the manufacturing process of concrete-related products, towards further waste disposal of recycled materials. SSA in both above-mentioned forms, like cement and aggregate ingredients were used in an extensive area of concrete-related materials, for example in the production of lightweight aggregates, clinker, slurries, natural weight of concrete blocks, aerated concrete, and foam concrete (Baeza-Brotons et al., 2014; Khanbilvardi and Afshari-Tork, 1995; Kosior-Kazberuk, 2011).

2.1.6.2 SSA in cement clinker production

The clinker procedure of cement production usually includes internal mixing and subsequent thermal operation of chalk, limestone, shale, or clay. A wide range of chemical activities from silicon, calcium, iron oxides and alumina are observed to lead to the formation of clinker by dicalcium silicate (C_2S), calcium silicate (C_3S), tetra calcium aluminoferrite (C_4AF) and tricalcium aluminate (C_3A) compounds. After storage and cooling procedure, the clinker must be crushed and mixed with fine cement powder and gypsum (Lin and Lin, 2006).

The usage of SSA as raw material to produce cement clinker were investigated in low amounts ranging from 1% up to 11% as illustrated in Table 2.1. This material was combined with an extensive ranged of other additive materials such as slag, copper

waste, iron waste, fly ash, water purified sludge ash (WPSA), industrial wastewater sludge ash (IWSA), sand, clay, and limestone. To assure the formation of the required clinker phases, the contents of many components are constantly tuned to meet the required oxide demand. These differences make the content of SSA difficult to determine the direct effect of SSA accurately, although there is a known tendency that could be distinguished from the performance (Lin and Lin, 2006).

The SSA production process showed that the combination importantly grows the phosphorus pentoxide (P_2O_5) and sulfur trioxide (SO_3) amounts of the cement clinker product. The formation of tricalcium silicate (C_3S) affect the setting behavior and early strength development which is generally suppressed by the excessively high oxide contents. However, when SSA content is limited to about 5%, setting behavior and compressive strengths are achieved for the Portland cement mixtures comparable to those of control samples (Lin and Lin, 2006).

Table 2.1 Contents of mixtures containing sewage sludge as part of the raw feed for cement clinker production (Dhir et al. 2017a)

Reference	Constituents, %										
	Blend no.	SSA	Limestone	Clay	Ferrate	Copper Slag	Sand	Fly Ash	MIBA	WPSA	IWSA
Kikuchi (2010)	1	1.1	61.8	6.0		0.3			30.4		
Lam et. Al (2010)	2	2.0	75.7			1.3	15.7	5.3			
	3	4.0	74.8			0.8	15.0	5.3			
	4	8.0	73.0			0.2	14.3	4.5			
Lin and Lin (2005)/ Lin and Lin (2006)	5	6.8	80.0		2.0					9.7	1.5
	6	8.5	80.1		1.7					8.7	1.0
	7	9.3	79.4		2.1					6.2	3.0
Lin et. al (2005)	8	4.2	81.5		1.9					12.5	
	9	4.7	80.4		1.9					13.0	
	10	9.0	79.6		2.1					9.3	
Lin and Lin (2004)	11	6.5	81.3		1.9					10.3	
	12	4.9	80.6		2.2					12.4	
	13	11.4	79.2		2.3					7.2	

With the organic part, the sludge material specifications have a much greater energy values than the other ash materials, and after drying, it could be a useful source of fuel and reduce the energy needs included in the heat treatment systems (Dhir et al. 2017a).

2.1.6.3 SSA as a Cement Component

Some waste materials (granulated blast furnace slag, fly ash, silica fume, burnt shale and limestone) have proven to be beneficial for improving some points of concrete performance. This is the benefit of protecting natural sources and decreasing the demands of cement clinkers. For example, it is well-known that the usage of some waste ashes improves the operation and stability of concrete against chloride attacks, and the highly reactive nature of the silica fumes makes it an appropriate choice of high-performance concretes regarding durability and strength (Luo et al., 2014).

Previous SSA articles (Tseng and Pan, 2000; Lin and Tsai, 2006; Lin et al., 2008a; Donatello et al., 2010; Baeza et al., 2014; Baeza-Brotons et al., 2014; Luo et al., 2014) as a known concrete component, the material must be able to provide an appropriate level of performance. Generally, this evaluation focuses on its interaction and possible effect on strength improvement.

The pozzolan activity of the material was assessed directly using a Frattini test, thermal gravity analysis and saturated lime test identified the amount of calcium hydroxide (Ca(OH)_2) due to the pozzolan reactions of SSA. The strength activity index (SAI) test, a secondary measure that compares the strengths that can be achieved under special conditions. The SAI results which are presented in Figure 2.5 are obtained according to the standard methods of ASTM C311 / C311M (2013) and BS EN 196-1 (2005). Figure 2.5 shows that SSA usually met the fly ash reaction requirements of more than 75% at 7 or 28 days in ASTM C618 (2015) and more than 75%, 85% in 28 and 90 days in BS EN 450-1 (2012). The use of pozzolanic materials generally results in lower early age strength. The same behavior is proven with SSA in many different mixtures, depending on the increased SAI's at subsequent treatment times, as shown in Figure 2.5.

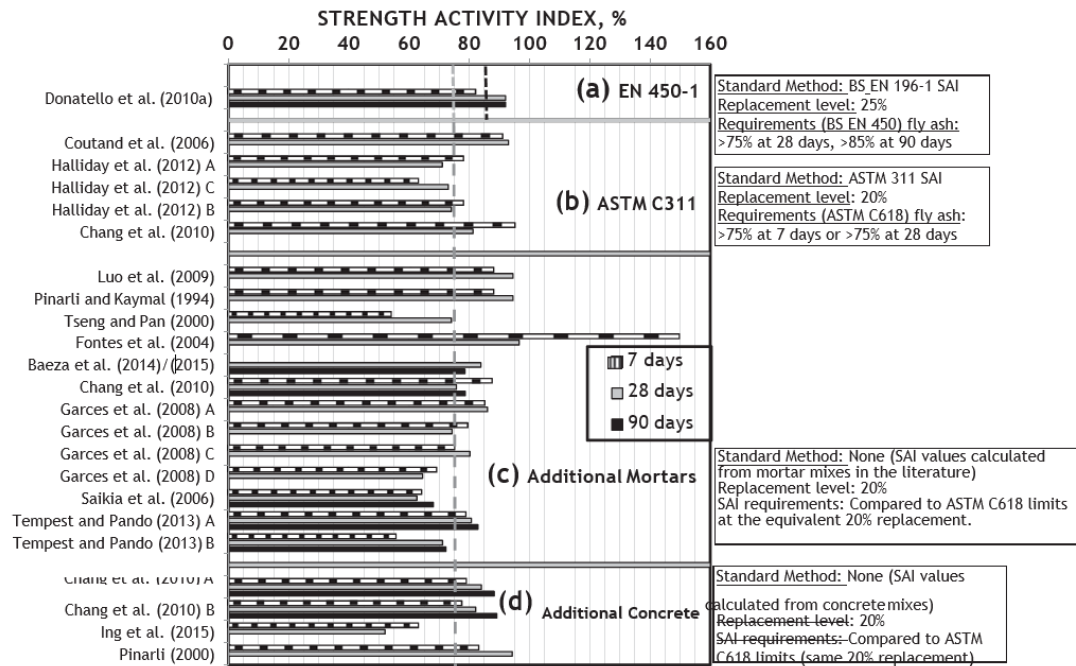


Figure 2.5 Strength activity index (SAI) results for sewage sludge ash (Lynn et al., 2015).

2.1.6.4 Aggregate

The possible usage of SSA as an ingredient in aggregates provide a clearer and less valuable option for incorporating additive materials into concrete uses. The aggregate component of the main mixture provides a possibility regarding the total amount of materials that could be used in the main mixture (Baeza-Brotons et al., 2015).

To change the old practice of the maximum usage of high-strength natural aggregates in all construction uses, a more effective technique matching the quality of aggregates is needed for the final product. This could cause a decrease in the requirement for natural aggregates, and economically it would avoid fees that have been developed to extract virgin aggregates. This method also permits an extensive range of materials that can be use, containing SSA, although these uses can't be considered as mere dumped on land, which is essential for the concrete development as well as sustainable use of materials. Details of concrete and mortar performance including SSA as filler or as an aggregate were investigated by Khanbilvardi and Afshari-Tork, 1995; Kosior-Kazberuk, 2011; Jamshidi et al., 2012; Baeza-Brotons et al., 2015 and De Lima et al., 2015.

The use of SSA was also explored as a manufactured/lightweight aggregate (Bhatty and Reid, 1989; Tay and Yip, 1989; Bhatty et al., 1992; Tay and Show, 1992; Federal

Highway Administration, 1997; Cheeseman and Viridi, 2005; Chiou et al., 2006; Lin, 2006; Tsai et al., 2006; Gunning et al., 2011 and Hu et al., 2012a, b). The production procedure contains heat operation of SSA incineration to cause expansion and this is resulting in a material with mild characteristics forming a strong layer of the outer surface.

2.1.6.5 Concrete and mortar

Concrete and mortar terms are from time to time used changeably, although the obvious difference between these two technical terms is that the mortar does not include coarse aggregate (i.e., gravel) and mortar is employed as a bonding material between bricks and stones together rather than as an independent construction product. These two products share the same performance and behavior requirements. In fact, mortar mixtures were sometimes chosen as an option to concrete by means of cementitious materials. SSA is used as a binder component and aggregate material (De Lima et al., 2015)

2.1.6.5.1 Aggregate component

SSA was investigated as a filler in aggregates and as a fine filler in other materials in less amounts. The SSA material was integrated in several ways: as a fine filler in aggregate De Lima et al., 2015, as a filler of cement Jamshidi et al., 2012 and as a macro fine aggregate alternative Khanbilvardi and Afshari-Tork, 1995; Kosior-Kazberuk, 2011 and Baeza-Brotons et al., 2014.

The compressive strength of concrete and mortar samples mostly were reduced when SSA were integrated, although Jamshidi et al. (2012), recorded significant increments with the addition of SSA up to 10%. The increase in strength could be specified how the material carried out in the mixture, in which case SSA was likely to have led the developments in aggregate mixing and particle filling levels. In general, it is known that SSA is more desirable for addition in less content (up to 20%) since the effects in any of these are more manageable than bulk or aggregate substitution. The results of bending strength reflected that the performance of the compressive strength decreases with an increased SSA amount. Despite the SSA characteristics, i.e., the absorption values of the low-content mixtures and their high porosity values were not importantly

different from the similar control mix, together with the mixture results of Baeza-Brotons et al., (2014). As an aggregate substitution, the results of SSA on absorption have been more marked, although previous strength results seem inappropriate to use in this way.

2.1.6.5.2 Compressive strength

Compressive strength is primarily the most critical characteristics to be considered in concrete and mortar, not only regarding mechanical properties but also as a parameter required in the arranging the classes of durability (Ing et al., 2015).

Figure 2.6 shows the impact of SSA contains on the performance compressive strength of mortar and concrete mixtures. For the analysis, the results were selected for 28 days, since in field, strength is mostly determined at this cure age (Ing et al., 2015).

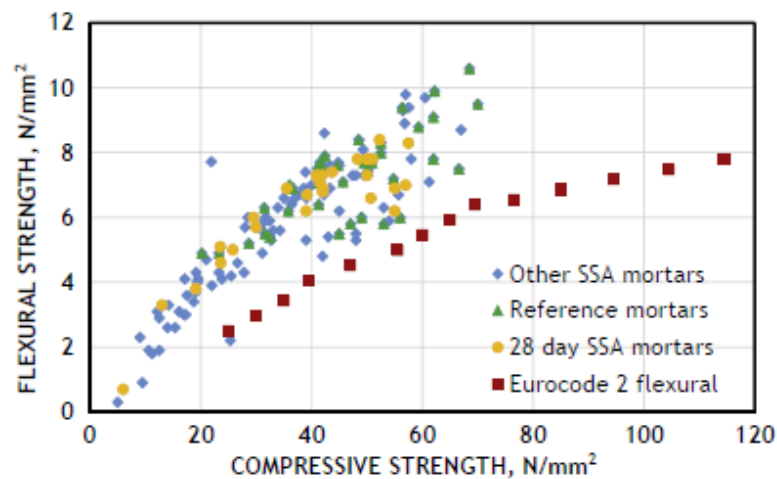


Figure 2.6 The relationship between the flexural strength and the compressive strength of sludge ash (SSA) (Dhir et al., 2017a)

Table 2.2 shows that the strength characteristics of concrete and mortar mixtures reduced with increased ash amount. It seems from researchers on Table 2.2 that the average strength loss rate is expected to be about 1% for each 1% SSA replacement level.

Table 2.2 Effect of SSA content on compressive strength for 28 days concrete (Dhir et al., 2017a)

Reference	w/c	Compressive strength (28 days), % control				
		5% SSA	10% SSA	15% SSA	20% SSA	30% SSA
Alcocelt et al. (2006) A	0.5		92.7		80.6	67.7
Alcocelt et al. (2006) B	0.7		85.5		71.1	56.6
Baeza et al. (2014)	0.5		88.1		83.8	61.9
Chang et al. (2010) A	?		94.9		82.1	69.2
Chang et al. (2010) B	0.5		94.6		75.7	64.9
Dhir et al. (2002)	0.77				61.5	
Fontes et al. (2004)	0.5		95.3	99.1	96.5	90.7
Garces et al. (2008)	?		95.2		74.3	49.1
Halliday et al. (2012) A	0.5		77.7		71.1	
Halliday et al. (2012) B	0.5		81.8		72.7	
Halliday et al. (2012) C	0.5		79.3		73.6	
Ing et al. (2015)	0.55	110.0	83.9	77.0	52.1	
Maozhe et al. (2013)	0.5-1.0		76.7		62.8	48.8
Pinarli (2000)	0.5	106.8	96.0	87.8	94.2	
Pinarli and Kaymal (1994)	0.5	103.2	100.9	96.8	94.5	

The impact of SSA on strength improvement with time, from 3 up to 90 days, is shown on Table 2.3. The effects are presented in the form of control mixtures, the average strengths are also given in parentheses, for example, at 10% of SSA with 3 days of curing time, the strength ranged from 70% up to 113% of the similar control strength and the mean strength of the SSA mixtures were 90% of the control mixtures.

Table 2.3 The SSA content and curing effect on the development of compressive strength (Dhir et al., 2017a).

SSA, %	Compressive strength range (Mean), % Control				
	3 days	7 days	28 days	56 days	90 days
10	70-113 (90)	84-113 (97)	78-95 (90)	90-93 (92)	93-96 (94)
20	55-100 (73)	61-97 (90)	55-96 (76)	78-83 (81)	79-88 (83)
30	35-93 (66)	41-91 (66)	49-90 (66)	70-73 (72)	69-76 (72)

The data on table 2.3 shows that the variation in strength between the SSA mixtures and the control mixtures was larger in the early curing period, although the curing period growth, the strengths get relatively higher, regarding the control mixture. This development at a late curing period is typical of a mixture including pozzolanic additives like ground granulated blast furnaces (GGBS) or fly ash. Compressive strength results for 28 days like control results were possible in various situations for different SSA amounts (Coutand et al., 2006; Cyr et al., 2007a; Fontes et al., 2004; Monzo et al., 1996, 1999a). It has been appeared that while the compressive strength

was higher for the low w/c proportions, there was no alteration in the rate of strength reduction with SSA (Alcocel et al., 2006).

2.1.6.6. Brick-tile-ceramic applications

The ceramics industry is an enormous marketplace, predicted to be account roughly \$250 billion world-wide (Winter Green Research, 2014). Conventional ceramic uses consist of glass, tiles, and bricks. Further, there is an enormous number of different sectors in which ceramics play a serious part as a component on the whole system, along with electronics, automobile, metallurgy, architectural, military, machine tool, optics, nuclear power, and medical industries (Anderson, 1999, 2002; Lin and Weng, 2001; Luo and Lin 2003; Tay, 1987). Clay is the most used raw material in ceramics industry. This material has a plastic nature that could be easily molded and formed the shape of ceramic products when mixed with water, and under thermal operations it is getting densified, this is leading to bigger mechanical characteristics without loss of shape, and as a result this is making it a very suitable alternative in the marketplace. SSA was examined for the usage of both as a clay substitution and a filler element. Concerning the addition of SSA in ceramics uses, the study performed with this new additive has only investigated the surface of the available ceramics in the industry, coating application as a ceramic material and in the more conventional form as a tile, glass and brick construction product is possible. Much research was conducted on the classification of SSA as specific ceramic additive, assessment regarding the ceramic manufacturing procedure, especially the incineration phase, and the characteristics of the resulting outputs were reviewed (Anderson and Skerratt, 2003; Cheeseman et al., 2003; Lin et al., 2006; Merino et al., 2005, 2007). The details of ceramic manufacturing process used with SSA have been given on Table 2.4. Raw materials which were used with or without additives, included water and dextrin adhesive, three clay (rich in kaolin, rich norite and rich in lights) and flat glass. Compressing technic was used to form the shape in most research and the compression pressure ranged from 3.5 MPa up to 60 MPa. Maximum calcification temperatures ranged between 600°C and 1200°C, although the major work was concentrated on testing higher temperatures of this range.

Table 2.4 Conditions for general ceramic treatment using SSA (Dhir et al., 2017a)

References	Initial Preparation	Forming	Sintering
Anderson and Skerratt (2003)	SSA dried; 12% (dry wt) dissolved dextrin starch binder added	Pressed into discs at 15.4 MPa	Electric kiln 1050°C, ramp rate 100 K/h, 30 min dwell time
Cheeseman et al. (2006)	No details provided	Pressed: 8, 16 and 32 MPa	Lab chamber furnace: 980-1080 °C, ramp rate 6°C/min, 60 min dwell time
Lin et al. (2006)	SSA dried, ground to powder	Pressed into cylinders at 3.5 MPa	Electric furnace: 600-1000°C, ramp 5°C/min, 30-240 min dwell time
Merino et al. (2005)	Dry SSA, wet SSA (7% water addition), ground 10 and 20 s, respectively	Pressed: 40 MPa (wet), 60 MPa (dry)	Nickel crucible: 900-1200°C, ramp 2°C/min, 60 min dwell time
Merino et al. (2007)	Dry SSA, wet SSA (7% water addition); ground additives of flat glass and three clays at 12.5-100%	Pressed: 15-59 MPa, depending on workability	Nickel crucible: 900-1200°C, ramp 2°C/min, 60 min dwell time

Due to the lack of plasticity in SSA, most of the above-mentioned experiments have been examined to add water or lubricants to enhance the workability. In fact, the compressive strength reaches the intended level of compaction for dry mixtures at 60 MPa and wet mixtures at 41 MPa (Merino et al., 2005, 2007). The less cohesion characteristics of SSA may indicate a better adequacy as a substitution of clay or filler; although, regarding the identification of SSA as a ceramic product, the above given studies are beneficial as a research. Some studies that indicate data on the density of SSA mixtures are presented at maximum sintering temperature in Figure 2.7. The effect of different dwell time, pressure force and dry versus wet sample preparation have been also presented in the figure as three shaded areas. Compressive strength and density relationship for SSA added ceramic mixtures have been shown for sintering temperatures from 600°C up to 1200°C on Figure 2.7.

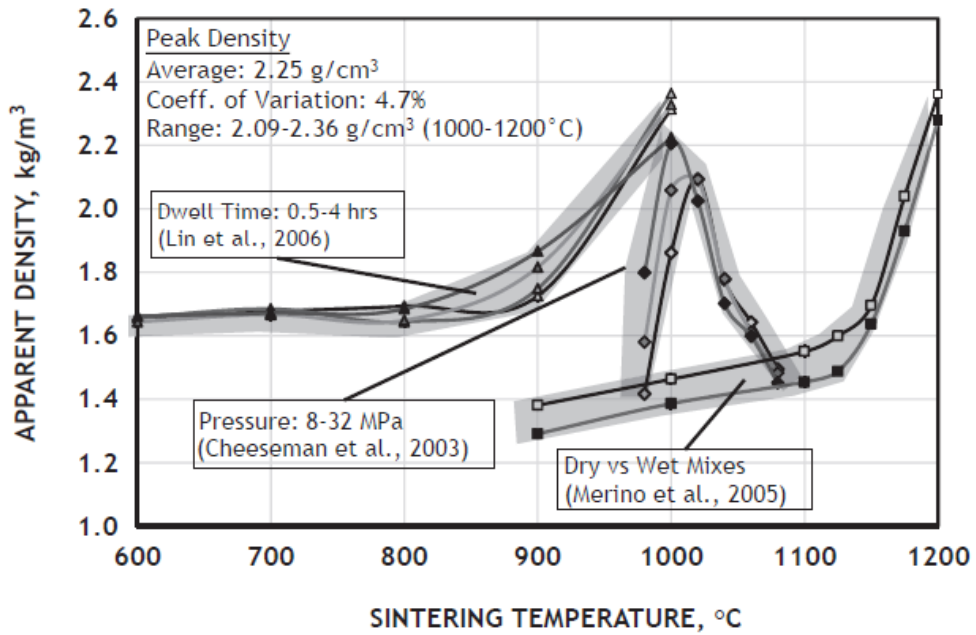


Figure 2.7 The response of the sewage sludge ash process for the treatment of sintering (Lynn et al., 2016).

SSA samples were found to have a mean density of 2.25 kg/m³ at a compressive strength around 155 MPa after sintering. The maximum density that is achieved was very low (from 2.09 to 2.36 kg/m³, a fluctuation ratio of 4.7%), although there appears to be a much greater variation in the temperatures. It seems that the increase in density starts at temperatures of 900°C up to 1150°C, and optimum conditions, ie, the peak intensity point, range from 1000°C up to 1200°C. This might be due to chemical differences in the composition of SSA since the flow characteristics of known oxides like phosphorus pentoxide (P₂O₅) and calcium oxide (CaO) could change the melting grade of the material. The best mechanical results were reported at 25% additives of montmorillonite clay although in the larger content, the products presented initial melting grades at 1200°C and their strengths were lesser (Lynn et al., 2016).

2.1.6.6.1 Bricks

Brick is among the most widely used construction material, with 1400 billion units being manufactured world-wide, although the most are produced in developed countries, especially in China, under weak situations using very simple brickmaking techniques (Clean Air Task Force, 2010). Due to this, even a small ratio of SSA replaced material in the brick industry is equal to the large size of the material used. Bricks are classified according to one of the following types:

- i. Joint Construction- applied in constructions of public buildings.
- ii. Facing modules- applications that require a good-looking aesthetic.
- iii. Engineering units- top quality products with stricter requirements for strength and absorption

The SSA manufacturing procedure include the usual main steps of thermal formation and condensation, using the material as an elemental substitute for clay in the raw form, with amounts close to 50% (Trauner, 1993; Anderson, 1999, 2002; Lin and Weng, 2001; Luo and Lin 2003; Tay, 1987). The bricks were manufactured at sintering temperatures of 300°C up to 1120°C, although the best performances were observed at higher temperature of this range.

During the production of bricks, excess water was found to be required by SSA due to high porosity, low plasticity and related to the low bonding property of mixtures. The results shown in Figure 2.8 give a good idea of SSA effect on the performance of the compressive strength of the bricks. In general, the compression strength decreases with increased SSA amount, despite the results of Lin and Weng, 2001 recommend that SSA flow characteristics might have beneficial effect to the strength in less amounts, but increased porosity becomes the predominant parameter in larger substitution levels. SSA bricks were accomplished to meet the ASTM C62, 2013; ASTM C216, 2015 and BS EN 771-1, 2011 strength standards. The behavior of freeze- thaw action also seems to be importantly influenced by the incineration standards. SSA enhanced the freeze-thaw resistance. All bricks examined in the studies have been used SSA (replacement levels from 0% up to 30%) for a satisfaction degree in the freeze- thaw weight loss limit by 0.5% for the class bricks in ASTM C62, 2013 and ASTM C216, 2015. Thus, SSA can help as a second option for the local supplier in areas that lack adequate natural materials.

The following findings have emerged in the literature:

- i. The density of the SSA brick was up and down, depending on the firing status (Lin and Weng, 2001; Trauner, 1993).
- ii. Weight loss when igniting bricks minimized with increased SSA content (Lin and Weng, 2001).
- iii. Drying shrinkage showed a reducing trend with SSA addition before incineration treatment (Anderson, 1999; Tay, 1987; Trauner, 1993). In

opposition, the overall shrinkage of fire seems to be increasing in SSA bricks (Anderson, 2002; Tay, 1987; Trauner, 1993).

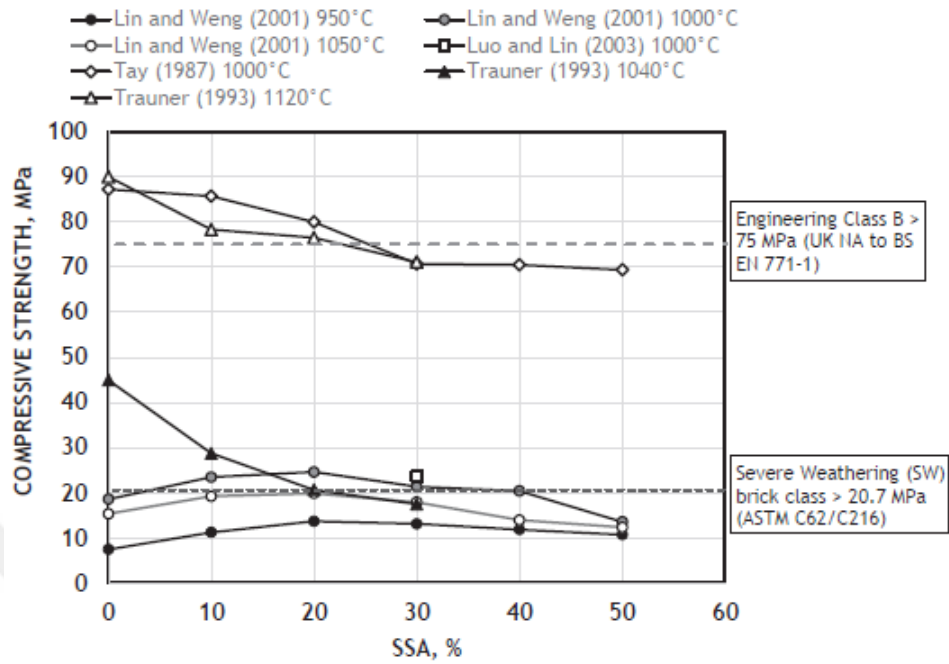


Figure 2.8 Effects of SSA content on the performance of brick compressive strength (Dhir et al., 2017a)

Many researchers in the literature examined this possible uses of SSA in bricks (Donatello and Cheeseman, 2013; Johnson et al., 2014; Kadir and Mohajerani, 2011; Smol et al., 2015; Tay and Show, 1992; Vouk et al., 2015; Wienerberger, 2012).

2.1.6.6.2 Tiles

Ceramic tiles are the most used construction products in walls, floors, tabletops, and surfaces. The main properties of tile materials contain dimensional stability and appearance. Water absorption is affecting the hardness, load resistance, scratching, and deterioration. Glaze is added repeatedly for decorative purposes, although it can also be used to enhance surface compressive strength to prevent fragile tensile failure (Kingery et al., 1976). Manufacturing procedures are like to those which were before described for bricks and general ceramics and include dehumidifying, drying, forming, and calcification in order to improve the required characteristics mentioned above (Chen and Lin, 2009; Dayalan and Beulah, 2014; Lin et al., 2005, 2007, 2008). The full details of the mixture design and characteristics used are given on Table 2.5. It must be pointed out that because of the shortage of natural sources, this study has

resulted in Asian countries and the materials have been examined and investigated according to Chinese standards (CNS, 1999).

Table 2.5 Description of work done with SSA in tiles (Dhir et al., 2017a)

Reference	SSA, %	Glaze, g/cm ³	Colourant	Nano-SiO ₂ , %	Pressure, kg/cm ²	Firing, °C
Chen and Lin (2009)	20, 30, 40, 50	-	-	0, 1, 2.5, 3	306	1000, 1100
Dayalan and Beulah (2014)	0, 30, 45	0, 0.03, 0.06, 0.1	Fe ₂ O ₃ , V ₂ O ₅ , CoCO ₃	-	300	1050
Lin et al. (2005)	0, 15, 30, 45	0.03, 0.06, 0.1, 0.15, 0.2	Fe ₂ O ₃	-	?	1050
Lin et al. (2007)	0, 20, 30, 40, 50	-	-	0, 1, 2, 3	300	1000, 1050, 1100, 1150, 1200
Lin et al. (2008)	0, 15, 30, 45	0, 0.03, 0.06, 0.1	Fe ₂ O ₃ , V ₂ O ₅ , CoCO ₃ , MnO ₂	-	300	1050

Table 2.6 presents data on water absorption effect for tiles including SSA. It was noted that water absorption characteristics grow with increased SSA amount, regardless of the data given by Lin et al., 2005.

Given the effect of other parameters regardless of the SSA amount on the absorption characteristic, the undermentioned deductions could be interpreted:

- i. It appears that firing at 1100 °C is optimal to reduce absorption, depend on the test from 1050°C up to 1200°C by Lin et al., 2007. Results indicate that sintering standards have a significant effect on the treatment procedure, rather than SSA amount.
- ii. Nano-silicon dioxide (SiO₂) reduces water absorption through the useful impacts of high-porosity decrease.
- iii. The top glazing ceramic cover reduces the water absorption of all tile products, as a strong preventative layer on the outer surface of the products.

Table 2.6 Performance of water absorption of sewage sludge ash and tiles

References	Mix/Production	Water Absorption, %					
		0 % SSA	15% SSA	20 % SSA	30 % SSA	40 % SSA	45 % SSA
Chen and Lin (2009)	Clay A, 1000 ⁰ C, 0% n-SiO ₂	<u>18,7</u>	-	<u>19,2</u>	<u>19,5</u>	<u>20,4</u>	-
	Clay B, 1000 ⁰ C, 0% n-SiO ₂	<u>19,1</u>	-	<u>19,4</u>	<u>20,2</u>	<u>20,6</u>	-
	Clay A, 1100 ⁰ C, 0% n-SiO ₂	<u>16,8</u>	-	<u>16,9</u>	<u>15,3</u>	<u>15,0</u>	-
	Clay B, 1000 ⁰ C, 0% n-SiO ₂	10,5	-	12,0	12,1	12,3	-
Lin et al. (2007)	0% n-SiO ₂ , 1050 ⁰ C	8,3	-	9,1	10,9	12,4	-
	1% n-SiO ₂ , 1050 ⁰ C	7,5	-	7,9	8,3	10,7	-
	2% n-SiO ₂ , 1050 ⁰ C	6,2	-	7,2	7,8	9,1	-
	3% n-SiO ₂ , 1050 ⁰ C	5,8	-	6,9	7,4	8,6	-
	0% n-SiO ₂ , 1100 ⁰ C	0,1	-	0,5	1,6	2,1	-
	1% n-SiO ₂ , 1100 ⁰ C	0,1	-	0,2	0,2	0,6	-
	2% n-SiO ₂ , 1100 ⁰ C	0,1	-	0,2	0,2	0,5	-
	3% n-SiO ₂ , 1100 ⁰ C	0,1	-	0,1	0,1	0,3	-
	0% n-SiO ₂ , 1200 ⁰ C	0,3	-	0,8	-	-	-
	1% n-SiO ₂ , 1200 ⁰ C	0,6	-	0,9	-	-	-
	2% n-SiO ₂ , 1200 ⁰ C	0,8	-	1,1	-	-	-
	3% n-SiO ₂ , 1200 ⁰ C	0,8	-	1,4	-	-	-
	Lin et al. (2005)	0% glaze, 1050 ⁰ C	1,0	8,6	-	11,4	-
0,03% glaze, 1050 ⁰ C		0,5	8,3	-	10,9	-	15,3
0,06% glaze, 1050 ⁰ C		0,4	8,3	-	10,9	-	14,5
0,10% glaze, 1050 ⁰ C		0,5	7,8	-	9,9	-	13,9
0,15% glaze, 1050 ⁰ C		0,4	7,6	-	9,6	-	13,4
0,20% glaze, 1050 ⁰ C		0,2	7,6	-	9,3	-	13,3
Lin et al. (2008)	0% glaze, red, 1050 ⁰ C	10,0	-	-	13,6	-	-
	0,03% glaze, red, 1050 ⁰ C	6,0	-	-	7,6	-	-
	0,06% glaze, red, 1050 ⁰ C	5,4	-	-	6,9	-	-
	0,10% glaze, red, 1050 ⁰ C	4,8	-	-	6,7	-	-
	0,03% glaze, yellow, 1050 ⁰ C	6,6	-	-	7,8	-	-
	0,06% glaze, yellow, 1050 ⁰ C	5,9	-	-	7,6	-	-
	0,10% glaze, yellow, 1050 ⁰ C	5,1	-	-	7,3	-	-
	0,03% glaze, blue, 1050 ⁰ C	6,9	-	-	7,8	-	-
	0,06% glaze, blue, 1050 ⁰ C	6,4	-	-	7,4	-	-
	0,10% glaze, blue, 1050 ⁰ C	6,0	-	-	7,1	-	-
	0,03% glaze, purple, 1050 ⁰ C	7,9	-	-	9,7	-	-
	0,06% glaze, purple, 1050 ⁰ C	7,6	-	-	8,7	-	-
0,10% glaze, purple, 1050 ⁰ C	7,2	-	-	8,3	-	-	

Black, no change from control; green, decrease from control; purple, minor increase from control (<2% rise); red, substantial increase from control (>4% rise); underline, exceeding CNS (1999) limit of 16%.

Bending strength is another significant mechanical property of tiles. When evaluating the effect of SSA tiles, the performance of SSA substitution has examined first, and

the results are shown in Figure 2.9 as a percentage of SSA control samples at release temperatures from 1050°C up to 1200°C (Chen and Lin, 2009; Lin et al., 2005, 2007). SSA permit a decrease in bending strength, averaging 6% for each 10% alternative level, based on the most appropriate linear trend line. The varied combustion temperature added changeable results, although there is no clear trendline with respect to temperature alterations to the rate of strength loss with SSA. The associated Chinese standards (CNS, 1999) identify the minimum bending strength of 60 and 100 kgf/cm² for ceramic pots and terracotta tiles respectively. SSA seems to have no problem with satisfying these needs, as in optimal operating conditions, all SSA tiles examined up to 50% of substitution levels and have met the maximum limit of 100 kgf/cm².

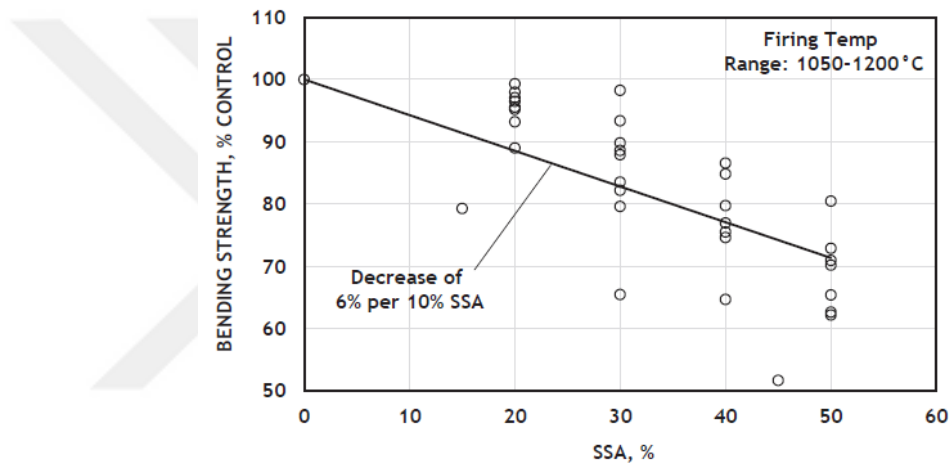


Figure 2.9 Effect of SSA content on the performance of tile bending strength (CNS, 1999)

As for the hardness and durability of glazed tiles, bending strength is improved with the inclusion of glaze due to the formation of a solid protective layer on surfaces after removal. Although, there is a significant increment in the cost of production and the amount of money spent for this purpose varies (Lin et al., 2005).

The SSA tiles met the limits of the above Chinese standards (CNS, 1999), although glazing has been necessary to perform as corrosion-resistant material for both control tiles and SSA tiles. Except for the warping, glazing has caused a development in tile characteristics, as well as the addition of nano- silicon dioxide (SiO₂), and these two could be used to offset the possible impact of SSA if necessary.

2.4.2.3 Glass-ceramics

Ceramics glass is produced from raw materials and controlled crystal glass. With SSA, the process involves rapid integration and separation to create a homogenous glass and make it first, followed by more heat treatment to induce the crystallization process. This type of product shares the properties of both ceramics and glass, containing low-porosity, high mechanical strength, and a strong chemical resistance performance. There is also a great deal of flexibility in the characteristics that can be achieved using glass ceramics, making them of great value in an extensive variety of applications, as an update to conventional products and specialty materials. The wide sort of glass-ceramic uses contains pipes, pumps, valves, condensers, insulators, telescope mirrors, aircraft, rockets, nuclear reactors, and biomedical engineering (McMillan, 1979; Donatello and Cheeseman, 2013; Isa, 2011; Rawlings et al., 2006; Smol et al., 2015).

The conversion of SSA material into the glass is significant that the temperature process will not cause to melt the material, which is found by the chemical composition. As this might result in larger degradation of current kiln, as well as higher energy is required. There is also a need of consistency in the chemical constitution of the raw material to assure the reliability of the resulting output (McMillan, 1979; Donatello and Cheeseman, 2013; Isa, 2011; Rawlings et al., 2006; Smol et al., 2015).

In opposition to tiles and bricks where SSA were used as a limited substitution of clay, the material was generally carried as a key element in the production of glass and ceramic. Although, several extra agents were added to assist fusion behavior and to aim a certain crystalline phase. Information about the mixtures and heat treatment, containing melting temperature and maximum crystallization, are given in Table 2.7.

Table 2.7 Mix type, design, and heat treatment are for ceramics and glass produced using Sewage Sludge Ash (Dhir et al., 2017a)

References	Mix	Thermal Treatment
Endo et al. (1977)	SSA+15-29% Cao	T _M 1490 ⁰ C T _C 1000-1100 ⁰ C
Park et al. (2003)	SSA+15-29% Cao	T _M 1500 ⁰ C, 1 h T _N 760 ⁰ C, 1 h T _C 1050 ⁰ C, 2 h and 1150 ⁰ C, 3 h
Suzuki et al. (1997)	100 g SSA, 50g LS, 50-60g Dol, 10-30 g SS, 10 g SA	T _M 1400 ⁰ C, remelt 1400 ⁰ C, 2h, refined 1300 ⁰ C, 1 h T _N 800 ⁰ C, 1 h T _C 1000-1200 ⁰ C, 1-8 h
Yoon and Yun (2011)	1:3 ratio of SSA/waste glass	No melting T _C 850,950,1050 ⁰ C, 1 h at rate of 5 ⁰ C/min
Wystalska et al. (2013)	SSA only, SSA +20% Dol	T _M ? T _C 1150 ⁰ C (SSA only), 871 and 986 ⁰ C for SSA + Dol, all 1 h Durations
Zhang et al. (2013)	SSA + unspecified CAO Percentage	T _M 1500 ⁰ C, 2 h T _N 837 ⁰ C, 1 h, 3 ⁰ C/min T _C 977 ⁰ C 1-3h, 5 ⁰ C/min
Zhang et al. (2015)	SSA + unspecified SiO ₂ and CAO percentages	T _M 1500 ⁰ C, 1 h T _N 790 ⁰ C T _C 870/945/1065 ⁰ C for 1-3 h

The properties of the glass-ceramic material, which is the result of SSA content, are given on Table 2.8, together with data of commercial used glass, ceramic, marble, and granite (McMillan, 1979).

Table 2.8 Properties of ceramic and glass produced using sewage sludge ash. (Dhir et al., 2017a)

Study	CS, MPa	BS, MPa	Hardness	TEC, 10 ⁻⁷ /°C	Density, g/cm ³	WA, %	AR, %
Endo et al. (1997)	164	n/d	n/d	67	n/d	0	0,1
Park et al. (2003)	n/d	75-92	5860-6230 MPa (V)	74-83	2,87-2,93	0	< 2
Suzuki et al. (1997)	n/d	n/d	5-6 (M)	67	3	n/d	0,1
Yoon and Yun (2011)	210-270	119-156	4790-5560 MPa (V)	n/d	2,32-2,69	n/d	0,13-0,14
Wystalska et al. (2013)	n/d	n/d	6.5 (M)	n/d	n/d	n/d	n/d
Zhang et al. (2013)	n/d	n/d	n/d	n/d	2,19-2,30	1,55-2,30	n/d
Zhang et al. (2015)	167-247	77-178	n/d	n/d	2,37-2,88	0,42-1,02	n/d
Reference Data for Natural Materials and Commercial Glass-Ceramics							
Marble	118	6-22	3-4	80	2,6 - 2,8	0,2	2,5, 10,3
Granite	130	6-30	5-6 (M), 5500 MPa (V)	50-150	2,7	0,35	1
Commercial glass-ceramics	n/d	n/d	7,5 – 9 (M)	50,4	2,42-5,88	n/d	n/d

SSA products have achieved much greater bending and compressive strength than granite and marble reference limits. It should be noted that for dissolved and crystallized SSA glass, the largest pressure resistance (247 MPa) is reached at the lowest temperature degree of 945°C from the pre-optimal crystallization range (945°C -1100°C). The glass-ceramics materials manufactured by Yun-Jun (2011) without SSA melting showed powerful mechanical properties. The densities of SSA material samples, under optimal crystallization states (see Table 2.7) are at a similar level to granite and marble. Conventional glass-ceramic densities are in a large level of diversity, which range from 2.42 g/cm³ to 5.88 g/cm³ (McMillan, 1979). Glass-ceramic samples containing SSA are located at a lower density range (Table 2.7). A good result was found for both ceramics and glass where the SSA has very low water absorption properties and this is a good practical side, indicating poor porosity and big strength properties.

2.4.2.4 Environmental assessment

The usage of additive materials like SSA in ceramic industry is consistent with long-term improvement strategies and procedures and is getting an essential part of the European and global legislation and is committed by companies, laboratories, and citizens. Using SSA as a resource can help to mitigate the demand for natural sources. This technique could be especially useful in fields where appropriate local clay is not available and could also decrease the amount of waste that might be sent to landfill as a disposal. The environmental evaluation should also take into account that the

possible release of heavy metals in the SSA, whether in the gas form of emissions during heat combustion or filtration from groundwater table (Wystalska et al., 2013).

The available data on emissions emitted during the production of bricks, tiles, glass, and ceramics with SSA is very limited, although the fact that ash itself arises from heat treatment organized similarly to sewage reagents are a positive sign. In an experiment conducted in the UK incorporating SSA at 5% in the brick manufacturing process, emissions from the furnace were found for two days below the standard limits specified in the (EPA, 1990) and (Anderson et al., 2002). In terms of practical applications and technical performance, SSA samples have reached worthy results in absorption, strength, and durability. Bricks containing SSA also required a high-water demand due to the lack of plasticity of the SSA material by comparison to clay. The optimum performance was achieved after it was released at temperatures ranging from 1000°C up to 1200°C, with a maximum density ranging between 2.1 to 2.4 g/cm³ and a maximum compressive strength of 350 MPa (Wystalska et al., 2013).

2.4.3 Road pavement applications

This part evaluates the use of SSA in road construction regarding its usage as an additive in unbound, hydraulically bound and bituminous material. The SSA material is not the most appropriate for unbound capping or subbase, because of its fineness classification. In hydraulically bounded road pavements, SSA was added to fresh concrete to get hardened material and then it was crushed to get a coarse aggregate. The material was commonly examined as a bituminous binding material, such as a filler or a fine state, containing several comprehensive projects (O'Flaherty, 2002).

The main role in construction of road pavement is to produce a durable layer for traffic movement. The purpose of road surface is to disseminate the traffic load of the vehicles to bottom soil under the road (subbase), to support traffic design loads. The pavement structure consists of multiple layers of varying thickness, including bound and unbound materials. The arrangement of a standard paving structure is illustrated in Figure 2.10, which shows the configuration of the subgrade, subbase, asphalt surface and capping (O'Flaherty, 2002).

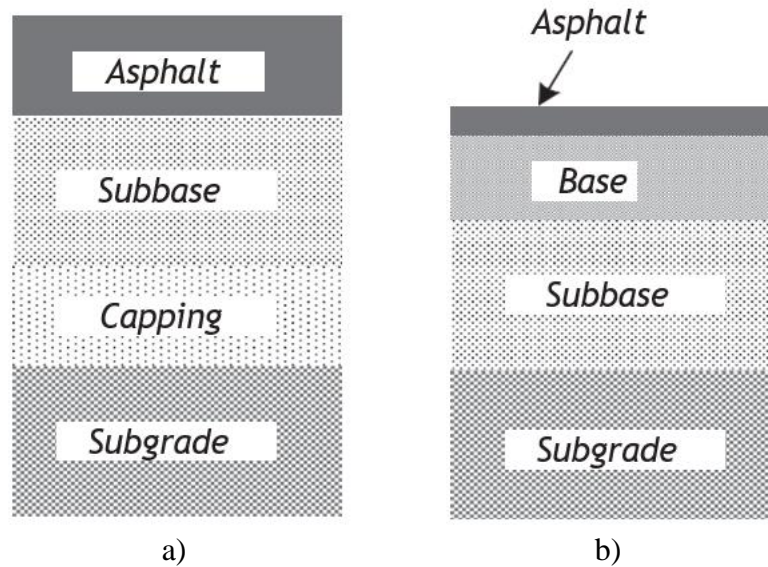


Figure 2.10 Flexible road structures typical of (a) highways and main roads; and (b) rural roads (Ravindra et. al, 2017)

The top surface function is to produce a homogenous, smooth but resistant path for a secure travel, moreover, to help the structural strength and durability of the road pavement. (O’Flaherty, 2002).

The enforced traffic load is enforcing the base/subbase layer and the needed thickness of this layer depends on the CBR value of the bottom soil. This layer is usually composed of well sorted granular or cementitious materials. A weaker capping layer could also be added as layer of soil. In the design of the road, it is not uncommon to encounter soil with a lower CBR of 5%. Therefore, the capping layer, which is 150 to 300 mm thick could be employed. The purpose of the capping layer is to produce an efficient layer so that it can be compressed by traffic loads to a tolerable limit. Well sorted granular materials, with less or zero plasticity index, are usually selected as capping (O’Flaherty, 2002).

Concerning the possible usage of sewage sludge in a wide range of functions as paving materials, publications in this field are less. Its usage as a fine mineral filler in asphalt structure is the most common alternative. Figure 2.11 is presenting the grain-size distribution curves for the SSA samples that are produced for Type 1 and 2 mixes. It is evident that the classification of SSA mixtures is much finer than the grain-size distribution for unbound and capping samples. However, SSA might be used as a mineral filler to enhance the gradation of base/subbase materials and to decrease the required thickness of the road pavement configuration.

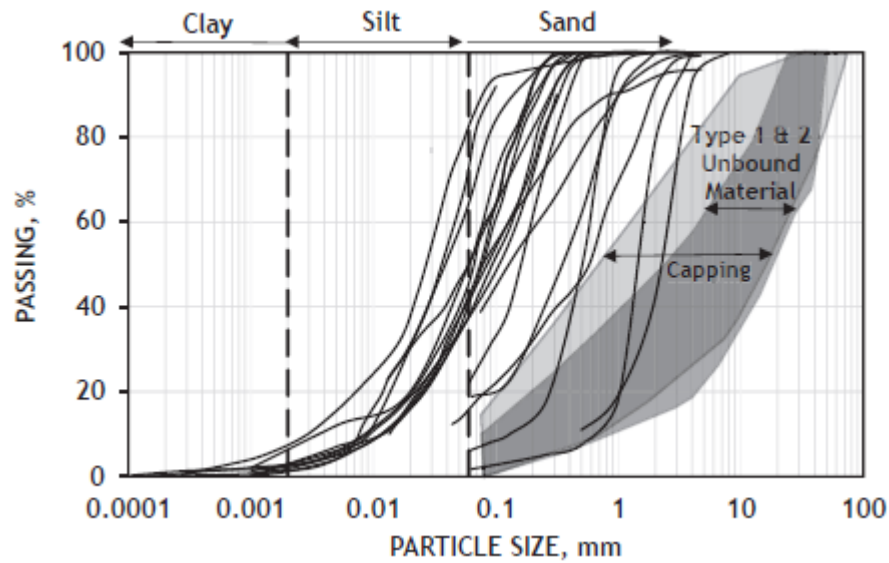


Figure 2.11 Particle size distribution curves for the waste dump produced for the work of highways (Ravindra et. al, 2017)

As a subbase material, SSA was used in original form ($D_{50}=104$ mm) and in a crushed pulverized material form ($D_{50}=10$ mm), where 15% and 30% of SSA addition were added to the concrete. In practical applications, extra water is also required to assure a good mixing. For this reason, SSA is included to the concrete material with a water amount of 135%. Although, due to segregation difficulties that occur with SSA, an extra mixture is prepared with a 65% of water amount. Table 2.9 shows the data illustrating the influences of the SSA increase on CBR and compaction properties for the subbase material (O’Flaherty, 2002).

Table 2.9 Sewage sludge effects on the properties of the pressure and dam ratio of the hydraulically related core materials (Sato et al. (2013).

Mix	Compaction			
	SSA, %	OMC, %	MDD, g/cm ³	CBR, %
Control	0	12.2	1.81	54
As-produced SSA (MC=135%)	15	16.4	1.83	107
	30	-	-	43
Pulverised SSA (MC=65%)	15	17.0	1.92	208
	30	18.7	1.85	143
Pulverised SSA (MC=135%)	15	19.9	1.90	-
	30	24.2	1.71	-

SSA addition of 15% has resulted in developments in the maximum dry density, especially the bearing capacity of the subbase layer. This is due to the filling performance of the SSA material. There was a larger increase in CBR and maximum

dry density with pulverized SSA due to its low porous form. Although, SSA additives are less efficient at 30% amount, because of the need of water for a satisfactory mixing.

It must be emphasized that the CBR value of the samples with 30% of the pulverized SSA were approximately three-times bigger than the originally produced SSA control samples. Despite that, in general, the most efficient results were reached by 15% of SSA content, in pulverized form to decrease porosity and water absorption characteristics (Khanbilvardi and Afshari-Tork, 1995; Khanbilvardi and Afshari-Tork, 2002).

The research conducted with SSA in bituminous bond samples were generally explored as a mineral filler constituent. This usage is most suitable for the grading of the material, although in any particular case SSA is examined as a fine aggregate inclusion (Khanbilvardi and Afshari-Tork, 2002).

Figure 2.12 shows the influences of SSA with various bitumen content on the stability associated with its usage as substitute for limestone and a mineral filler component (at 6.4% of filling content for the total mixture) (Al Sayed et al., 1995). SSA could be used as a partial filler substitute up to 45% and as an alternative replacement component up to 15% of fine aggregate (Khanbilvardi and Afshari-Tork, 2002).

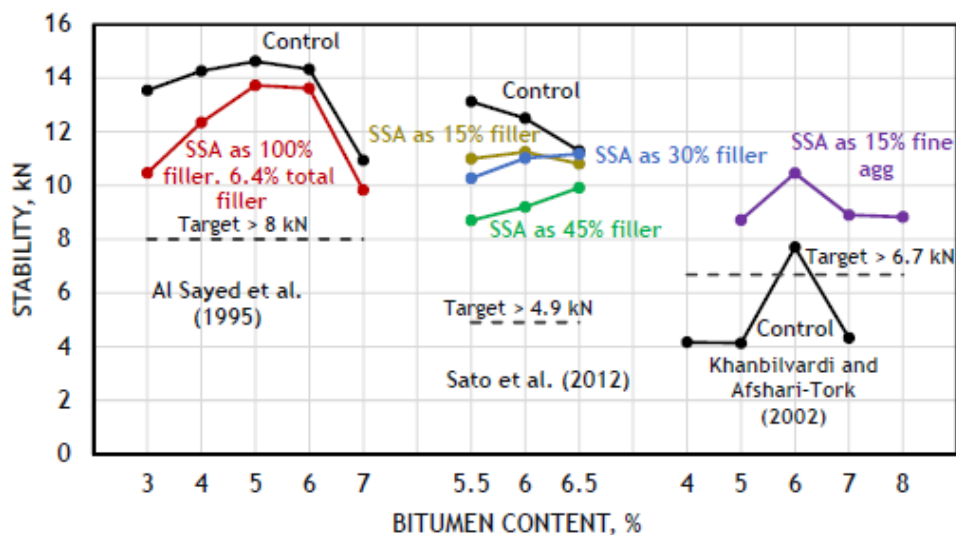


Figure 2. 12. Effect of SSA, with different contents of bitumen on the stability (Ravindra et. al, 2017)

It seems that as a direct substitution of the filler, SSA addition results in a decline of the stability of the mixture, although the losses are controllable, especially in the study with SSA as a substitute of filler component (Al Sayed et al., 1995), and, the stability

targets are fulfilled with all SSA mixtures. SSA is considered to have an effective performance on the stability of the mixture when it is used as a fine aggregate material. Increase in stability could be assigned to the SSA filling characteristic. According to this conditions, developments and instability were indicated by Envirosience (1982) and the Federal Highway Administration (1997) where SSA is added as an inclusion to the mixture, at amounts lower than 5%.

The findings of the flow tests were observed from the vertical deformation of the bitumen-bound samples under loading and are shown on Table 2.10 for the same contents of the SSA and the bitumen. It is evident that, usage of SSA as filler or as a fine aggregate substitute helps to increase the flow. It comes as no surprise, SSA is assumed to have less stiffness characteristics than sand and natural limestone. Although, for the great part, SSA samples have met the targeted limits. The flow is becoming problematic at the highest bitumen content, in every state this will be less economic Tenza-Abril et al. (2014).

Based on the stability and flow of the above content, the impacts of SSA on optimum bitumen amount compared to limestone control samples appear to be much small. As a mineral filler alternative, findings from Al Sayed et al. (1995) and Tenza-Abril et al. (2014) showed that the optimum bitumen content corresponding to limestone samples could be selected at 5% and 4.5-5.5%, respectively. Sato et al., (2012) have been reported that the usage of SSA in its original form as manufactured requires an increase of about 0.5% in bitumen for each 15% of SSA amount. Also, it has been indicated that 15%, 30%, 45% of SSA contents were used as a partial filler in bitumen mixtures. Although, the SSA pulverizing procedure ($D_{50}=104$ mm decreased to $D_{50}=10$ mm) decreased the porous of the SSA grains that ash can add as a filler alternative, with no important rise in bitumen need.

Table 2.10 Sludges of sewage and sludge ash with bitumen content on the flow of bituminous mixtures (Sato et al., 2012)

References	Mix	Bitumen, %	Flow	Target Limits			
(a) Al Sayed et al. (1995)	Control 0% SSA	3	mm	BS 598-3			
		4	2.7	2-4			
		5	2.3				
		6	2.6				
		7	3.7				
		4	4.6				
		5	3.7				
	100% as filler	3	2.8				
		4	2.9				
		5	3.1				
		6	3.9				
		7	6.1				
		6.1					
(b) Sato et al. (2012, 2013)	Control 0% SSA		1/10 cm	Japan specifications			
		5.5	30.7	20-40			
		6.0	37.0				
		6.5	44.1				
		15% as filler	5.5	29.0			
			6.0	34.8			
			6.5	42.1			
		30% as filler	5.5	20.4			
			6.0	27.8			
			6.5	33.3			
		45% as filler	5.5	22.3			
			6.0	27.9			
			6.5	31.0			
		(c) Khanbilvardi and Afshari-Tork (2002)	Control 0% SSA		0.01 inch	New York State limits	
				4	7.9	8.18	
				5	7.9		
				6	9.6		
				7	9.8		
				15% SSA as fine aggregate	5	11.9	
					6	11.0	
					7	12.9	
8	18.0						

2.4.4 Geotechnical properties and applications

In this part performance of SSA is evaluated according to the scientific studies in the literature which are examined in geotechnical applications, such as an additive for soft soil stabilization and as a fill material. Performance aspects addressed the plasticity index, compaction characteristics, shear strength, unconfined compression strength, California bearing ratio, swelling and pH change.

Geotechnical engineering could be explained as the uses of geological, geophysical, and hydrogeological fundamentals to solve engineering problems on or within earth. Geotechnical engineering includes a wide range of usage types, containing earthworks (cut and fill), foundation design, soil improvement techniques, slope stabilization and the construction of retaining walls.

Geotechnical engineering suggests favorable uses of additives and waste materials, due to large amounts and low mechanical strength needs. However, such waste materials can not be easily disposed in dumping areas. These materials must demonstrate that the usage of them could provide the required level of geotechnical demand.

2.4.4.1 Grading

Grading is a significant part for soil measurements, and it is forming the basis with consistency parameters like plasticity index, for soil classification systems that are developed. Classification as an international use in geotechnical engineering is a need to collect the soils into groups that behave similarly. Figure 2.13 presents the grain size distribution curves for unprocessed SSA samples, along with the size fraction limits and soil type. The samples on Figure 2.13 seem to be generally well-graded. The effective grain size (D_{10}) and the coefficient of uniformity (C_u) for SSA mixtures are between 0.003-0.7 and from 3-12, respectively.

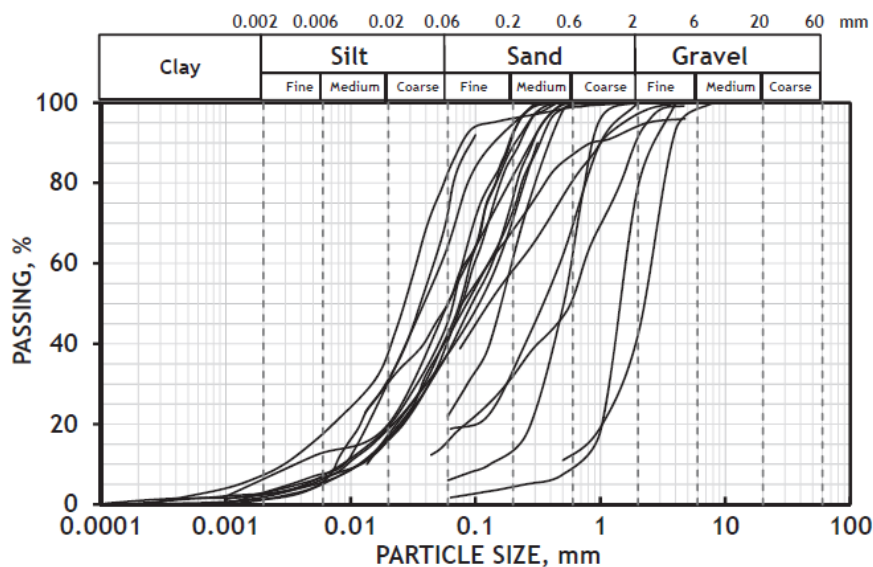


Figure 2.13 The particle size distribution curves of SSA are combined with soil size fractions.

The data and information in this study used from Sharif and Atom (2014), Alcocel et al. (2006), Anderson and Skerratt (2003), Bhattu and Reid (1989), Cheeseman and Viridi (2005), Donatello et al. (2010a, b), Franz (2008), Garces et al. (2008), et al. (2002), Koesor Kasperok (2011), Kriskirikova (2015), Ksepeko (2014), Mauzi et al. (2013), and Petavratzi (2007).

2.4.4.2 Plasticity

Plasticity index is the property of the material to undergo permanent deformation under stress without cracking. The fine granulated soil becomes plastic with increased water amount, resulting in loss of shear force and stability. The findings for the SSA's composition were mixed and varied from nonplastic to highly plastic. The scientific researchers who have investigated plasticity index of SSA but have not provide the data of the Atterberg limits, tend to classify the SSA as nonplastic (Wegman and Young, 1988; Yusuf et al., 2012; Sato et al., 2012; Tempest and Pando, 2013 and Al-Sharif and Attom, 2014). The Atterberg limit results of SSA are displayed on the Casagrande chart in Figure 2.14. This chart is divided into areas with low plasticity and high plasticity values. The "A" line presents the border between the silts/organic soils (under line) and the clay (over the line) and. Although depending on the limited results, SSA seems to have plasticity characteristics like high plasticity silts/organic materials. This recommends that, regarding the strength, SSA might be fairly sensible to water changes during the usage in geotechnical engineering applications.

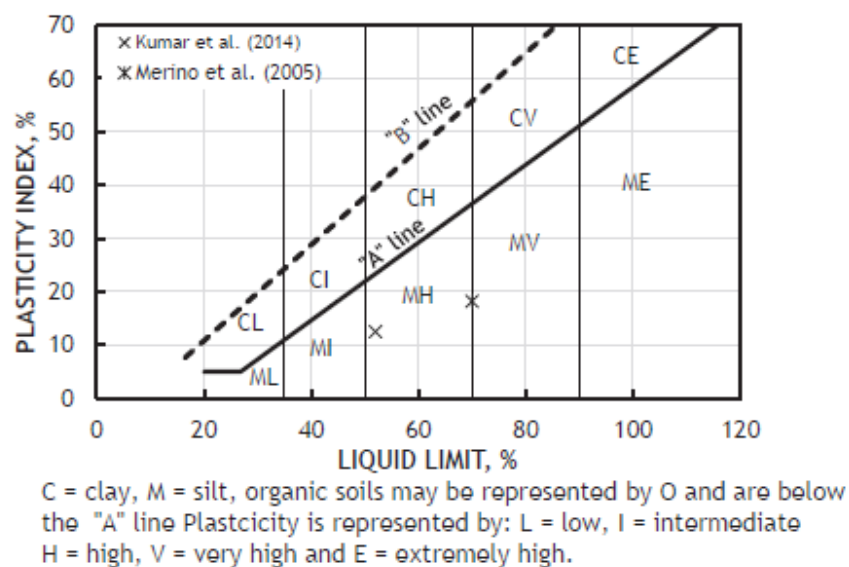


Figure 2.14 The plasticity of SSA on the Casagrande scheme (Ravindra et. al, 2017)

2.4.4.3 Permeability

Permeability is soil characteristic at which liquid or gas can pass through the entire material with a rate under a pressure. In geotechnical engineering applications, this information is significant on soil stability due to weak drainage and could result in excessive pore water pressure in soils. From an environmental aspect, the permeability rate of SSA is also affected by heavy metals content that could leach out and affect the permeability. The permeability rate of SSA was measured to be between 1×10^{-4} to 4×10^{-4} cm/s (Federal Highway Administration, 1997; MPCT, 1980; Yusuf et al., 2012; NCHRP, 2013 and Al-Sharif and Attom, 2014;). This puts SSA on the boundary of clean sand, sand-gravel mixtures and very fine sands, silts categories as described in BS 8004 (1986). As long as the classification of SSA was matching the above soil categories, it could be emphasized that SSA has similar permeability values to that found similarly in gradient soils. The results of the permeability indicated that this material would supply good drainage characteristics as filler and is improbable to result in excessive water pressure accumulation. In contrast, this may make SSA more sensitive to leakage controlled by the closure, especially when used in applications that are not limited.

2.4.4.4 Compaction characteristics

Compaction property is used to enhance soil strength and density. The achievable degree of compressibility depends on grain morphology, grading, organic amount, water amount, and applied stress. Compaction is tested in a fixed mold by compressing the soil in a series of layers. For a particular pressure, the maximum dry density that is reached in a series of water content is listed. Figure 2.15 shows a relationship between maximum dry density and water amount, along with the similar California Bearing Ratio (CBR), and permeability behaviour.

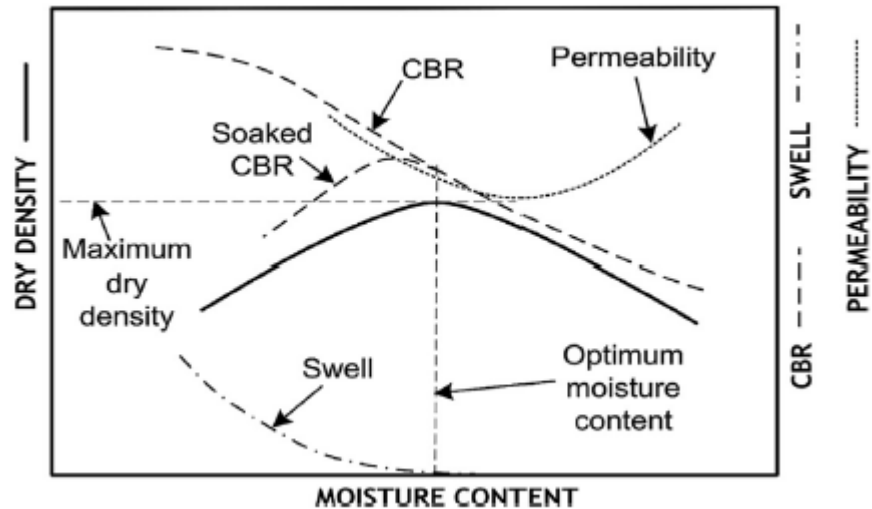


Figure 2.15 Relationships between dry density and moisture content for CBR and both permeability and swelling characteristics. (Al-Sharif and Attom, 2014)

Unfortunately, there is no data in the literature on the behavior of water amount and maximum dry density for SSA. The material was found to have an average a specific gravity greater of 2.6. The average specific gravity is classified less than natural sand (specific gravity 2.65), whereas the low mass of particles indicates the porosity. The irregular SSA particles may prevent the form of compression that can be achieved, given the high degree of friction between the particles, however, this may be useful for total shear strength.

2.4.4.5 Organic content

Organic matter is burned in the original form of sludge during incineration, although it is common to find small fragments in the SSA. The organic part could overlap with the density, compatibility, and safety of the material, as well as the natural interactions between lime/cement and ash in soil stabilization uses. The SSA organic matter was generally less than typical clay content. Although this parameter does not appear to be a major inhibitor, it was still in the interest of the engineer to try to minimize the residual organic matter in SSA.

2.4.4.2 Soil stabilization

For the purpose of achieving and applying sustainable improvement goals that are becoming significant in the construction industry today, the applied hand is further directed towards easing the excessive demand for natural sand and gravel materials in

the construction process. And by the most efficient use of materials of lower quality can be achieved and obtained, especially in cases where the performance requirements are low, as well as through the inclusion and use of additive materials and recycled. In geotechnical engineering, the suggested usage of SSA for soil stabilization seems to be an ideal possibility, as it might make it easy for greater use of lower quality clay soil, while at the same time, SSA could be used as a valuable source instead of the landfill.

Stability is a treatment used to improve the strength and durability of soft soil. Major stabilization methods include the integration of low contents of materials such as cement, hydraulic lime, and bitumen with soil. Treatment methods have evolved to include secondary materials such as fly ash as an additive to stability, due to its activity as a pozzolanic agent and its beneficial effects in filling pores as fillers. In a similar context, this section aims to assess the possibility of including SSA.

Table 2.11 shows the various tests and mixtures that were used in soil stabilization applications with SSA since 2000. SSA were used on its own and as a common part with lime and cement as an additive to soil stabilization. The total amount of the stabilization additives is ranging up to 30% for each dry mass of soil, and in all instances, the soil improvement was applied to cohesive clays, weak and soft soils.

Obviously using SSA in original form is the most economically appropriate alternative, although the advantages were assumed to be in the mechanical stability by improving grades and of decreasing plasticity index and swelling potential. Mixtures, containing lime or cement, together with SSA, were assumed to propose better developments in strength, not only from the binding aspect but also from the pozzolanic activity of the SSA.

Table 2.11 A series of designs for soil stabilization treatments containing SSA.
(Ravindra et. al, 2017)

Reference	Mix Design
Al-Sharif and Attom (2000)	SSA only-0%, 2.5%, 5.0%, 7.5%, 10.0%, 12.5% SSA mixed with three cohesive soils
Al-Sharif and Attom (2014)	SSA only-0%, 2.5%, 5.0%, 7.5%, 10.0%, 12.5% SSA mixed with three cohesive soils
Lin et al. (2005)	SSA only-0%, 2%, 4%, 8%, 16% SSA added to cohesive soil
Lin et al. (2007c)	SSA only-0%, 2%, 4%, 8%, 16% SSA added to cohesive soil; compared to pulverized fuel ash
Tempest and Pando (2013)	SSA only-5%, 10% SSA added to clay
Chen and Lin (2009)	SSA+cement- 4:1 SSA/cement ratio; 0%, 2%, 4%, 8%, 16% added to soil
Ingunza et al. (2014)	SSA+cement-0-9% cement, no SSA; then 9% cement + 5%, 10%, 20%, 30% SSA
Lin et al. (2007b)	SSA+cement-4:1 SSA/cement ratio; 0%, 2%, 4%, 8%, 16% added to soil
Luo et al. (2012)	SSA+cement-3:1 SSA/cement; 15% addition, also with 0-4% Al_2O_3
Lin et al. (2007a)	SSA+lime-4:1 SSA/hydrated lime; 0%, 2%, 4%, 8%, 16% added to soil

The impacts of the above fixation improvements on soil properties were then investigated, covering effects on Atterberg limits, compression characteristics, UCS, CBR, stress relationship, swelling/shrinkage, pH and permeability behavior.

2.4.4.2.1 pH

The assessment of pH is providing useful insight into soil stability behavior. Calciumoxide (CaO) is the main reactive element found in abundant amounts in both lime and cement. When these substances are included to clay soil type, the pH rises to alkaline state strongly as the ions are entering the soil/water solution. This results in soil grains to sinter and changes into coarse form. This initial reaction occurs quickly when the additives were added with the soil and the clay result in reducing water retention capacity. Then, under high pH states, both alumina and silica in the soil turn into the solution and interact with calcium ions from lime to form aluminum silicate hydrates, which crystallize over a time to bind the soil grains.

The pH behavior of many of the soil stabilization mix designs detailed in Table 2.11 was recorded in different treatment periods. Results are shown after treatment for 3 hours and 21 days in Figure's 2.16 (a) and (b), respectively (Lin et al., 2005a, 2007a, b, c; Chen and Lin, 2009). The soil pH stabilized with SSA has obviously not changed significantly in both treatment times and with all added content, indicating that there were no important interactions between the soil and SSA. Research has shown important grow in pH for soil mixed with a combination of SSA and SSA-cement regarding its highly alkaline composition of the documented sample. The soil reaches

the top of the alkaline immediately after treated with the additives, presented in the treatment results for 3 hours on Figure 2.16 (a). As can be seen, significantly lower pH values in 21 days (Figure 2.16 (b)), alkalinity dissipates gradually over time due to the reduction of calcium ions as the water reaction continues. This continuous consumption of alkali shows that bonding formation (cementation) and soil strengthening is occurring.

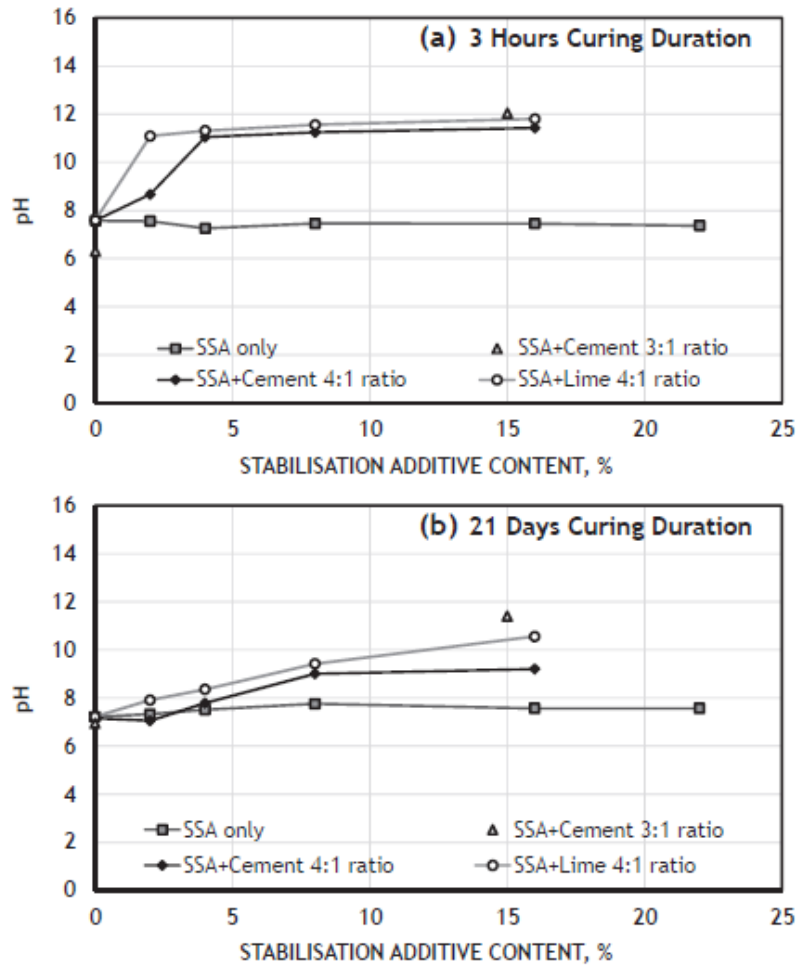


Figure 2.16 Effect of pH stabilizes treatments after (a) 3 treatment hours and (b) 21 treatment days. (Chen and Lin, 2009; Lin et al., 2005a, 2007a, b, c)

2.4.4.2.2 Plasticity

As established previously, soil gums have a major impact on parameters such as shear strength of foundation, stability, and possible swelling of the soil. The effects of including additives (SSA only, SSA-cement and SSA-lime) are examined in this soil property, measured by PI, in Figure 2.17, for treatment of up to 28 days.

It is evident that all additives for the purpose of soil stabilization led to noticeable reductions in plasticity, which turns soil properties from high plasticity to low-quality. There is little adjustment in the improvement made with treated SSA soil only, compared to soils that also contain lime and cement, suggesting that useful developments in plasticity indexes are often attributed to ash. Development in plasticity index occur mostly in the first days after treated with SSA and seem to achieve the equilibrium point in about 6 days of treatment, after which the behavior stays constant.

For this purpose, the effect of SSA fixation on soil elasticity was discussed in Figure 2.18, which illustrates the effect of soil supplemental content. This test provides 28 days of results, apart from Al Sherif and Atom (2014), who did not define the time period of treatment for the soil.

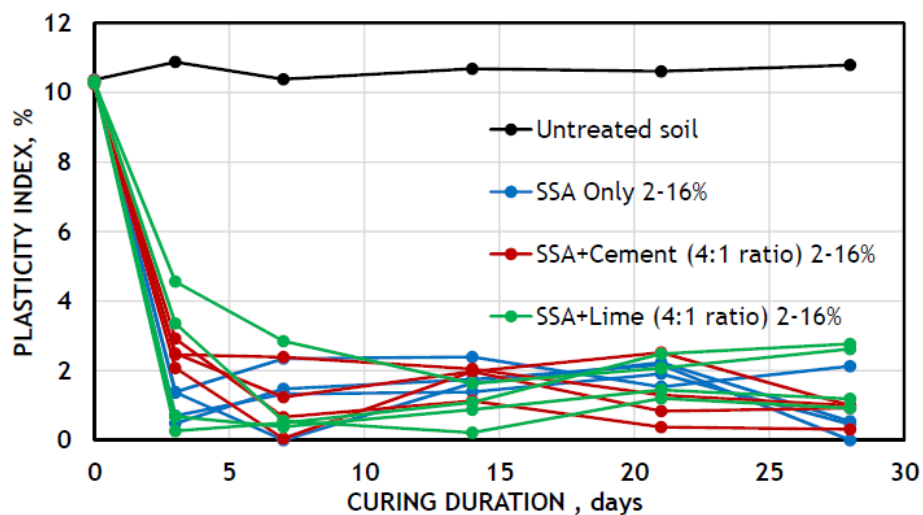


Figure 2.17 Effect of SSA and additives on soft soil and plasticity with curing time. Al Sherif and Atom (2014)

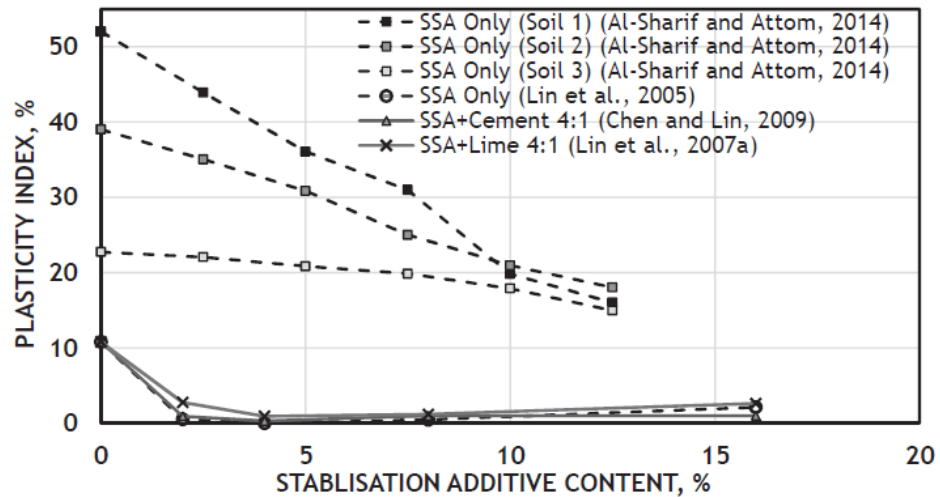


Figure 2.18 Effect of additive content of stabilizing SSA on soil softness and plasticity properties. (Al Sharif and Attom (2014))

Laboratory results have clearly shown that the choice of additives to stabilize the characteristics of plastic behavior depends heavily on the initial performance of untreated or clean soil. Soil using basic PI has achieved full benefits of 10% to reduce soil plasticity with the addition of static content from 2% up to 4%. Another soil samples, with an extraordinarily high PI content of up to 50%, continued to decrease soil plasticity index.

2.4.4.2.3 Compaction properties

Dry soil density can be increased by increasing strength, low permeability, and higher volume stability. SSA impact were assessed as a part of the fixation additives on soil compaction characteristics using the standard Proctor (ASTM D698, 2012), and modified Proctor (ASTM D1557, 2012). The testing results are shown on Figure 2.19, which has been improved and obtained acceptable results by tracking changes in optimum moisture amount and maximum dry density points on compaction curves with different amounts of SSA and SSA-lime additives.

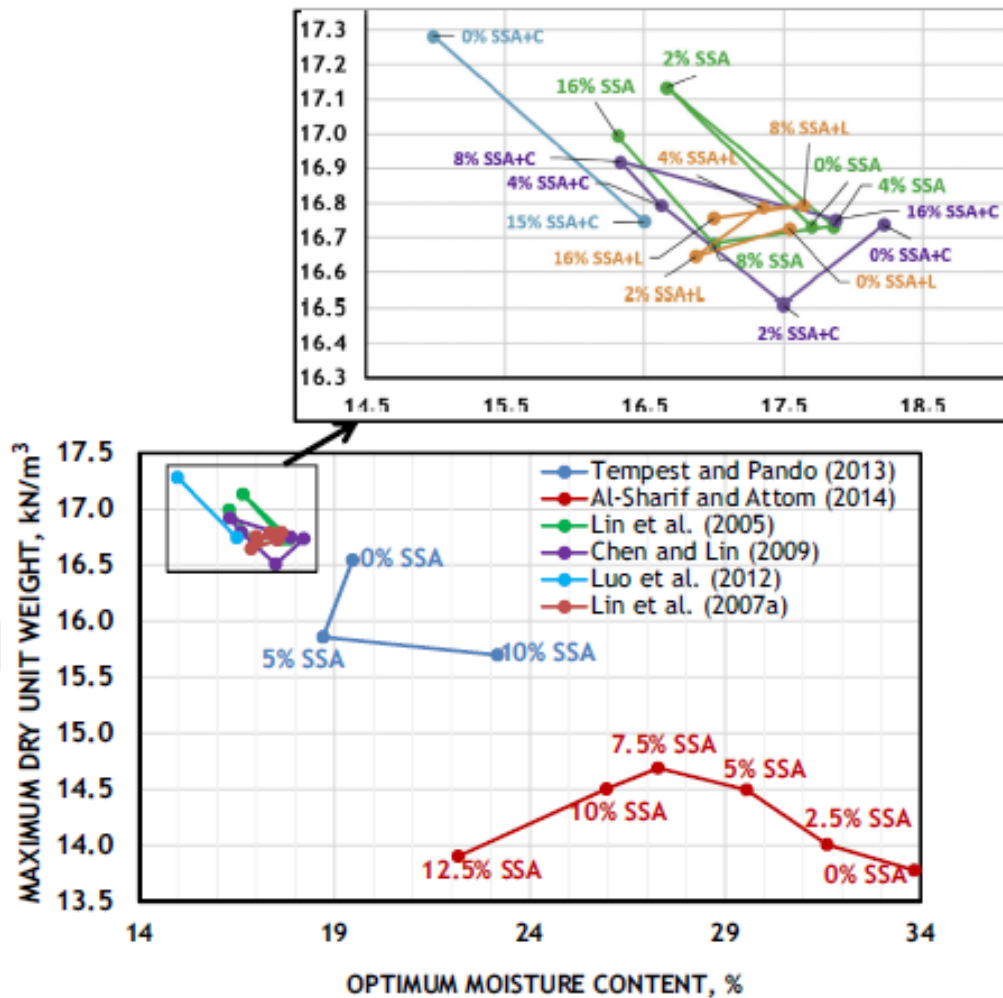


Figure 2.19 Effect of additives on optimum moisture content and maximum dry unit weight characteristics (Ravindra et. al, 2017)

The information and extra testing results on the direct relationship between dry density and SSA amount are supported as a valid addition to these behaviors. A grow in dry density was expressed for SSA quantities from 2% up to 7% (Lin et al., 2007c; Al-Sharif and Attom, 2014), another study results of SSA were indicating a decrease in the dry density for bigger SSA amounts of additives (Ingunza et al., 2014). Straight cuts were reported for all levels of SSA added up to 30%, although they were only examined at 5% intervals.

2.4.4.2.4 Unconfined compressive strength

Improving the strength parameter is the main goal of soil stabilizing that can be built upon. The effects of SSA additions on UCS were assessed from soft soils in accordance with the ASTM D2166 (2013) test procedure. The mixing results of

different additives, when soil treatment reaches 90 days, were displayed in Table 2.12, with color coding based on the density variation.

Installation additions were found to be useful in raising the soil strength. The behavior of the former dry unit density recommended that higher performance levels could be achieved at lower SSA substitution levels; although, continuous developments in strength were clear to increase the added content. There is considerable variation in UCS initiation of untreated soil, although similar increases of up to 30-45 kPa are reached up to 16% of SSA. The soil mixed with SSA progressed to see improvement in strength as treatment period continued. High strength improvements were apparent when lime and cement were combined with SSA. A 4:1 ratio of SSA/cement or SSA/lime, the strength has been achieved up to seven times higher than the soft soil without treatment. The inclusion of SSA was also useful for top-grade soils with UCS that were more than 2000 kPa (Ingunza et al., 2014), indicating that the SSA can have a valuable usage in a large application area.

It is interesting that there is an abnormality reported by Sharif and Atom, 2000. Stability was not too much effective with SSA, perhaps because of the very high elasticity of the soil. These UCS results reflected dry density behavior, presenting peak development strengths with 7.5% SSA, and then the strength performance decreases.

Table 2.12 Effect of sewage sludge ash addition on unconfined compression strength for soft soils

Reference	Additive %	UCS at various curing durations, kPa					
		≤1 day	2/3 days	7 days	28 days	56 days	90 day
(a) SSA only							
Tempest and Pando (2013)	0				203.5		
	5				227.8		
	10				240.3		
Lin et al. (2007c)	0	33.1		33.1		33.1	
	2	37.8		46.9		63.0	
	4	41.8		47.4		67.1	
	8	42.7		54.6		69.8	
	16	47.1		60.8		67.8	
Lin et al. (2007c)	0	31.5	32.4	32.5	30.0	29.0	31.4
	2	37.8	51.8	46.6	55.7	65.2	70.8
	4	40.8	53.5	47.9	57.4	65.8	71.4
	8	42.8	55.5	54.3	59.1	69.2	75.6
	16	47.2	59.2	60.6	62.8	71.2	78.6
Al Sharif et al. (2000)	0				Soil1 Soil2 Soil3	(all 28 days)	
	2.5				164.6, 190.4, 147.2		
	5.0				164.8, 193.7, 155.4		
	7.5				171.9, 201.7, 161.1		
	10.0				175.6, 209.9, 170.2		
	12.5				161.1, 198.4, 156.4		
					149.1, 178.4, 136.2		
(b) SSA+Cement							
Ingunza et al. (2014) mixes contain 9% cement	3				2261.3		
	9				2403.9		
	15				2514.0		
	20				2831.5		
	30				2708.4		
Luo et al. (2012) 3:1; SSA:Cement	0	38.8		39.1	40.1	39.1	38.8
	15	44.0		137.8	181.5	211.1	214.8
Chen and Lin (2009) 4:1; SSA:Cement	0	32.2	33.3	33.4	31.3	29.9	32.2
	2	53.2	61.7	61.1	69.5	72.5	95.8
	4	60.7	68.5	74.6	82.9	92.0	116.0
	8	68.1	102.2	127.7	141.3	141.4	158.7
	16	74.9	144.1	155.4	209.5	209.5	224.5
(c) SSA+Lime							
Lin et al. (2007a) 4:1; SSA:Lime	0	31.5	32.0	33.0	30.0	29.1	31.0
	2	43.3	59.1	64.0	67.0	64.5	73.4
	4	47.8	73.4	70.0	108.4	103.4	129.6
	8	53.2	79.3	97.0	119.2	117.7	148.8
	16	56.7	79.3	124.1	143.8	162.6	189.7

Brown, 0-25% increase; blue, 25-100% increase; green ≥100% increase; red, decrease

2.4.4.2.5 California bearing ratio

The CBR process provides an indirect evaluation of soil strength, resistance quality and measures the load resistance versus penetration. This is stated as a fraction of the resistance given by broken rocks. As an easy and fundamental test which is a part of the pavement design procedure to calculate the thickness of the layer is used widely in geotechnical engineering applications.

For soil mixed with SSA as a single or basic component of lime or cement the fixing sample, CBR values were identified in three different energy performances (10 strokes, 25 strokes, 55 strokes), together with a value measured at 95% of the maximum dry density. The data in Table 2.13 present that SSA in original form resulted in significant improvements in CBR values, soil is improved to "fair subgrade" and "good subgrade" in addition of 2% and 8% of SSA, respectively, based on the AHS-181 (1981) standard.

The inclusion of limestone or cement as a secondary element in the additional stabilized mixture could lead to greater soil developments. For instance, CBR values reach the "excellent sublayer" rating with an inclusion content of 8%. Of the two binders, cement is providing the highest CBR values, although the variation is becoming particularly noticeable only at additive levels of 8% and 16%.

Table 2.13 The percentage of California Bearing Ratio soil treated with sewage sludge ash (SSA) as a stabilizing component.

Reference	Additive, %	CBR per Blow			95% CBR Value	AAS-181 Category
		10 Blows	25 Blows	55 Blows		
SSA only						
	0	1.0	2.3	7.6	1.7	Poor
	2	1.9	3.8	7.1	3.5	Fair
Lin et al. (2005)	4	1.6	5.4	11.1	7.0	Fair
	8	2.1	8.1	27.1	15.6	Good
	16	2.1	10.7	24.4	14.2	Good
SSA+cement (4:1 ratio)						
	0	1.0	2.3	7.6	2.5	Poor
	2	2.8	13.5	14.9	13.0	Good
Chen and Lin (2009)	4	2.9	13.5	15.1	14.2	Good
	8	23.7	38.9	97.6	60.6	Excellent
	16	58.4	64.1	107.4	81.5	Excellent
SSA+lime (4:1 ratio)						
	0	0.8	2.2	7.5	1.6	Poor
	2	1.5	4.9	17.0	9.9	Good
Lin et al. (2007a)	4	3.1	10.3	26.0	13.6	Good
	8	11.7	25.1	38.7	32.8	Excellent
	16	8.7	25.9	35.2	45.7	Excellent

2.4.4.2.6 Shear strength

Shear strength depends on particle friction and soil bonding, and it is significant to examine them when determining bearing resistance and overall stability. A brief definition of the studies done and results from the performance of soil stabilization improved with SSA on stress-strain behavior and shear strength were given in Table 2.14. There is a current tendency in all the results, increasing the additive content of SSA, SSA-cement, or SSA-hydrated lime has increased the maximum shearing strength and decreased failure strain of soils. The stress-strain relationship after improvement with SSA represented a more brittle failure state, especially with 7.5% of SSA amounts and bigger ratios. This behavior could be result in a decrease in soil plasticity as shown in Figures 2.17 and 2.18. The effect of stabilization with SSA on stress-strain relationship was also found to be similar to the equivalent effect with coal ash.

Table 2.14 The work and results arising from the shear resistance properties of soil stabilized with sewage sludge ash

Reference	Additive	Test	Findings
SSA only			
Al Sharif and Attom (2000)	0-12.5% SSA	UCS (ASTM D2166-13)	Decreased failure strain and toughness, increased brittleness (mostly at $\geq 7.5\%$ SSA)
Lin et al. (2005)	0-16% SSA	UUU Triaxial (ASTM D2850-87) CP25, 50kN	Failure more brittle with SSA; shear strength increased, cohesion increased (32 up to 65 kPa), friction angle decreased (35 to 24°)
Lin et al. (2007c)	0-16% SSA	UUU Triaxial (ASTM D2850-87) CP25, 50kN	Failure close to brittle failure; cohesion increased, friction angle decreased; stress-strain behaviour with SSA similar to fly ash
SSA+cement			
Chen and Lin (2009)	4:1, SSA/C, 0-16%	UUU Triaxial (ASTM D2850-87) CP25, 50kN	Shear stress increased with additives; more brittle failure mode; decreased failure strain (maximum stress at 10% strain).
SSA+lime			
Lin et al. (2007a)	4:1, SSA/L, 0-16%	UUU Triaxial (ASTM D2850-87) CP25, 50kN	Higher shear strength, more brittle failure with additive; increased cohesion (up to 58.8 kPa), reduced friction angles (minimum of 30.9°)

UUU, unconsolidated undrained unsaturated; CP, confining pressure; C, cement; L, lime

Strength parameters, cohesion and angle of friction were also calculated by Mohr-Coulomb's failure envelope for undrained, unsaturated and unconsolidated test results. Cohesion was determined to increase from 32 kPa to a maximum of 65 and 59 kPa after treatment using only SSA and SSA-lime, respectively, in contents up to 16% of SSA. In contrast, the friction angle was reduced from 35 degrees to at least 24 degrees, with the same treatments, although the increase in shear strength was generally evident.

2.4.4.2.7 Swelling

The increase in soil volume is due to the increase in excess pore water pressure where it includes soil swelling and this behavior is causing a negative effect on the surrounded layers and structures. Volume variation or swelling is also affected by other parameters such as organic content, mineral types, and absorbed cation properties of soil. Figure 2.20 presents the swelling performance of SSA, SSA-lime and SSA-cement additives on the behavior of soft soil. Potential swelling tests were performed according to ASTM D1883 (1987), with changes in the volume of the treated soil.

Figure 2.20 presents that the inclusion of SSA on its own led to an immediate reduction in soil swelling and already treated with only 2% of SSA resulting in a lower risk of swelling. This is due to Ca^{2+} in SSA for the replacement of the hydrogen bonding of the clay.

SSA-cement addition also limited the behavior of soil swelling, and it should be noted that the 2% content of SSA appears to be more effective. With the inclusion of cement, C-S-H gel might have an extra restrictive impact, although it is noteworthy to emphasize that the rate of development of swelling is similar to that of only SSA mixed soils. However, the correlation associated with the final improvement of Ca-Si and Al-Si hydrates eventually resulted in a clear development in the swelling behavior of the 16% SSA-lime amount.

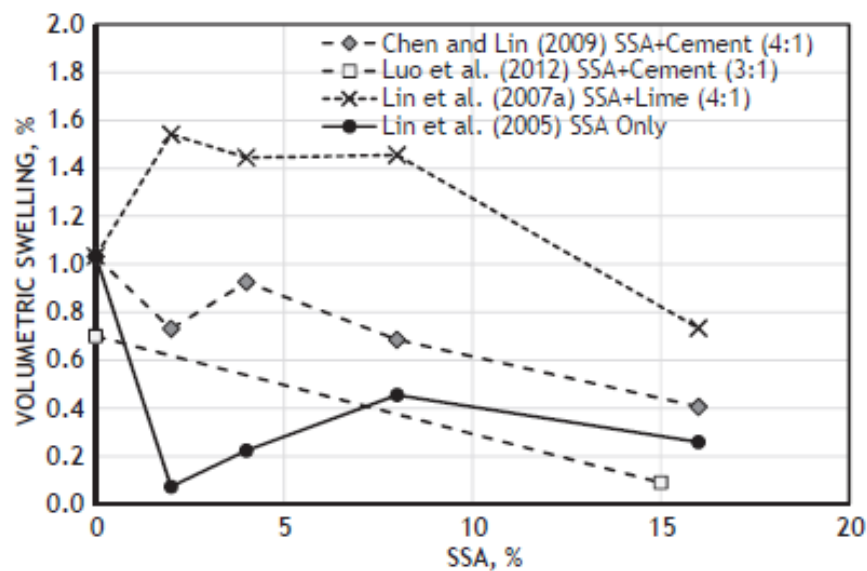


Figure 2.20 Effect of soil stability treatment with SSA on the behavior of soil swell.

2.4.4.3 Fill material

The geotechnical characteristics of SSA material and the less demanding performance needs to indicate that its usage as a filler might be encouraging. Although, known that the usage of the SSA will be in an unbound form on the ground, the environmental effects must be safely achieved at first. Unfortunately, as a result of this research, found that there are only a few research available on this application of SSA and have not found enough scientific applications for this article. The information reported is as follows:

- According to information from the 1984 report, more than 23,000 tons of SSA manufactured per year at the time in Sapporo, Japan, had been generally used for the purpose of reclamation of agricultural land (Uozumi et al., 1984).
- SSA was examined as a fill between the covering top layer and the bottom filtration layer, although the full concentration of this work was on the environmental evaluation (Kamon et al., 2001).
- The design of an experimental mix of synthetic aggregates used in plastic pipe fillings contained 20% SSA as a partial substitution of fly ash. The mixture also contained dredged materials (45%), sludge (10%) and remaining fly ash (25%). It has been found to manufacture mechanically strong and easily compactable lightweight aggregates (Newport et al., 2004).
- Several projects including applications and usage of SSA as a cover for waste landfill sites and as a fill in Branford, USA (The State of New Jersey, 2011).
- SSA was also classed as an alternative feedstock generally used in landfills in Connecticut and Massachusetts, USA (California Integrated Waste Management Board, 2009).

2.4.4.4 Environmental impact of SSA

The resulting positive environmental effects related with SSA applications in the geotechnical application process are well established in environmental engineering and engineering work in general, including reductions in potential fracture of waste, landfill taxes, preservation of natural sources and general promotion of sustainable building quality practices. Although, there has been less research conducted to consider the possible effects of the potential released heavy metals in SSA in the environment, especially around cities. The lack of clarity in this area might have contributed to the reluctance to allocate sources for the mechanical properties of SSA in geotechnical engineering applications. As briefly described in section 2.4, the stages of environmental evaluation procedures for the usage of SSA as a fill material between the top layer of soil and the bottom filtration layer were carried out in various engineering work (Kamon et al., 2001). It has been shown that by configuring the cover and filtration layer thicknesses and controlling the leakage rates, the time spend

by the components in the SSA to reach groundwater for hundreds of years can be postponed, in accordance with the assumption of the model studies (Kamon et al., 2001).

As a stabilizing soil additive, SSA is sometimes mixed with lime or cement to improve clay soil. Although not reflected in geotechnical engineering technology research, depending on the evidence in section 2 on applications of concrete, it is assumed that lime, cement and, to a lesser extent, cohesive soil materials will limit the leaching effect of heavy metals included in SSA.

2.4.4.5 Case studies in geotechnical engineering

Several case studies provided a useful soil assessment and geotechnical science of performance under real-world situation; although, these projects were usually implemented after building a strong information based on the assumed characteristics with new materials. As the improvement of SSA in geotechnical engineering applications is still new and it is in the first level, it is no wonder that case studies are limited and therefore lack of scientific sources are in this field. SSA was manufactured in Sapporo City of Japan at that time, it was used as a filler for land, roads, and reclamation of land (Uozumi et al., 1984). SSA was also been effectively used as cover material at several landfill sites in Massachusetts, Pennsylvania and Connecticut, USA (California Integrated Waste Management Board, 2009; The State of New Jersey, 2011). In addition, SSA performance was effective as an additive to soil stabilization in field tests, resulting in important developments in the stiffness and strength of the SSA treated soil (Tempest and Pando, 2013).

2.4.4.6 Conclusions

This part evaluated the effect of SSA in geotechnical engineering applications, containing the initial characterization of it, followed by its usage as soil stabilization and filling additive. SSA is composed of silt and sand sized fractures and is often well-graded. The plasticity index of SSA differs from non-plastic to a level similar to highly plastics. SSA permeability values are on the boundaries of "clean sand and sand gravel" and "very fine sands, and silts" and are assumed to present good drainage characteristics. This material has a mean specific gravity (2.60) less than normal sand and has a porous microscopic structure. Its irregular particles might inhibit the degree

of compressibility that can be achieved, although friction between particles should enhance strong shear resistance. Organic amount within an the SSA material has a mean ratio of 3.4% and is usually less than organic content within the clay material. SSA is an effective alternative material for treating soft soils when used alone or as a major component with cement or lime. Stabilization using SSA material has reduced the plasticity index values of the soil. With regard to the compaction properties, for extremely high plastic soils, SSA could result in important decreases in optimum water amount. For a clay with low degree of plasticity index, SSA-based mixes work more successfully in less content, provide higher maximum dry densities. SSA stabilization addition increases the UCS of soil, benefiting both high and low upgraded soils. The strength improvements were even more pronounced, reaching seven times bigger than the untreated soil, when simple cement or lime ratios were mixed with SSA material. The CBR values of the soft soil enhanced from the quality of "poor" subgrade to "good" through 8% of SSA addition and from "poor" to "excellent" upgraded with 8% of SSA and cement or lime. The shear strength of soil was rising with SSA additions; however, the failure state is becoming more brittle. The treated soils are showing lower swelling potential, although SSA-only and SSA-cement additives were the most effective.

Depending on previously concrete results (section 2), SSA mixing with cement, lime and to some extent with clay as part of the stabilization is expected to reduce heavy metals leaching from SSA. In a field study, decreases in settlement and developments in bearing capacity are also apparent after stabilization treatment using SSA.

For very high plasticity index values ($PI > 20$), SSA could result in important decreases in the optimum water amount (34% to 22%, with 12.5% of SSA stated by Al-Sharif and Attom, 2014).

For clays with a lower degree of plasticity index values, the effects of additives on compaction characteristics were varying, although the volume of change is less indicated. The additives tend to provide greater benefit for maximum dry densities when used in less amounts. This is probably due to the pore-filling effect of the additives. Although, the conflicting behaviors of decreasing dry density and increasing water amount were sometimes obvious, as the amount of SSA, SSA-lime and SSA-cement additions were increasing. This might be because of the low specific gravity

of SSA compared to clay and its high absorption characteristics. As a fill material, SSA were used in the previous in big amounts in Japan for reclaimed land cover. The SSA material also provided extra positive performance, as a filling material, waste landfill cover, and a partial component of the aggregate product produced for backfill of plastic pipes.

2.5 Model test studies

Many researchers used models to obtain soil properties that represent a real simulation of the field situation. In general, the studies were divided into three types. The first category was dealing with theoretical models only, using some analytical programs or solutions. Type II used real models and conducted soil tests using a different type of material for models. Another one uses vehicle models including theoretical and experimental work to get results. The review focused on practical model studies to find good information about the design of the fund, which would be useful for its design. The box is used to consider a large soil field condition in the laboratory environment. Some information that is built on the scale model box is provided in the literature as follows:

Love (1984) studied a detailed model study into constructed of laboratory devices and their construction to conduct full-scale work. Simple tests of the plane strain, monotonous systems performed consist of a compressed fill layer on a sublayer of a standard clay, with and without incorporating a typical mesh into its interface. The test technique included a comprehensive study of the images taken of the marking movements in the mud through the transparent aspects of the test box during the tests. An 18-ton hydraulic loading jack (Figure 2.21a) and a perspex sided aluminum box, (Figure 2.21b) which fitted inside the press, constituted the main pieces of equipment. The size of the sample (300mm by 1000mm in the plan, by 400 mm in depth) was such that $\frac{1}{4}$ full-scale tests could be carried out without the significant effects from boundary conditions.

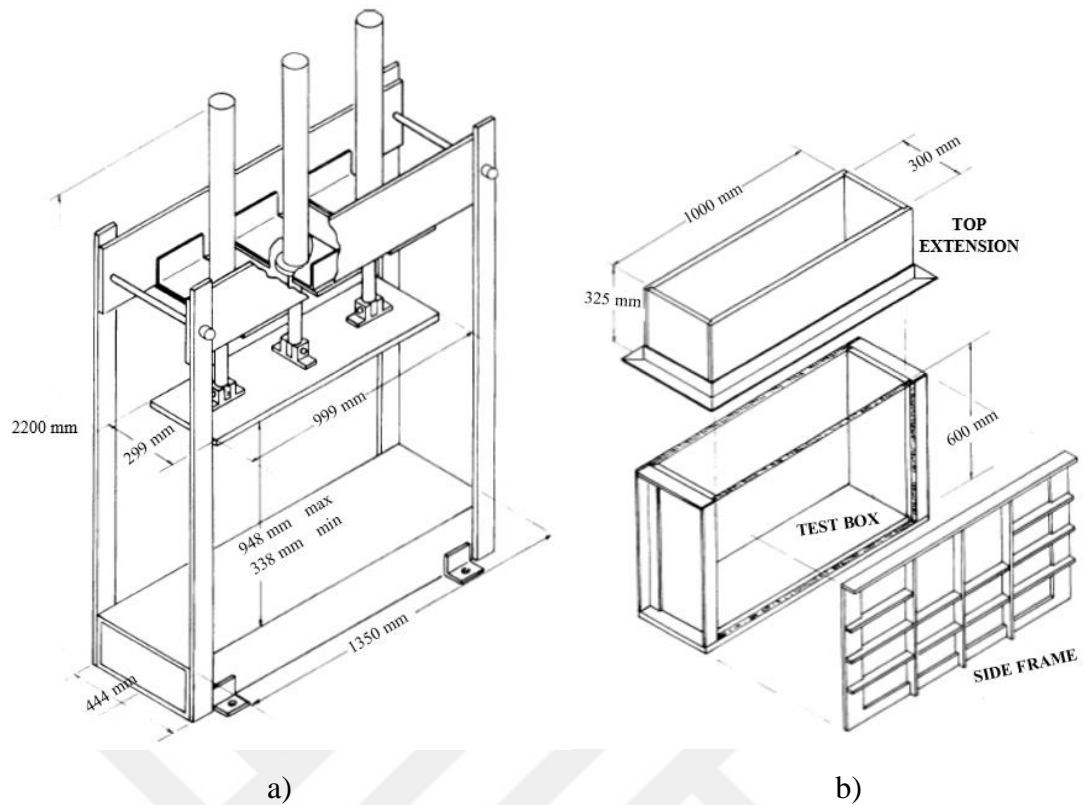


Figure 2.21 Test box, (a) load-press and consolidation plate (b) side frame and top extensions (Love, 1984)

Park et al., (2000) designed a model box which is shown in Figure 2.22 and studied the liquefaction effect of embankments on sandy soils. The shaking table tests were conducted for 12 different cases to investigate the behavior of embankments on sandy soils in the model box. The dimensions of the transparent model box were 194 cm wide, 44 cm wide and 60 cm deep. The test box was made of plexiglass.

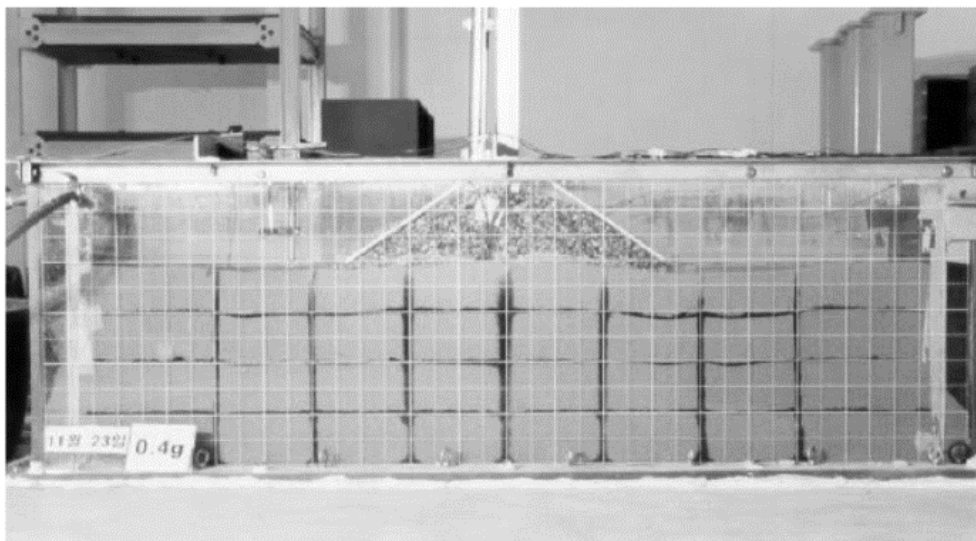


Figure 2.22 Image of the demining of the dam fund model (Park et al., 2000)

Kumar et al., (2006) investigated the effect of ultimate bearing capacity on strip footings which consist of reinforced or unreinforced strong sand layer. Three main problems were analyzed on the basis of the results achieved from the footing tests as listed: (1) the bearing capacity effect of stratified soil layer on the foundations; (2) the bearing capacity effect of geogrid reinforced horizontal top layer; (3) the settlement effect of reinforced stratified subsoil of the foundation. The model footing was made up of mild steel. Also, the footing was designed to examine strip shaped loads. The footing dimensions were 0.15 m x 1.19 m. The size of tank is configured considering the front view to be tested and the zones of influence. The inner dimensions of the tank were installed at a length of 1.8 meters, a width of 1.19 meters and a height of 1.2 meters. It is assembled by steel channels. The bottom and sides of the tank were consisting of light steel plates with a thickness of 9 mm and welded to the base frame of the angles and steel plates. Loads were applied vertically to the model footing by a hydraulic jack. A sensitive proving ring with a capacity of 50 kN were used to record the applied loads. To record the correct vertical settlement of the footing for each increase in the applied load, two dial gauges were used. Measuring dial gauges devices were installed on the beam through a magnetic base.

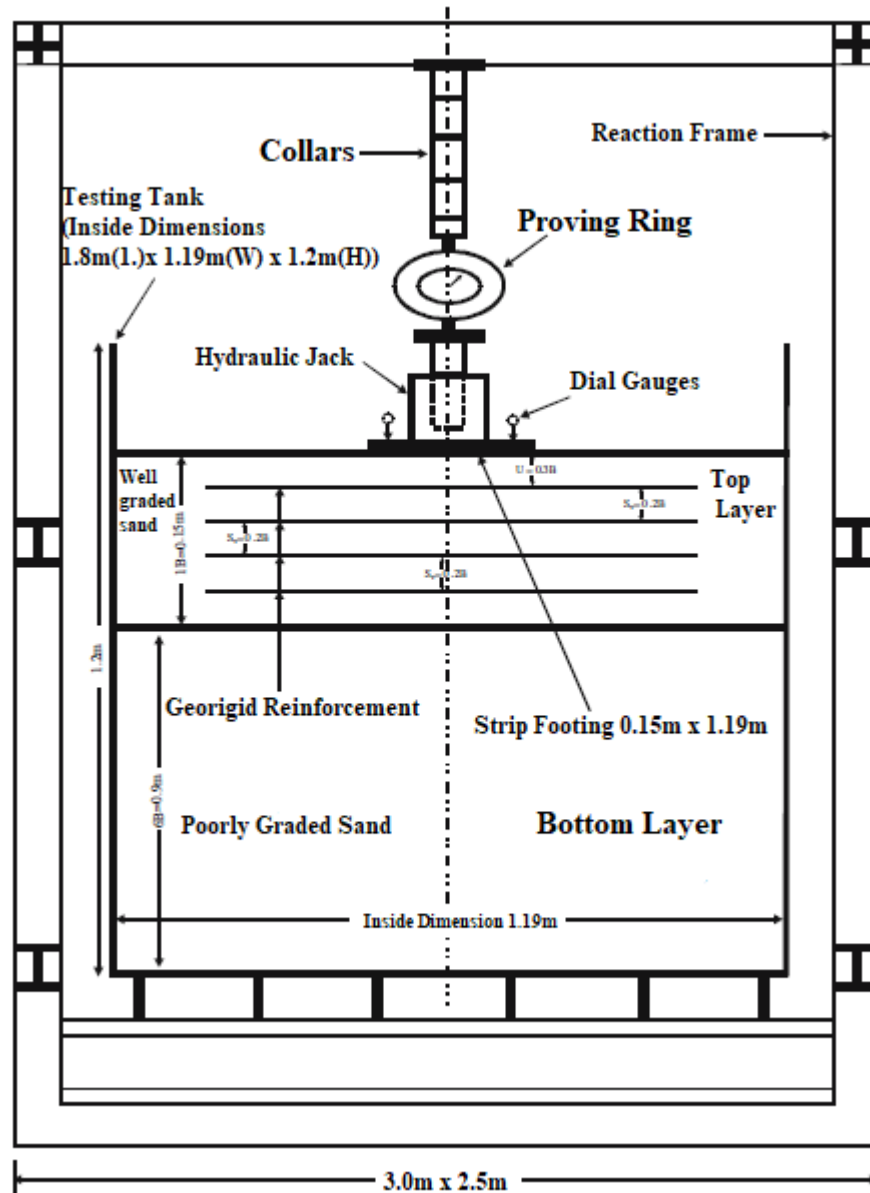


Figure 2.23 Set up preparation for tests presented footing test model (Kumar et al., 2006)

Cerato and Lutenegger (2007) performed tests on two compacted sands at three different relative densities in a circular and square model scale footing tests varied in width from 0.025 to 0.914 m. The model scale tests were conducted in three different test trenches; the initial test was carried out in a steel box 0.762 x 0.762 x 0.305 m with a concrete base as shown in Figure 2.24. Square and circular footings with widths of 0.0254, 0.0508 and 0.1016 meters were used with two sands, at three different relative densities. The winter sand and brown mortar sand were compacted by hand, little moist, at 0.0508 m lift with a steel tamper 0.152 m² to 1.44, 1.52 and 1.60 Mg/m³, $D_R=13\%$ 43% and 70%, 1.68, 1.79, 1.91 Mg/m³ $D_R=24\%$, 57% and 87%, respectively. All the tests were examined in a new test bed.

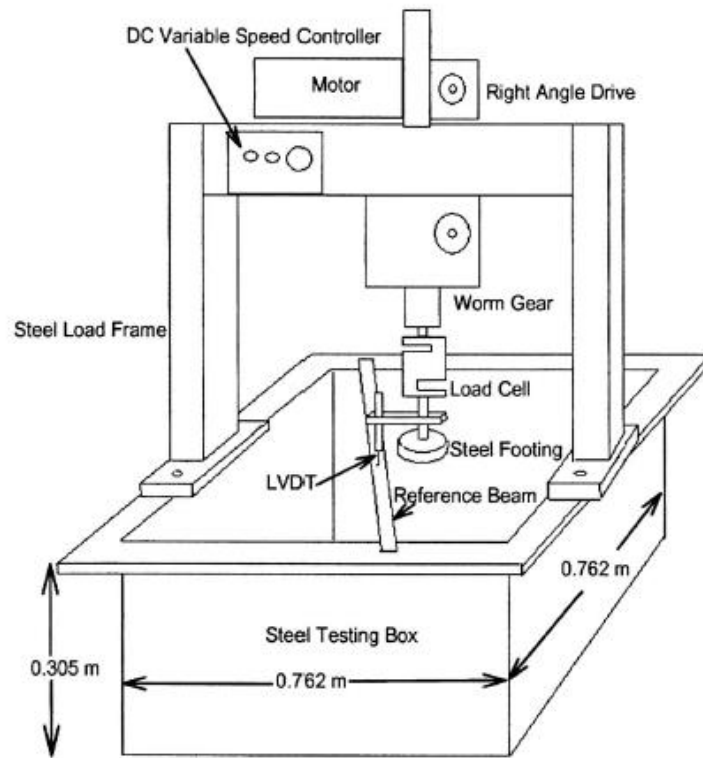


Figure 2.24 Set up preparation for tests presented footing test model (Cerato and Lutenegeger, 2007)

Thallak et al. (2007) employed a laboratory model to improve the knowledge of the behavior of geocell reinforced soft clay footings under circular loading. During this study natural silty clay was used. Geocells were made of polymer-grids. The load carrying capacity of the clay bed was increased by about 4.5 times the non-reinforced capacity. Loading tests were employed in a model footing frame. The test tank used in the probe was a square shaped model and had dimensions of 900 x 900 x 600 mm. The sidewalls of the testing tank are firmly anchored at an iron angle to prevent yielding while loading. The model footing was circular and composed of a solid steel plate. To have a rough base inside the circular model footing a thin layer of sand using epoxy was glued. A hydraulic jack supported against the frame were used in the model footing. Figure 2.25 illustrates the schematic testing diagram which was used during the investigation.

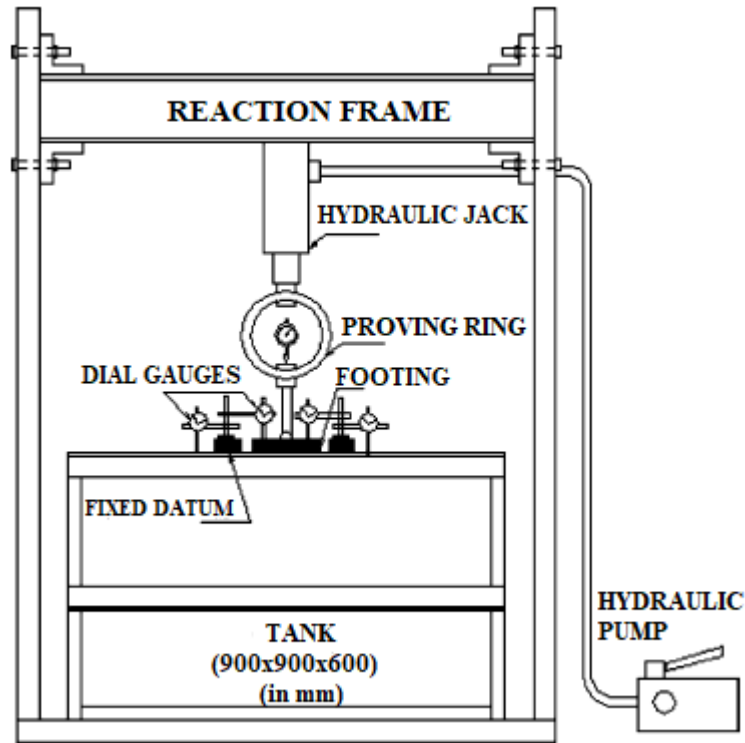


Figure 2.25 Schematic diagram of the test set up (Thallak et al., 2007)

Kumar and Bhoi (2008) studied the impact of interference of two closely spaced strip footings on the ultimate bearing capacity using dry sand and small-scale tests. The effect of spacing (s) between two footings was clearly investigated. A rectangular steel tank with a width of 2.0 m was chosen with a length of 0.37 meters and a depth of 0.65 meters. The tests were employed on a steel base with a width of 7.0 cm and a length of 36.0 cm and a thickness of 2.5 cm. The clear distance between the fixed glass panels and the edge of the footing varied between 0.5 and 60 cm; this is corresponding the value of s/B between 0.14 and 17.14. The location of the glass sheet was different to achieve different values of s/B . The horizontal distance between the edge of footing F and the boundary wall AG of the tank was always equal to 96.5 cm, which corresponds to 13.79 times the width of the footing; it is worth noting that this odd value of distance increases because the center of the footing is constantly in the similar state as the center of the testing tank. A hydraulic jack was installed between the strong horizontal reaction beam and footing base as shown in Figure 2.26 to apply vertical load.

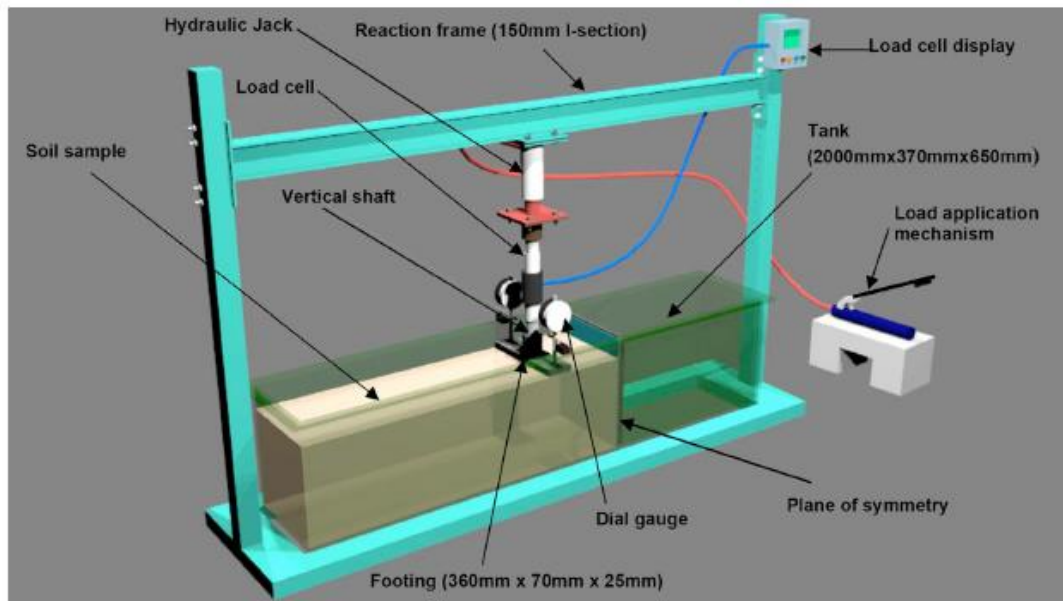


Figure 2.26 A 3D view of the selected pilot setting (Kumar and Bhoi, 2008)

Gupta and Trevid (2009) investigated the behavior of the circular model on the silty soil with cellular support. They conducted an extensive laboratory tests in a model box with a frame. Soil layers were placed in a test tank of internal dimensions (0.60 x 0.60 x 0.60 m). The tank was placed in a large box. All device dimensions are displayed in Figure 2.27.

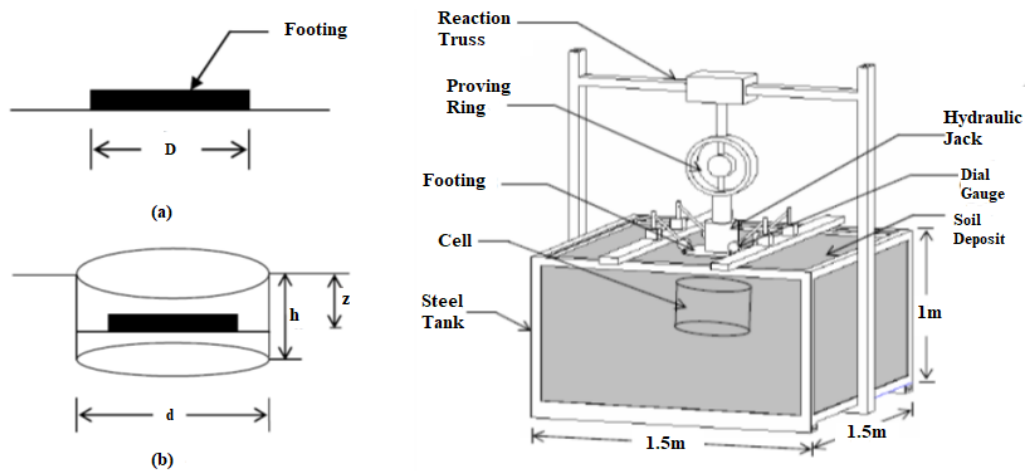


Figure 2.27 Model square foot circular (Gupta and Trivedi, 2009)

Kumar and Prasada (2009) studied the use of lime and cement to stabilize the pavement in road construction. The tests were employed on a flexible pavement model in a circular steel tank with a diameter of 60 cm as shown in Figure 2.28. The load is carried out through a 10 cm circular metal plate, which is placed on top

of the pavement layer. The steel tank was positioned on the base of a compression testing device.

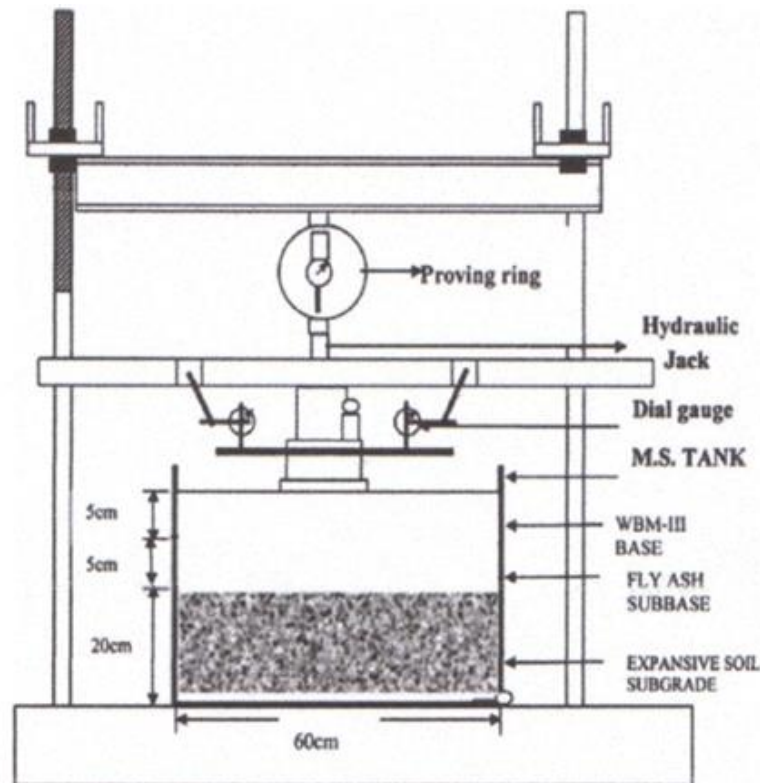


Figure 2.28 Install the pavement by lime and cement using a circular model box (Kumar and Prasada, 2009)

Nazir and Azzam (2010) improved the layer of soft clay using sand piles partially replaced with/without confinement by testing a laboratory model. This study was conducted to examine the impact of the sandpile to develop the bearing capacity and to handle the settlement behavior. Also, this study aims to examine the variation of the subgrade coefficient and the induced failure mechanism of the shallow circular footing. Figure 2.29 presents a schematic diagram of the testing device used in this research. The testing box was in the shape of a cylinder, with an inner diameter of 90 cm in the plane and a depth of 120 cm, and the thickness of the sidewalls was 6 mm. The model box was designed with sufficient rigidity to maintain the loading conditions for displacement control in all directions. The sidewalls of the box were installed from the outer surface using a horizontal beam installed in the middle of the testing tank. The interior walls of the testing tank were smoothly polished to minimize friction with the soil as far as practicable using a galvanized layer on the inner wall. The loading system made of a manually operated hydraulic jack and a precalibrated loading ring to manually employ the load to the system.

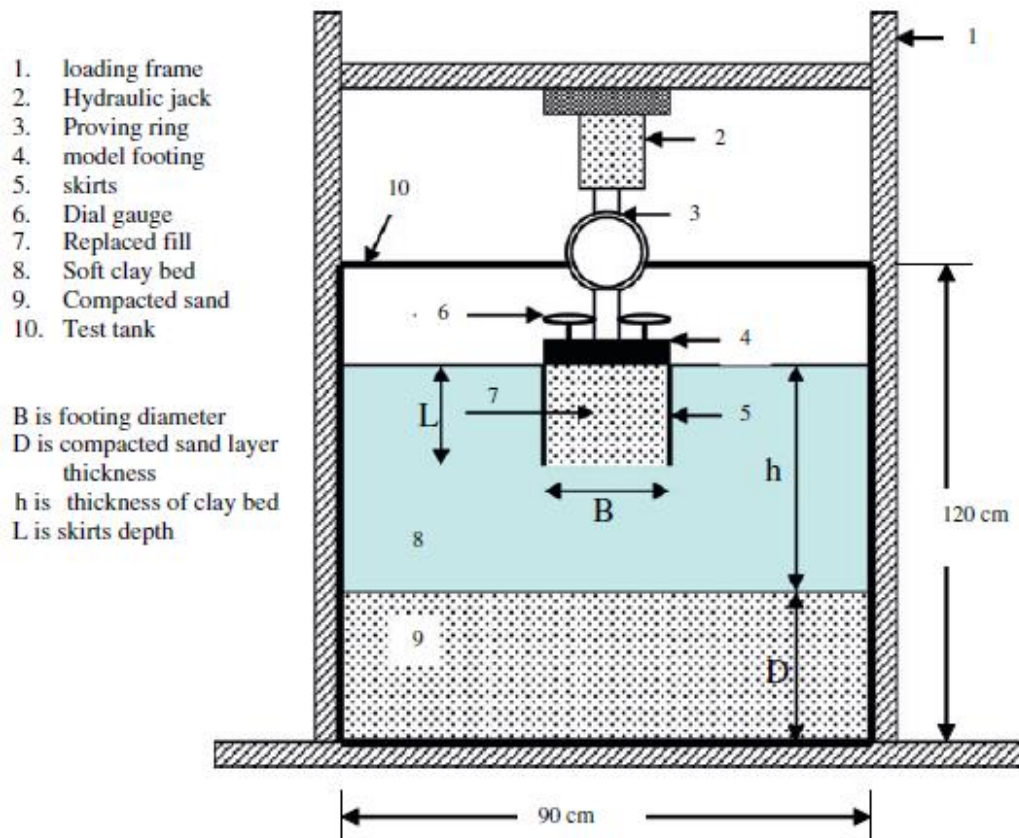


Figure 2.29 Schematic of view of the test set up (Nazir and Azzam, 2010)

Oh and Vanapalli (2013), conducted an extensive laboratory of footing model tests in statically compacted unsaturated fine grained (UFG) soil. The testing results were interpreted employing two different stress approaches: effective stress approach (ESA) and total stress approach (TSA). The accuracy of using TSA approach has been tested on plate load testing to investigate the behavior of UFG soil. The limitations, advantages, and disadvantages of the use of ESA approach and the overall stress approaches for applications of geotechnical engineering were discussed in this study. The footing model (50 x 50 mm) was tested in a high-strength cylindrical plastic tank (HSPT) (diameter 300 x 300 x 12.7 mm high) on fine granulated soil statically compacted (see Figure 2.30) The HSPT is selected since it is lighter than the steel tank and is easy to handle during the testing program. Three HSPT clips are connected to remove potential strain on HSPT while compaction of model footing tests.



Figure 2.30 Equipment set up used for conducting model footing tests (Oh and Vanapalli, 2013)

Kolay et al. (2013) published a study on geogrid reinforced silty clay and sand to improve the bearing capacity for shallow foundations. A typical testing tank with dimensions of 76.2 cm length, 30.5 cm width, and a depth of 74.9 cm were used. Steel angle sections at the bottom, top and in the middle of the tank were used to manufacture the designed test tank with vertical and horizontal stiff sides. The stiffener was to prevent any lateral yield while the applied load to the footing model, and when the soil was compacted in the tank during the experimental study. Two sides of the testing tank were consisting of 2.5 cm thick plexiglass panels; the other two sides of the tank were consisting of 1.9 cm wooden plates as a support and 1.2 cm thick plexiglass panels.

The inner sidewalls of the testing tank were smooth to minimize lateral friction as shown in Figure 2.31.

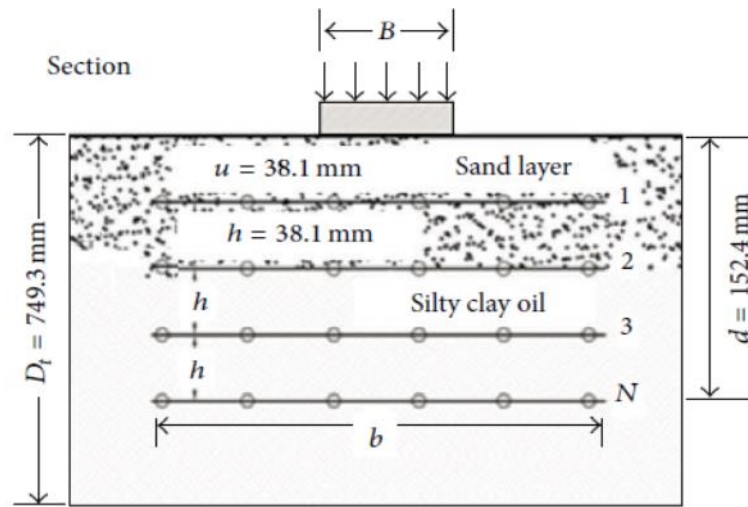


Figure 2.31 The shallow foundation model on the soil supported by the geographic network (Kolay et al., 2013)

Sanjeev et al. (2013) studied the usage of a plate loading test to predict bearing capacity of granular stratified soils. Load-settlement behavior for different sizes of plates on coarse soils was investigated in a large testing tank. The tests were examined using light steel plates of square shapes on two layers of soils; the fine-gravel layer was placed on the top of the sand layer. During this study, the influence of the thickness of the top layer on settlement and bearing capacity were investigated. The large testing tank which is shown in Figure 2.32 had internal dimensions of 2.0 m x 2.0 m as in the scheme and a depth of 1.50 meters. The tank was made of steel sheets and is directly supported by 50 mm x 50 mm steel angle sections. Iron panels and angels at the corners, bottom, and top reinforced the testing tank against the loads. The testing tank were placed on a stiff concrete base. A cross beam on the vertical sides were installed to support the loading equipment. The horizontal cross beam was laid across the middle of the testing tank. A schematic diagram of the testing system is shown in Figure 2.32.



Figure 2.32 Image of the load test of the plate on the soil with granular layers (Sanjeev et al.,2013)

Abd Elsamee (2013) studied the effect of foundation shape and depth as well as the the subgrade reaction modulus (or static spring stiffness, k_s) of cohesionless soils. A square plate load test was placed in an open box as shown in Figure 2.33. Different soil layers were used to fill the box by compaction for different densities, which were determined by the sand cone test. Nine solid steel panels were used in the tests, which were split into three sets. The first set contained three rigid circular plates. The second is like the first shape but had a square shape. Besides, the other two square plates had an equivalent area. The last set were three rigid rectangular plates having the same areas as the first set.



Figure 2.33 Effect the dimensions of the base and shape using the square model with the frame (Abd elsamee, 2013)

Wakil (2013) performed eighteen laboratory tests on a circular steel footing with different diameters and skirt lengths. These laboratory tests aimed to enlighten the impact of skirts on shallow footings. The effect of the lengths of the skirts and the relative densities of the sand on the ultimate bearing capacity were studied. The soil

box consists of two 300 mm steel rings and a diameter of 750 mm (see Figure 2.34). These rings were combined to build a soil box with a total height of 600 mm. The soil box features have been enhanced using circular steel plates and steel rings to avoid any lateral yielding of the sidewalls. Also, the vertical steel ribs were inserted to each ring and welded on the circular plates of the border of each ring. The soil box was put on a rigid steel beam for a vertical precision.

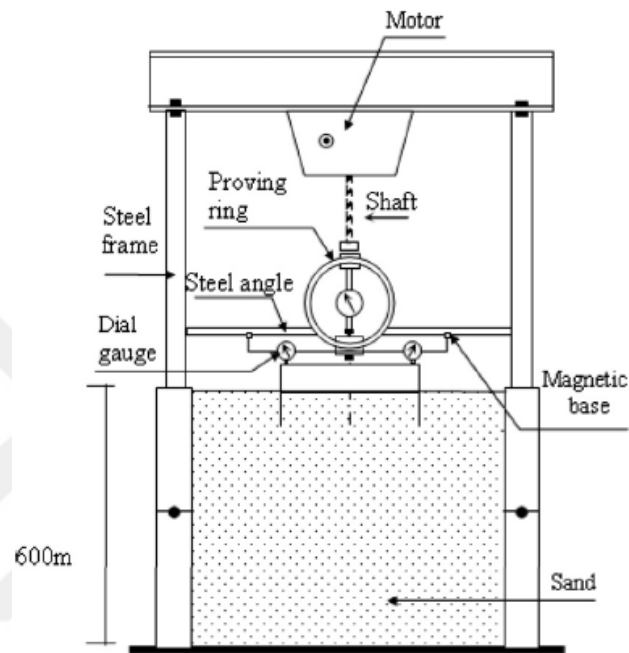


Figure 2.34 Set up of testing procedures (Wakil, 2013)

Azzam and Nasr (2014) observed the ultimate load capacities of shell foundations on the treated and untreated sand by experimental work. A series of laboratory tests were performed on the model shell footing with and without a single layer of treatment. The tests were conducted on shell foundation at various depths and soil densities. Figure 2.35a presents a schematic diagram of the laboratory model device which was used during the study. The model box, with internal measurements of 90 x 30 cm in the plane, a depth of 120 cm, and the thickness of the testing tank walls were 6 mm. The model box was designed with sufficient rigidity to maintain plane strain conditions in all directions. The sidewalls of the testing tank were installed from the outer surface and using a horizontal beam to combine them in the middle of the tank. The inner sidewalls of the tank were polished smoothly to minimize contact with the soil as far as possible using a galvanized layer in the inner wall. The loading system made of a hand operated hydraulic jack and a precalibrated loading ring to manually employ the

load to the soil footing system. The settlement is observed by the dial gauge devices installed on the footing surface.

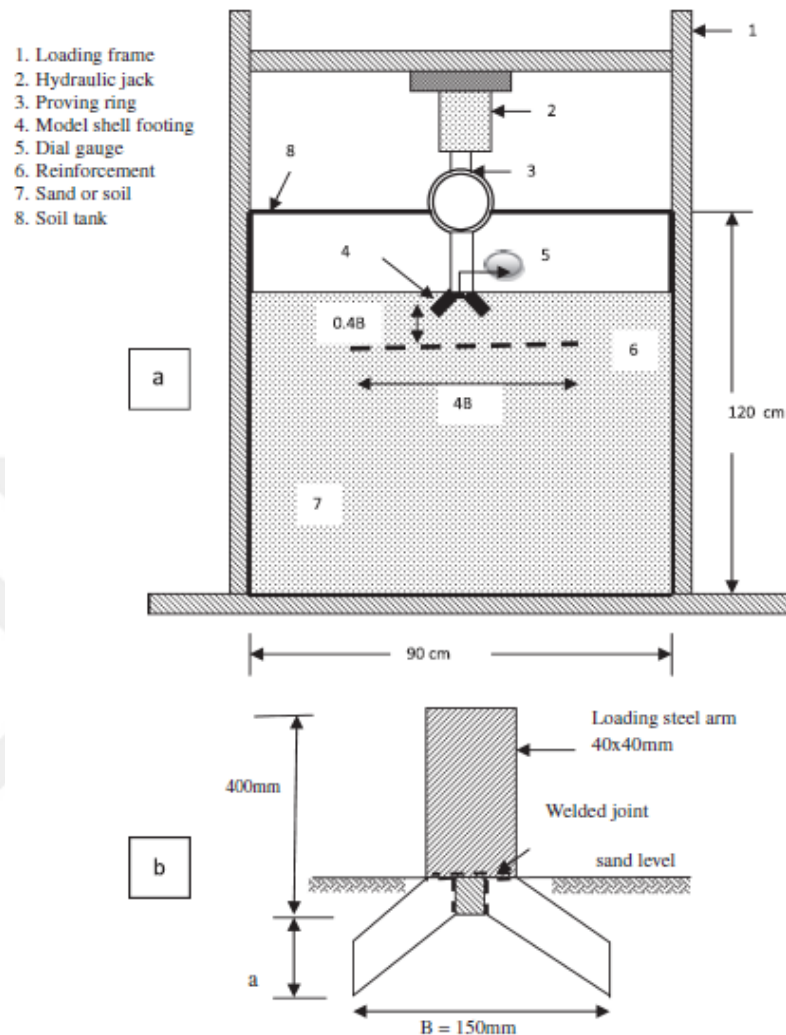


Figure 2.35 Schematic view of (a) Test preparation and (b) Shell base model (Azzam and Nasr, 2014)

Bazne et al. (2014) investigated the performance of geogrids if it could contribute to the bearing capacity of clay when used in drainage applications. To achieve that objective, a series of experimental and analytical work were carried out on different configurations to investigate the influence of geogrids on the bearing capacity of soft-grained soils. Physical models designed with four different plate shapes (rectangular, square, and two circular) and were tested through different configurations on the reinforced soil layer (i.e. length, number, depth and spacing) in the laboratory. A steel container with inner measurements of 60 cm length x 50 cm height x 50 cm width was constructed as shown in Figure 2.36. The container was made of 5 mm thick steel sheets and a 6 mm thick plexiglass front panel. In general, the container sidewalls were

configured and manufactured so that no side deformations could occur during sample preparation and loading. Figure 2.36 presents a schematic diagram of the container. As shown in Figure 2.36, a steel shaft was used to transfer the load applied to the footing. The shaft was installed on a solid steel plate that represents the base in the physical model. The base plate was solid enough to show no lateral deflection while the load is applied. One square footing (5 cm x 5 cm), one rectangular footing (10 cm x 5 cm) and two circular footings with various diameters ($B=5$ cm and $B=8$ cm) were carried out with various combinations of geogrid reinforcement layers.

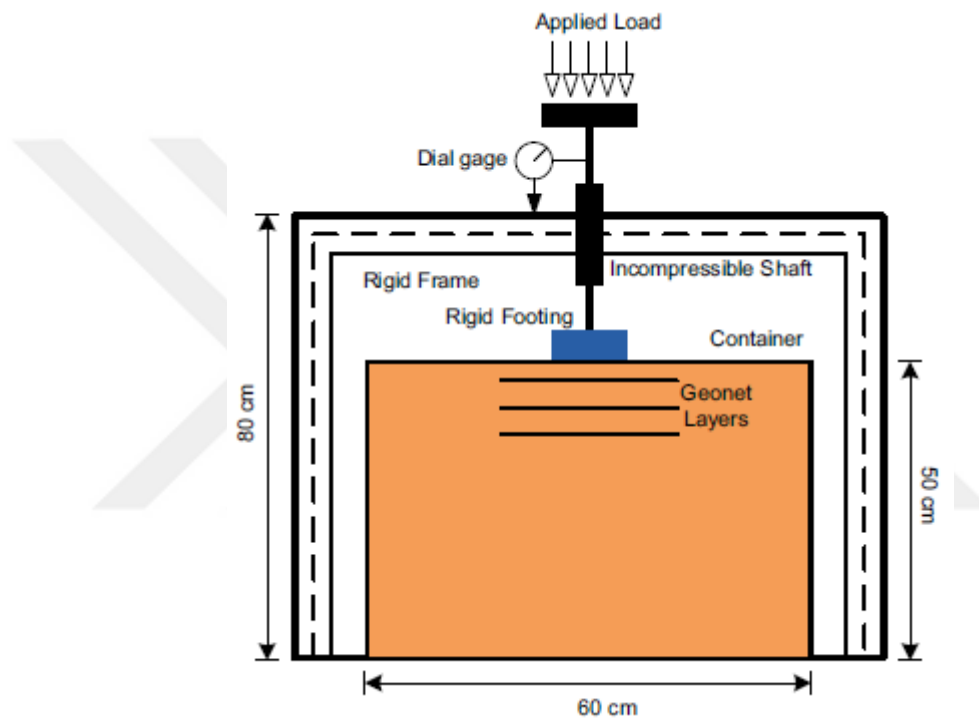


Figure 2.36 A schematic presentation of the test preparation used in the study (Bazne et al., 2014)

Elsaied et al. (2015) examined three-dimensional testing models to study the effect of soil confinement on circular footing of granular soil. Totally, 23 model footing tests were employed. Nine hollow cylinders with different diameters and heights were fixed around the model footing for soil confinement. Square shaped geogrid layers were put at various depths under the bottom edge of the cylinder. Various parameters such as diameter, length, and depth were studied. Also, the width, number, and position of geogrid layers were also examined. The model was manufactured from a steel circular footing device which were tested in a three-dimensional framed tank with inner dimensions of 1000 mm length, 1000 mm width, 600 mm depth and 200 mm diameter (see Figure 2.37). The height and width of the tank were chosen three and five times

the footing width, respectively. The testing tank was configured to reduce the boundary effect on the footing settlement behaviour.

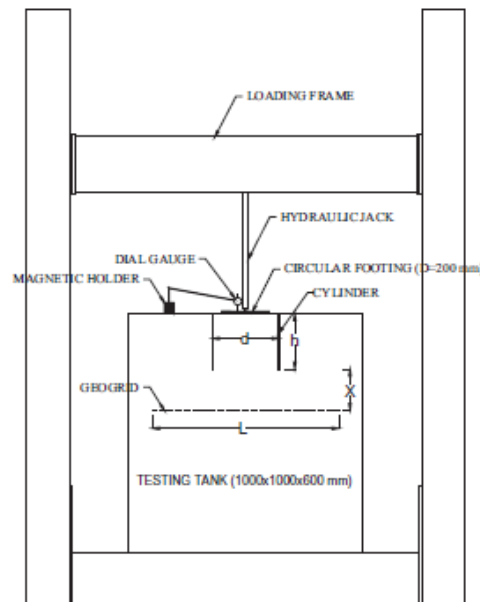


Figure 2.37 (a) Schematic view of the set-up, (b) photographic view of the set-up (Elsaied et al., 2015)

Ramadan and Hussien (2015) performed a series of experiments on strain by using finite element method (FEM) simulations of these tests in PLAXIS software. The 3-D tunnel was designed to observe the behaviour and failure mode of sand overlying clay under a vertical load. Experimental and numerical results were compared and reported to ensure that the study of such a FEM model would solve such geotechnical applications. The testing apparatus of the experimental system was displayed in Figure 2.38. The figure shows a rigid steel frame (1) and a steel tank (2), 1.0 x 1.0 x 1.0 m which were employed as a soil testing tank.

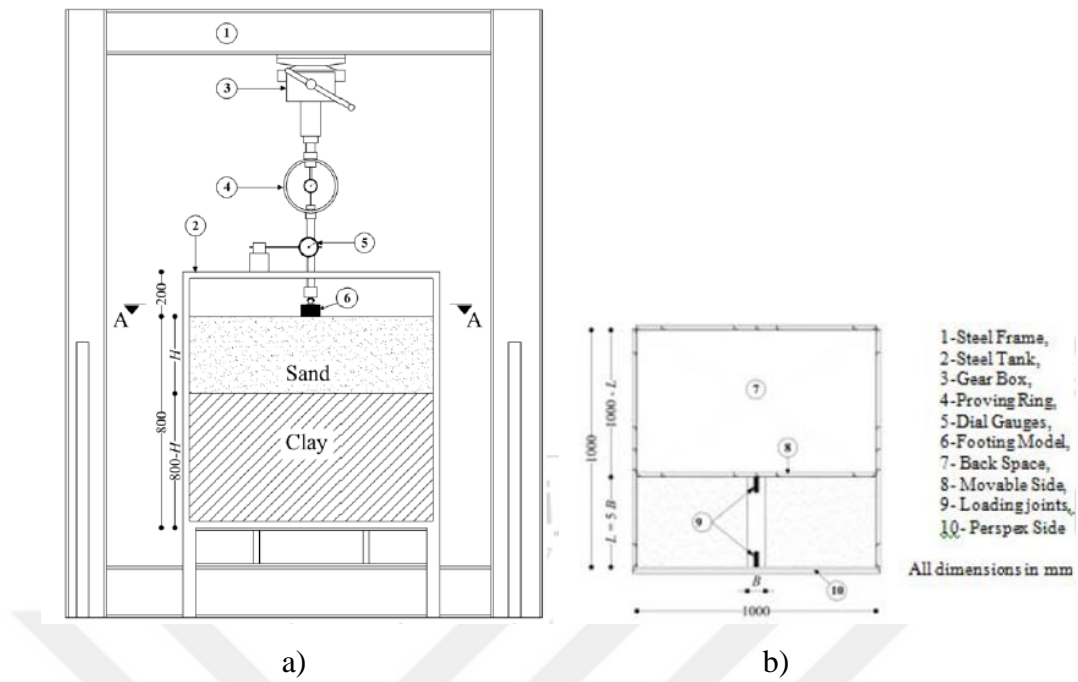


Figure 2.38 Test Setup: (a) Elevation, (b) Section A-A (Ramadan and Hussien, 2015)

Hegde and Sitharam (2015) carried out a laboratory study to explore the possibility of using natural bamboo to increase the bearing capacity of a soft soil. To extract the effect of additional confinement on the soil, three-dimensional bamboo cells, locally available, known as bamboo cells, were formed. The performance of bamboo cells was compared with commercial geo cells. Furthermore, the planar reinforcement of bamboo grid was compared with the clay layer improved by a combined geocell and geogrid mix. The model load tests were performed in the laboratory on a clay layer. The testing tank had dimensions of 900 mm length, 900 mm width, 600 mm height. The plate used in that study was square with 150 mm sides and a thickness of 20 mm (see Figure 2.39).

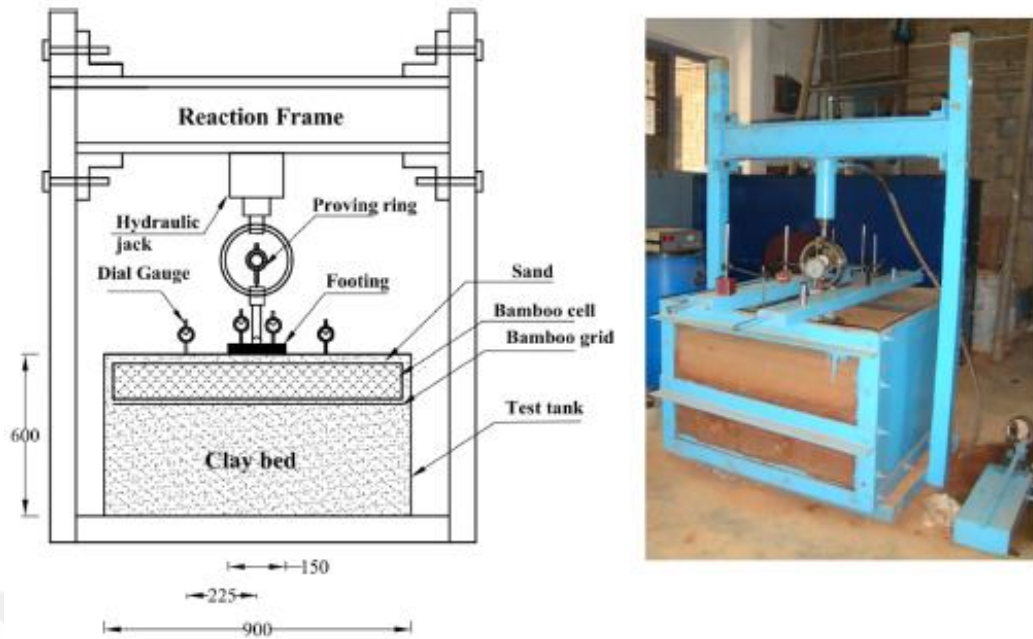


Figure 2.39 Test the setup tool (a) the schematic display; (b) photograph (Hegde and Sitharam, 2015)

Sadoglu (2015) studied the load settlement behavior of strip footings numerically and experimentally. The ultimate load on treated and untreated sand for plane strain conditions were determined. The sand was compacted in a testing tank with a relative density of 0.74 to achieve the shear failure point. The numeric model of the testing setup was performed using a Plaxis 2D software. As a soil reinforcement woven geotextile was used. The basic components of the experimental setup included a tank, a strip footing, a loading system, geotextile, sand and so on (see Figure 2.40). These primary components were explained below on the schematic view. The interior dimensions of the reservoir containing the sand were 0.9 m length x 0.10 m width x 0.65 m height (Figure 2.40). The bottom and sides of the tank were produced using stiff wood. The front and back faces are made of 20 mm plexiglass panels to see the failure surface. Two steel frames made of hollow sections were produced and joined together by steel bolts along the sides of the frame.

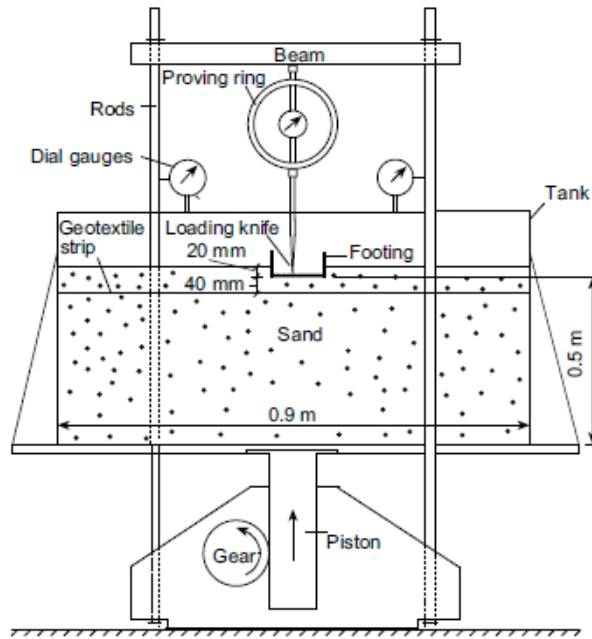


Figure 2.40 Schematic view of the experimental set up (Sadoglu, 2015)

Tafreshi et al. (2016) performed an extensive laboratory study on circular footings supported by reinforcing the sand with geosynthetic materials. These materials were investigated by multiple layers of the geocell and the footing performance was compared to one on the same sandy soil containing a multi-layer geotextile strengthening. The comparison contained geocell and geotextile layer of the same geosynthetic material with the same properties. Figure 2.41 illustrates the schematic diagram of the physical test preparation and its components, which include the testing tank, the loading system, and the measurement system. The testing tank was a rigid box with dimensions of 1000 mm x 1000 mm and a depth of 1000 mm. The backwall and sidewalls of the tank consist of 20 mm medium density fiberboard (MDF) sheets. The front face of the testing tank consisted of 20 mm thick plexiglass. This plexiglass allowed to observe and measure the surface plane strains. The hardware system was enhanced to show both the loading and the settlement results automatically. A S shaped load cell with a precision of 70% and with a full scale capacity of 20 kN was installed between the loading shaft and the footing system to evaluate the implemented load sensitively.

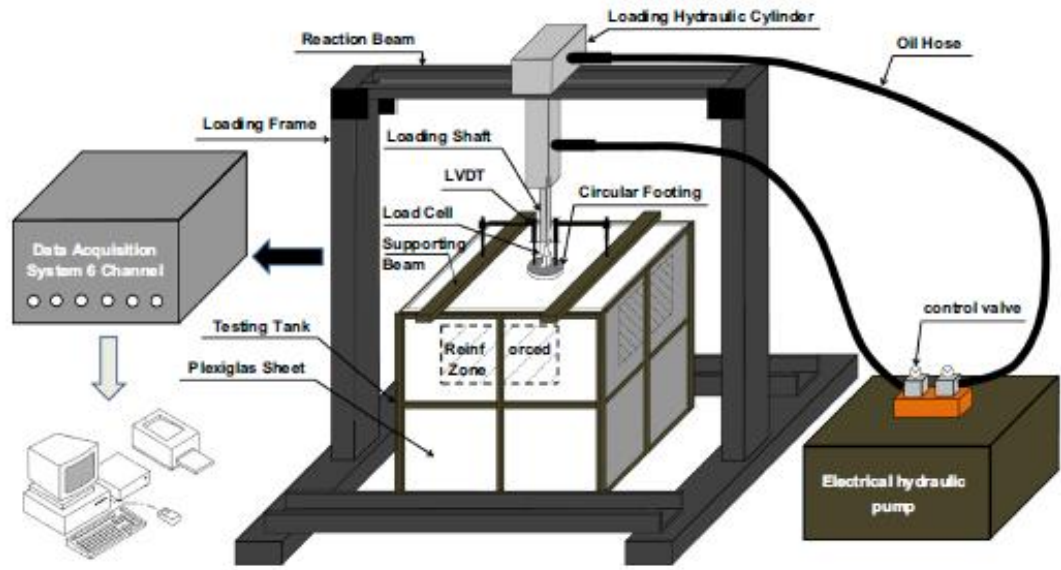


Figure 2.41 Schematic representation of test preparation and trench planning (Tafreshi et al., 2016)

CHAPTER 3

MATERIALS AND EXPERIMENTAL TECHNIQUES

The materials that have been used during this research were clay and SSA. Samples were prepared by mixing clay and SSA in different proportions of SSA by dry weight, with SSA content ranging from 0- 30%. This chapter is including the details of a comprehensive laboratory study to investigate the effect of various ratios (0%, 5%, 10%, 15%, 20%, and 30%) of SSA on engineering properties of clay. Also, this chapter presents the characteristics of the clay and SSA used during this study. As a first stage of the experiments, different samples of clean clay with SSA mixtures were prepared in the laboratory and the index properties of them were defined by relevant experiments. The chapter also describes the procedures and details of sample preparation techniques of tests that were carried out. Also, a basic design, construction, and characterization of a large-scale circular model footing set-up and steel reaction frame were illustrated for the field tests. Scanning Electron Microscope (SEM), X-Ray Fluorescence (XRF) and Energy Dispersive X-ray (EDX) analyses of clay and SSA were presented.

3.1 Material properties

3.1.1 Clay

The type of the soil used in all tests of this study was a low plasticity clay (CL) obtained from the Gaziantep University campus, Turkey. The gradation of clay was fixed between the 4.75-0.075 mm and prepared by sieving it through standard sieves. The grain size distribution of this soil was determined according to ASTM D422. The grain size distribution curve is presented in Figure 3.1. The plastic limit and liquid limit values were 13 and 27, respectively (ASTM D4318).

The specific gravity of the clay was found to be 2.70. Scanning Electron Microscope (SEM) photo and Energy Dispersive X-ray (EDX) analyses of the clay has been shown in Figure 3.2a and Figure 3.2b. X-Ray Fluorescence (XRF) analysis of clay has been given in Table 3.1.

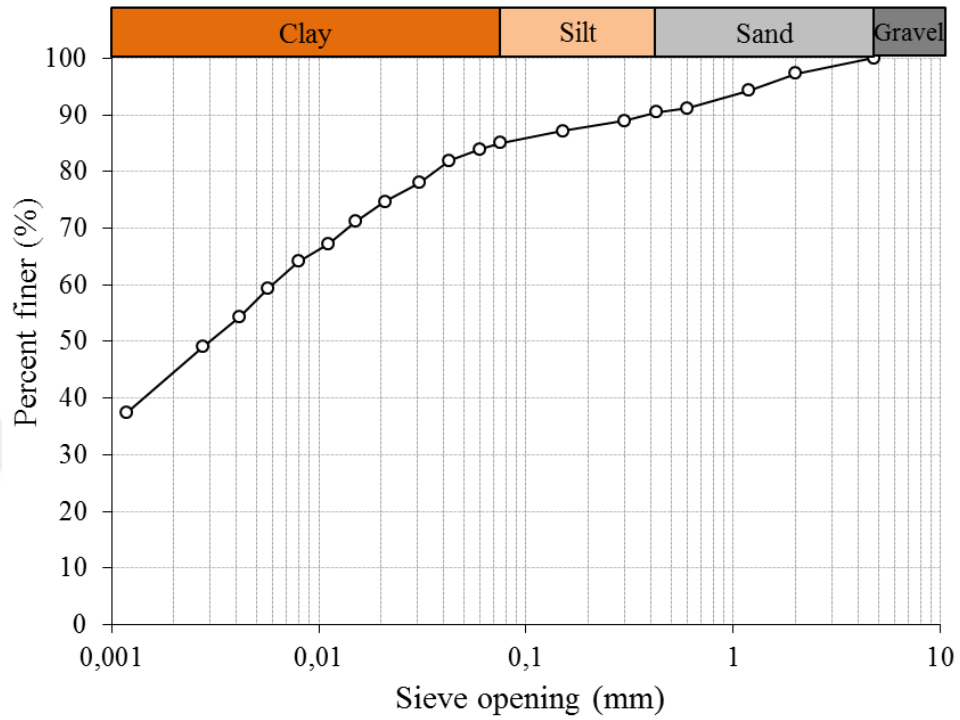
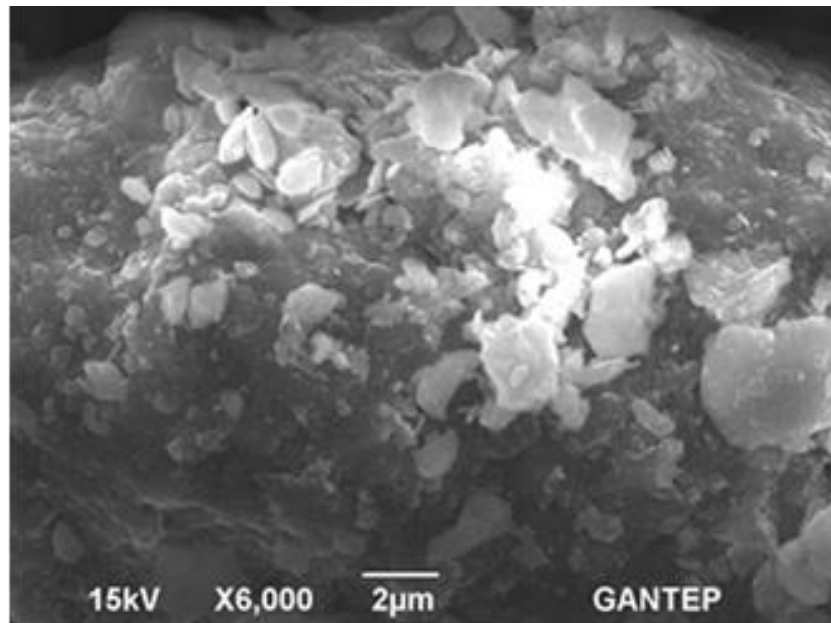
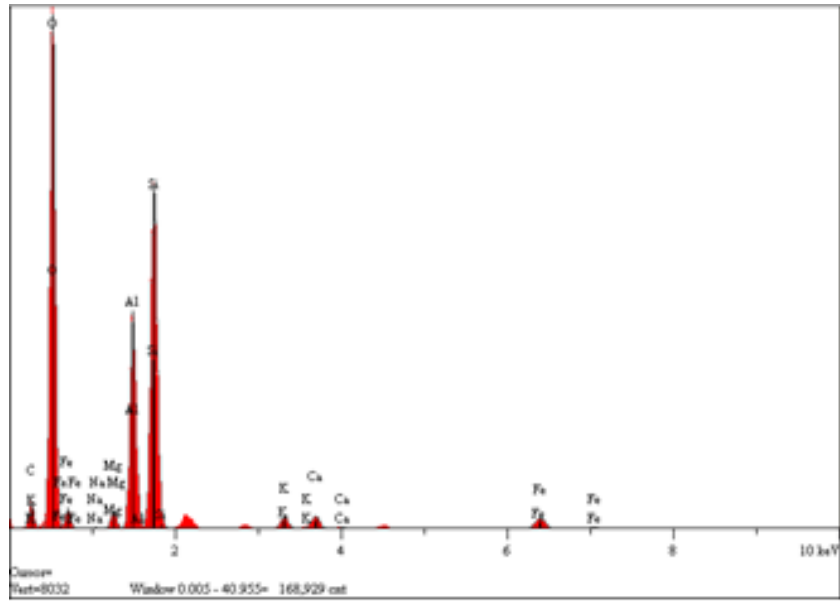


Figure 3.1 Grain size distribution curve of the soil used in this study.



(a)



(b)

Figure 3.2 (a) Scanning Electron Microscope and (b) Energy Dispersive X-Ray analysis of clay.

Table 3.1 X-Ray Fluorescence (XRF) analysis of clay.

XRF Parameters	Clay
SiO ₂	32,83
Al ₂ O ₃	11,91
Fe ₂ O ₃	6,55
CaO	20,92
MgO	1,22
SO ₃	0,17
K ₂ O	1,36
Na ₂ O	0,00
TiO ₂	0,81
P ₂ O ₅	0,39
Mn ₂ O ₃	0,16
LOI	22,44
LSF	18,98
SM	1,78
AM	1,82
Specific Gravity	2,70

3.1.2 Sewage sludge ash

The ash used in this study was collected from Gaziantep water and sewerage administration (GASKI) burning wastewater treatment facility. The specific gravity of this ash was found to be 2.65. The grain size distribution of SSA was determined according to ASTM D422 and is shown in Figure 3.3. The SEM photo and EDX analyses of SSA have been shown in Figure 3.4a and Figure 3.4b. Also, the XRF analysis of SSA has been given in Table 3.2.

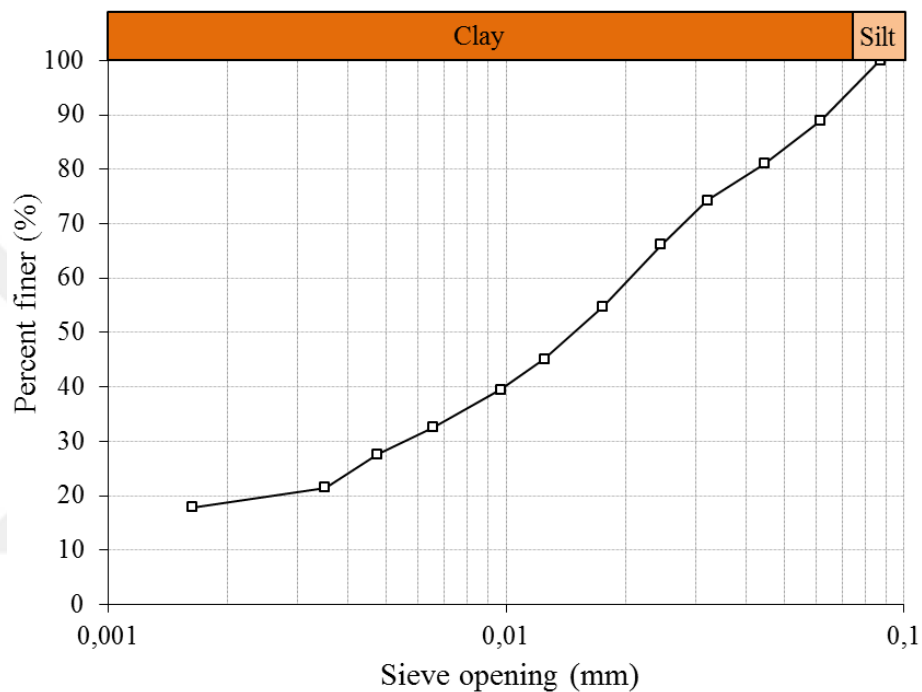
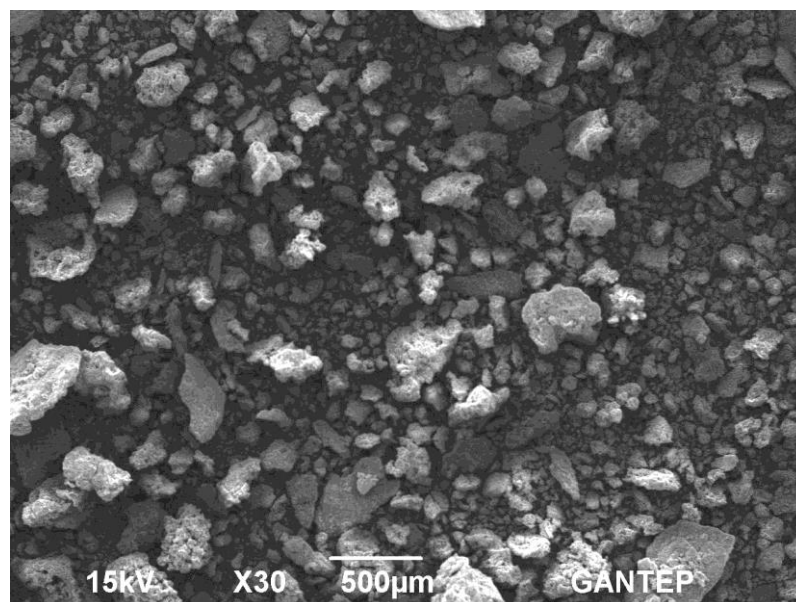
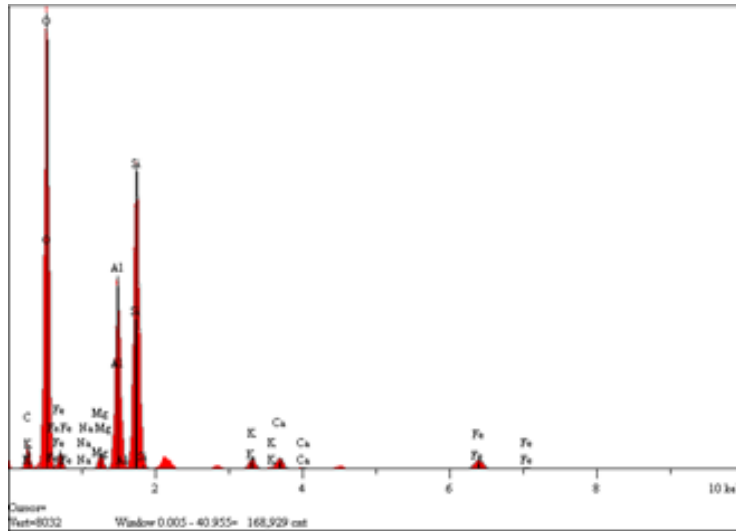


Figure 3.3 Grain size distribution curve of SSA used in this study.



(a)



(b)

Figure 3.4 (a) Scanning Electron Microscope and (b) Energy Dispersive X-Ray analysis of sewage sludge ash.

Table 3.2 X-Ray Fluorescence (XRF) analyses of sewage sludge ash.

XRF Parameters	SSA
SiO ₂	25,01
Al ₂ O ₃	8,21
Fe ₂ O ₃	6,63
CaO	33,95
MgO	2,85
SO ₃	7,24
K ₂ O	1,01
Na ₂ O	0,26
TiO ₂	0,84
P ₂ O ₅	7,36
Mn ₂ O ₃	0,15
LOI	6,17
LSF	40,40
SM	1,69
AM	1,24
Specific Gravity	2,65

The GASKI treatment plant was built in 1990 as a sewerage system for Gaziantep. The project is planned in two phases to reach the wastewater treatment capacity of a population for 2.5 million in 2022. The plant is in operation since 1999 and currently can operate 230 tons of wastewater per day. The plant that generates this ash used in the study is treating about 91.000 m³/day of municipal wastewater (Gaziantep Metropolitan Municipality, 2011).

Thermal processing reduces the overall mass of sludge to 85 %. The volume is also reduced to 90 %, thermal processing destroys toxic organic components, minimizes unpleasant odors and facilitates further management, and there is also the possibility of power generation (Tantawy et al., 2012).

Since 2008, a total of 5.272,000 kWh of electricity has been generated in the Cogeneration Unit used to meet the power needs of the plant. As a result of the sludge incineration process, ash is produced as a by-product at the end. SSA was obtained from the exit outlet of the furnace and was preserved in a dry state (see Figure 3.6e). This process results in approximately 9.342,4 tons of incinerated SSA per year (see Table 3.3 and Table 3.4) (Gaziantep Metropolitan Municipality, 2011).



(a)



(b)



(c)



(d)



(e)

Figure 3.5 Photo of (a) Gaziantep Wastewater Treatment Plant, (b) Digester tanks in the plant, (c) Digestion plant of the sludge, (d) dried/dewatered sludge and (e) ash occurred after the incineration process of dewatered sludge (Directorate of GASKI, 2018)

Table 3. 3 Sewage sludge statistics per day (Directorate of GASKI, 2018)

Sewage Sludge Statistics of GASKI (December 2017)			
Days	Amount of digested sludge (m ³ /day)	Density of digested sludge (g/l)	Amount of dewatered sludge (m ³ /day)
1	1.672	38,3	245
2	1.667	38,8	240
3	1.680	38,4	254
4	1.700	37,2	251
5	1.760	36	256
6	1.612	37,7	228
7	1.782	38,2	271
8	1.687	37,4	262
9	1.465	38,1	182
10	1.575	37,3	218
11	1.856	38	261
12	1.723	37	261
13	1.798	38,1	258
14	1.654	37,9	258
15	1.702	37,2	252
16	1.687	37	237
17	1.690	37,8	221
18	1.655	37,2	250
19	1.657	37,6	231
20	1.609	36,9	246
21	1.766	37,2	261
22	1.783	37,5	243
23	1.767	38,1	263
24	1.789	37,1	242
25	1.631	37,9	215
26	1.583	38	200
27	1.678	37	225
28	1.723	38,5	207
29	1.601	39,2	227
30	1.698	37,1	245
31	1.587	36,5	217
Total	48.898		7.427

Table 3.4 Incinerated sewage sludge ash statistics per month (Directorate of GASKI, 2018)

Dewatered Sludge and Ash Statistics of 2017				
Month	Amount of dewatered sludge (m ³ /month)	Incineration	Amount of produced sewage sludge ash (ton/month)	
January	6.360			732,7
February	6.020			693,5
March	6.540			753,4
April	6.630			763,8
May	6.600			760,3
June	6.570			756,9
July	6.960			801,8
August	7.020			808,7
September	7.110			819,1
October	6.900			794,9
November	6.960			801,8
December	7.427			855,6
Total	81.097		9.342,40	

After the incineration process, approximately 9.342,4 tons of ash was produced. The average production of SSA is about 25 tons per day (Directorate of GASKI, 2018).

3.1.2.1 General characterization of SSA

The general chemical and physical characteristics of SSA can widely vary due to the concern with difficulty in the texture of treated wastewater as well as the type of incineration system and chemicals used during wastewater treatment (Gray and Penessis, 1972). Donatello et al. (2010) and Cyr et al. (2007) reported that silicon (Si), iron (Fe), aluminum (Al), calcium (Ca) and phosphorus (P) were the major elements present in the SSA materials they investigated, other elements reported as being present included potassium (K), sodium (Na), magnesium (Mg), and sulfur (S) (Lin and Weng, 2001). The presence of P in SSA is mainly due to the removal of soluble P from wastewater during the wastewater treatment process. The most crucial metal phases found in SSA are silicon oxide (SiO₂), calcium phosphate (Ca₃(PO₄)₂), iron oxide (Fe₂O₃), calcite (CaCO₃), anhydrite (CaSO₄) and a significant amount of amorphous phases (Cheeseman et al., 2003).

Table 3.5 Chemical characterization of GASKI sewage sludge ash.

Sample	Compounds											
	SiO ₂	Al ₂ O ₃	Fe ₂ O ₃	CaO	MgO	SO ₃	K ₂ O	Na ₂ O	TiO ₂	P ₂ O ₅	Mn ₂ O ₃	LOI
SSA	32,83	11,91	6,55	20,92	1,22	0,17	1,36	0,00	0,81	0,39	0,16	22,44

3.2 Evaluation of index properties

The first tests are aimed a complete experimental index investigation program. This program included relevant tests to assess the distribution of grain size, hydrometer test, specific gravity, Atterberg limits (liquid and plastic limit), for the used clay, SSA and various combinations of clay-SSA mixtures.

3.2.1 Particle size analysis

Particle size analysis determines the gradient (particle distribution, by size) with the scope of the compliance assessment of the verification specification. Gradient data can be used to determine soil properties. The grain size characteristics were determined following the method ASTM D422. Sieve analysis was performed on the clay between 4.75-0.075 mm while the hydrometer test has been conducted on the clay passing 0.075 mm (#200). The grain size distribution curves of clay and SSA are shown in Figure 3.1 and Figure 3.3.

3.2.2 Specific gravity

The specific weight of solid substance is the ratio of the weight of a given volume of material to an equal volume of water. In geotechnical engineering, the determination of the specific gravity of the soil is necessary to calculate the soil's voids and for the determination of the distribution of grain size in the hydrometer analysis. For many geological and waste materials, the specific gravity has values in range between 2.65 to 2.75 (Blight, 2010).

Clay and SSA specific gravities were determined in the same manner as ASTM D854 (see Figure 3.7). It should be noted that the specific gravity of the clay-SSA mixtures were calculated for the consistency of each soil in the entire mixtures. Table 3.6 shows the specific gravity of clay, SSA, and clay-SSA mixtures used during the experimental program.

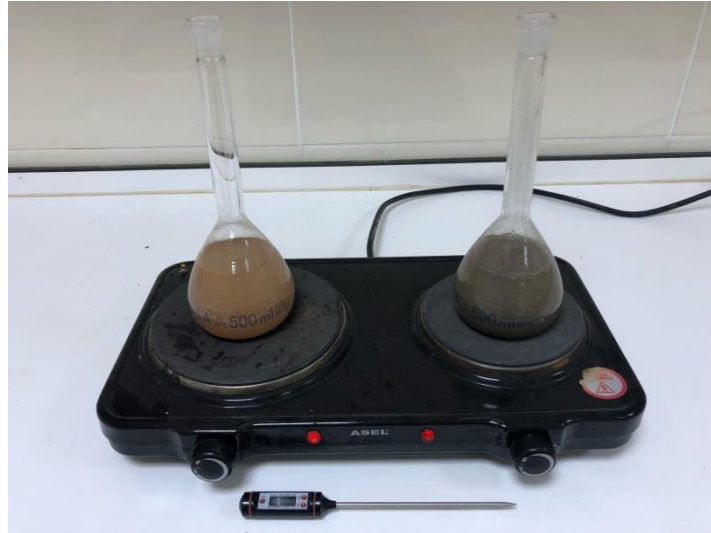


Figure 3.6 Specific gravity test for clay (left) and sewage sludge ash (right side)

3.2.3 Hydrometer test

Precipitation analysis (fluid weight scale, pipette, buoyancy analysis) is known as the grain distribution curve for soil that can not be tested by sieving. Sediment analysis computes soil particles by size using the physical deposition process, a process described in the Stokes law (Stokes, 1891). The grain size is calculated from the sedimentation distance of the soil particles. The percentage by weight is determined by measuring the weight of the soil suspension unit. This method also separates micro-soil particles so that the end of this experiment can produce the full-grain size distribution curve. From this curve, many vital aspects of the soil can be identified, and a general classification of the soil can be made. This test was conducted according to ASTM D7928-17 that deals with standard test methods for particles- size analysis of soils. The hydrometer's used during the tests are shown on Figure 3.8. All the appropriate corrections, such as dispersion agent correction, hydrometer reading correction, temperature correction, and hygroscopic correction, have been done. The diameter of soil particles was calculated according to stoker's law (ASTM D7928-17).



Figure 3.7 Hydrometer testing equipments' (left) and hydrometer testing on clay and sewage sludge ash (right)

3.2.4 Atterberg limits test

The liquid limit, plastic limit, and plasticity index were determined both for clay and SSA samples using Casagrande and Rolling method. The amount of clay-SSA mixtures to be worked with was chosen from 0 – 30% of the SSA by dry weight. The percentage was varied at an interval of 5%. All the Atterberg limit tests were carried out following ASTM D4318. Based on the results that were obtained from particle size analysis and Atterberg limit tests, the samples of the soils were classified using unified soil classification system (USCS). Casagrande and rolling method testing photos on clay and SSA are shown in Figure 3.9.



Figure 3.8 Photos of Casagrande and rolling spaghetti test methods.

3.3.1. Compaction test

The laboratory test described here was performed to measure the maximum weight of the dry unit (MDD) (γ_{drymax}) and the optimum moisture content (OMC) (w_{opt}) of different clay-SSA mixtures that were subjected to standard compaction effort. According to the results, these laboratory experiments are also useful in determining the quality of the relationship between the compaction water content and the dry unit weight of the clay-SSA mixtures tested. The effect of SSA on clay with various ratios (0, 5, 10, 15, 20, and 30%) was investigated to obtain MDD and OMC. The standard Proctor test was performed according to ASTM D 698-12 standards. Following this test, the soil was compacted in a 102 mm (4 inches) mold in five equal layers with each layer receiving 25 blows of a 44.5 N (10.0 lbf) height of 457 mm (18 inches). The total pressure energy applied during the standard Proctor compaction test is 594 kJ/m³. Figure 3.11 is a photograph of the laboratory equipment required for the standard Proctor test.



Figure 3.10 Photo of standard Proctor testing equipment's.

3.3.2. Vane shear test

SSA with a percent of 0%, 5%, 10%, 15%, 20% and, 30%, by total weight of clay-SSA materials were prepared during these tests. For each mixture, five various ratios of the water content have been added and mixed. After that, the prepared samples were tied in a plastic bag to prevent the loss of the water content. In the beginning, the samples were cured for 24 hours to get homogenous mixtures. However, due to chemical reactions between the water and high SSA contents, the curing time has been changed to 1 hour for high (>15%) SSA mix ratios. The higher the SSA ratio is, the

more the water loss is. Due to this fact, for the SSA ratio higher than 15%, the curing time was 1 hour. After the curing period, the samples were mixed again within the plastic bag, and then the samples were poured on the table. After this, the samples were divided into three equal parts and placed part by part in the specimen cup. After placing these three parts of the specimen into the cup, the surface of the specimen was made smooth and clean. The laboratory vane shear test was carried out according to the ASTM D 4648-00 standards. With the steps as following for each clay-SSA mixture:

- Connect the rotary shear unit as well as the sample container so that the table or frame does not move during the experimental study.
- Insert the vane in the sample at a minimum depth equal to double the blade height. To ensure that the top of the vane blade is embedded at least, there is one vane blade below the sample surface.
- By rotating the hand knob device, be sure that the graduated reading is at zero points on the secondary scale. After that, take an initial reading.
- Hold the sample tightly to prevent rotation
- Start mechanical rotation of the feather to rotate the top of the spring or transformer at a steady rate of 10 revolutions per minute by the hand knob.
- Pulse deflection readings or torque converter shall be recorded at least every 6 degrees of rotation until the spring deflection stops the increase (which is a failure) or even obtains a maximum of 180 degrees of rotation.
- During vane rotation, hold the blade of the vane at a constant height.
- Record maximum and medium torque readings.
- Remove and clean the vane blade
- Take a small sample of the specimens and put it in the oven to get them dry weight and evaporated water content to determine the moisture content.

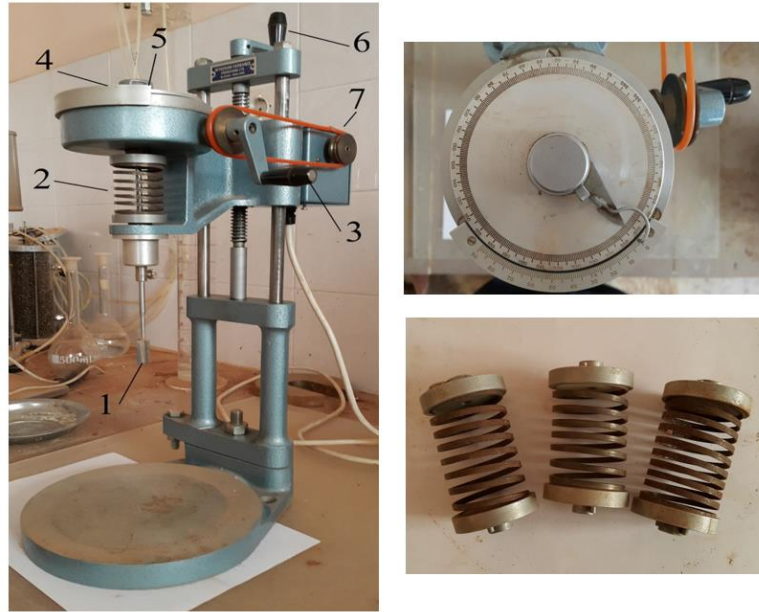


Figure 3.11 Laboratory vane shear device; 1-Vane, 2-Spring, 3-Rotating hand knob, 4-Graded scale, 5-Secondary scale, 6-Raising hand knob, 7-Motorize unit.

3.3.3 Fall cone test

A cone, manufactured by UTEST with a 30° cone and weighing 0.785 N, was used during the experimental studies. The equipment has a specimen cup of 40 mm in height and 55 mm in diameter. Specimens at different mix ratios (0, 5, 10, 15, 20, and 30%) were prepared on dry weight basis by using the clay and SSA mixtures dried in an oven for 24 hours and at 105°C temperature. The appropriate quantities of clay-SSA mixtures were determined, and then mixed in dry condition until the specimens are noted to be uniform. The specimen was mixed with a certain amount of water and left for curing over 24 hours to allow entire water diffusion. The arranged specimen was pushed gently into the cup in three layers using a knife. The excess soil on top of the cup was levelled-off using a ruler. Finally, the specimen was gathered on the equipment with tip of the cone just touching the top. The penetration was found at the end of a five second. Several trials were carried out to control the repeatability of the testing results. At the end of the test, water content in the specimens were identified.



Figure 3.12 Photo of fall cone testing apparatus.

3.3.4 Oedometer test

The one-dimensional consolidation testing equipment in Figure 3.15; a conventional laboratory testing method was used to show the compressive properties of clay and clay-SSA mixtures to estimate its effect on settlement properties. A sample of undisturbed soil with a height of 20 mm and a diameter of 50 mm in a welded steel ring immersed in a water bath. It is subjected to compressive stress by applying a vertical load, which is supposed to operate uniformly on the soil sample area. Two-way drainage is allowed through the porous disks at the top and bottom as described in Figure 3.15a and Figure 3.15b.



Figure 3.13 Photo of oedometer cell components and testing apparatus.

Within-laboratory work, vertical compression of the soil sample was recorded using highly sensitive dial gauges. Initially, 100% of the vertical load was taken by pore water due to the reduced permeability of the studied soil sample. The result was that

pore water was unable to flow from the blanks rapidly. Therefore, there is very little compression to the soil sample immediately after vertical loading. Soil can only be compressed when effective pressure is increased. For each increase in stress, the final settlement of the soil sample, as well as time, was recorded to reach the final settlement. Loading and unloading endpoints were used to plot a standard stress-void ratio curve. The tests were completed as described in the ASTM 2435 standard.

During this experimental study, the compressibility characteristics of clay-SSA mixtures were conducted in different relative densities (loose and dense state), by the oedometer test. The loose state samples have been prepared in the laboratory by pouring the clay-SSA mixtures slowly in the consolidation cell. Various ratios (0, 5, 10, 15, 20, and 30%) of clay-SSA mixtures were prepared in this manner. The dense state samples have been obtained from the circular model footing. The samples were obtained by the consolidation ring, as shown in the figure and tied in a polythene bag to protect the moisture content. Dense samples obtained from the circular footing included 0, 10, 20, and 30% ratios of SSA by total dry weight.

3.3.5. Hydraulic conductivity test

Permeability is a measure of the ease with which water can flow through soil volume. It is one of the most critical geotechnical features. However, it is probably the most challenging parameter to determine. Moreover, it controls soil strength and deformation. In this study, the permeability test was carried out on clay-SSA mixtures by using the falling head permeability test. Testing samples were prepared in two methods. Falling head permeability samples were prepared at optimum water content and maximum dry density according to the results of the standard compaction test. The coefficient of hydraulic conductivity has been obtained following the procedure described in Head (1994) and BS 1377 (part 6). Furthermore, to compare the results of falling head permeability test, samples from the circular footing have also been taken. Figure 3.16 shows the sampling of falling head permeability test from the circular footing model. Samples have been taken both before and after the plate load test, to compare the hydraulic conductivity parameter before and after loading.



Figure 3.14 Photo of falling head specimens, manometer stand, and water bath.

3.3.6 Unconfined compressive strength test

During this experimental study, UTEST unconfined compressive strength testing equipment was used to determine the stress-strain behavior of clay-SSA mixtures according to ASTM 2166 standards. The unconfined compression strength tests were conducted on clay-SSA mixtures at various ratios (0, 5, 10, 15, 20 and 30%) of SSA using a special rammer and mold system. The molds were obtained from a 2.0 meter long and 5.0 cm diameter tube that had been cut into 10 cm lengths. A rammer system that had been developed by Cabalar (2013) was used during this experimental study (see Figure 3.17). The samples were compacted in the molds by this special rammer which was designed for this purpose and calibrated with the standard compaction test effort. Therefore, to attain the standard compaction effort, the number of blows was

calculated, and each layer was compacted with 31 blows. After the compaction process, the test samples were removed from the split molds and tied in a polythene bag for four different curing periods (4, 8, 16, 32 days) to allow the distribution of moisture.



Figure 3.15 Photo of rammer system components; steel plate, mold, and hammer (Cabalar, 2013)

3.3.6.1 Testing procedure of unconfined compression strength test

- The first step in the procedure is to check the download window. Determine the calibration constant for the proving ring and the units of the deformation dial gauge.
- The strain rate for shearing the samples was 1% per minute. It is crucial that the soil sample is not cut faster than this rate.
- The initial height and diameter of the soil sample should be measured. The sample is unlikely to be a perfectly suitable cylinder. Therefore, it will be necessary to find the average height and diameter by taking several measurements in different places with the soil sample.
- The weight of the soil sample and the total weight of the unit (wet)
- Place the soil sample in the loading frame, seat the proving ring, and zero the dials.
- During this experimental study, the load must be applied at specified strain values. Readings were taken at strains of 0, 0.1, 0.2, 0.5, 1.0, 2.0, 3.0, 4, 5.0,

6.0, 8.0, 10, 12, 14, 16, 18 and 20%. The vertical deformation dial readings at these strain values were recorded.

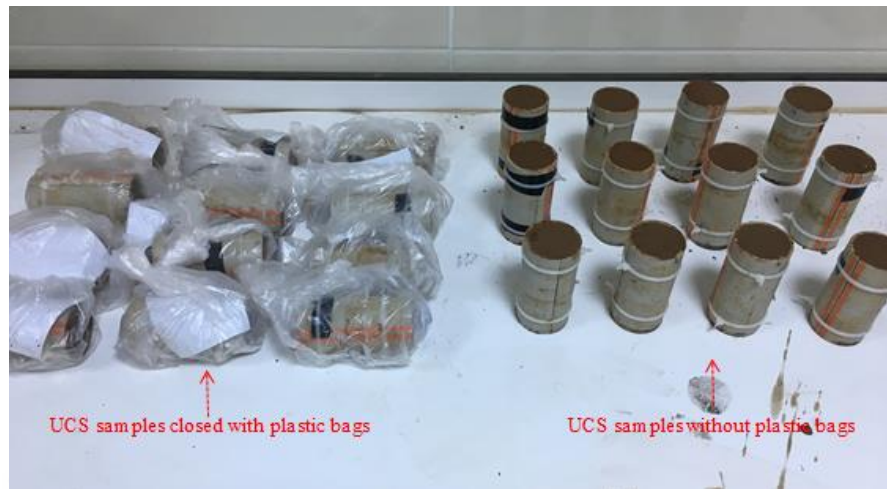


Figure 3.16 Photo of UCS specimens.



Figure 3.17 Unconfined compression strength testing machine.

3.3.7 California bearing ratio test

In this study, ELE CBR testing type of equipment, which is shown in Figure 3.20 and Figure 3.21, were used to determine the behavior of the stress and penetration of the clay-SSA mixtures according to ASTM 1883 standard. The CBR samples were prepared at MDD and OMC. Laboratory investigations have been carried out on 56 clay-SSA samples. The samples have been divided into two groups as soaked and unsoaked CBR samples. All the CBR samples have been conducted for different curing (4, 8, 16 and 32 days) periods, due to emphasis on the effect of moisture content on the CBR value of the soil samples.



Figure 3.18 CBR testing equipment.



Figure 3.19 Photo of CBR mold, compaction hammer, and surcharge load accessories.

3.5 Model set-up tests

3.5.1 Sample preparation

3.5.2 Plate load test

The experimental program consisted of carrying out five series of tests in the circular model footing to study the effect of SSA on bearing capacity and settlement of clay-SSA mixtures. A steel reaction frame assembly have been used during the tests. (Figure 3.25b) The samples were prepared inside this circular footing with dimensions of 2.0 m diameter and 1.5 m depth. The clay-SSA mixtures were compacted in the footing according to the OMC and MDD results which were obtained by standard proctor test. The model footing was constructed as a reinforced concrete wall with 0.4 m thickness. The footing was loaded with a hydraulic jack supported against the reaction frame. A steel company designed the reaction frame with a 0.5 m height a 2.0 length. It was designed to react against 40 tons. The steel company combined 2U channel profiles and constructed a I profile reaction frame. (see Figure 3.26)



Figure 3.26 Photos of circular model footing and steel reaction frame.

Before the mixture compacted into the circular model footing, the surface was set up, and the pressure cells were installed down into the soil deposits at the desired locations. The geometry of the circular model footing and pressure cells are shown in Figure 3.27.

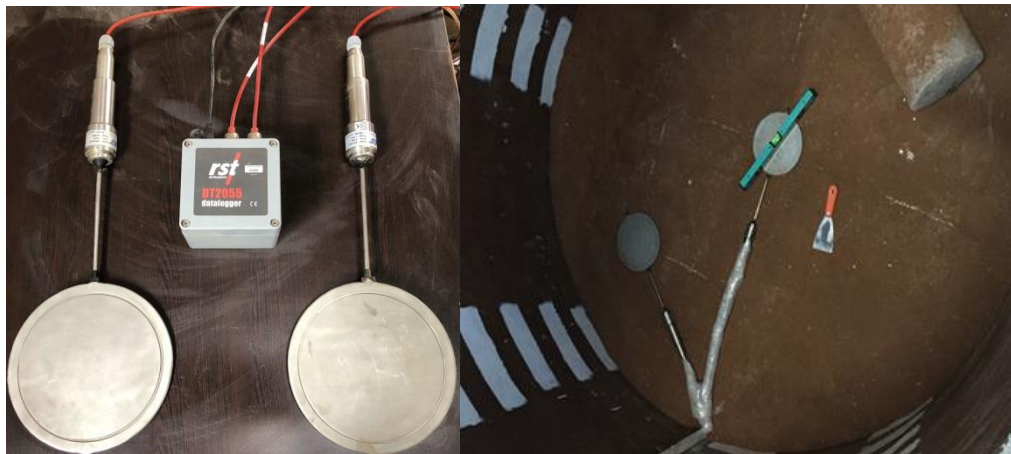


Figure 3.27 Photos of (a) pressure cells and (b) installation into the soil deposit

The experiments were performed with a 30 cm diameter circular plate, and the plate was placed in the middle position of the steel reaction frame as shown in Figure 3.28, and the load was applied in increments by a hydraulic jack. Each load increment was maintained according to the ASTM D1195 standards. The tests are completed and either the stress reaches 1,000 kPa or the soil collapses. The failure or collapse of the

soil is the point where deformations reach and pass 2.5 cm in the stress-deformation graph. In all the plate loading experiments conducted, all samples were initially loaded to 1,000 kPa or collapse of the soil and then unloaded to make comparisons. For each stress level, it was kept waiting at each level until deformations stopped. As a result of this loading and unloading behavior, plate loading unloading figures, and the permanent deformations that occur on the surface were evaluated and compared.



Figure 3.28 Photo of 30 cm diameter steel plate that used during the plate load test

The settlement of the plate was measured using three equilateral angle dial gauges placed on sides of the plate. The entire assembly, including the hydraulic jack, proving ring, and the plate was aligned with the help of plumb bob to attain the verticality.

3.5.2 Field California bearing ratio test

Both laboratory and field CBR tests have been examined during this thesis. The field CBR test was conducted in the model circular footing, according to ASTM D4429 as seen in Figure 3.29. The large-scale samples were tested at the optimum moisture content, which was obtained from the laboratory compaction test. Bearing property of the clay-SSA mixtures were determined in the circular footing set up during the field CBR test. The field CBR tests were conducted before and after the plate load test. The first field CBR tests were conducted immediately after filling the circular model footing. So the second tests of field CBR were performed with a cure time reaching up to 4 days. Field CBR values have been obtained in three different locations on the compacted soil surface inside the model circular footing. The figure shows the

locations where the field CBR tests were carried out. This study also discussed the relationship between laboratory and field CBR values.



Figure 3.29 Photos of field CBR during and after the test

CHAPTER 4

RESULTS AND DISCUSSION

This chapter describes the interpretation, analysis, and discussion of the physical properties of test results that attained from the inside laboratory and field-testing program. Also, it presents the effects of SSA on compaction, index properties, consolidation, permeability, strength and bearing capacity on the laboratory and field test results. The following procedures discussed about the test results of clay-SSA mixtures.

4.1 Compaction testing results

The compaction test was performed on clay and clay-SSA mixtures at different percentages from 0% to 30% by the weight of the mixture. In this study, the compaction curves for each percent were determined according to ASTM D698. The compaction curves obtained at laboratory test results as shown in Figure 4.1. In addition, the peak point of each curves represented the optimum moisture content (OMC) and maximum dry density (MDD) of clay ad clay-SSA mixtures as shown in Table 4.1. It is explained by increase percentage of SSA the compaction characteristics of clay was changed. Figure 4.2 and Figure 4.3 explains the variation of OMC and MDD with SSA contents, respectively. The results indicated that the MDD of clay and SSA mix decreased from 17.3 kN/m³ to 11.2 kN/m³ as the percentage of SSA increases up to 30%. It is due to increase in the percentage of voids (high water absorption) and due to the specific gravity of SSA is smaller than of clay soil particles. Furthermore, decrease in the MDD due to replacement of more solids with respect to interaction between clay and SSA particles. Ingunza et al., (2014) indicated decreasing values for all SSA additive levels up to 30%, all the tested samples were at 5% intervals. On the other hand, the OMC increased from 18.0 to 32.6 when the percentage of SSA increased from 0% to 30% as shown in Table 4.1. The increment in OMC is due to replacement of clay by SSA particles that increased the intake more moisture than clay.

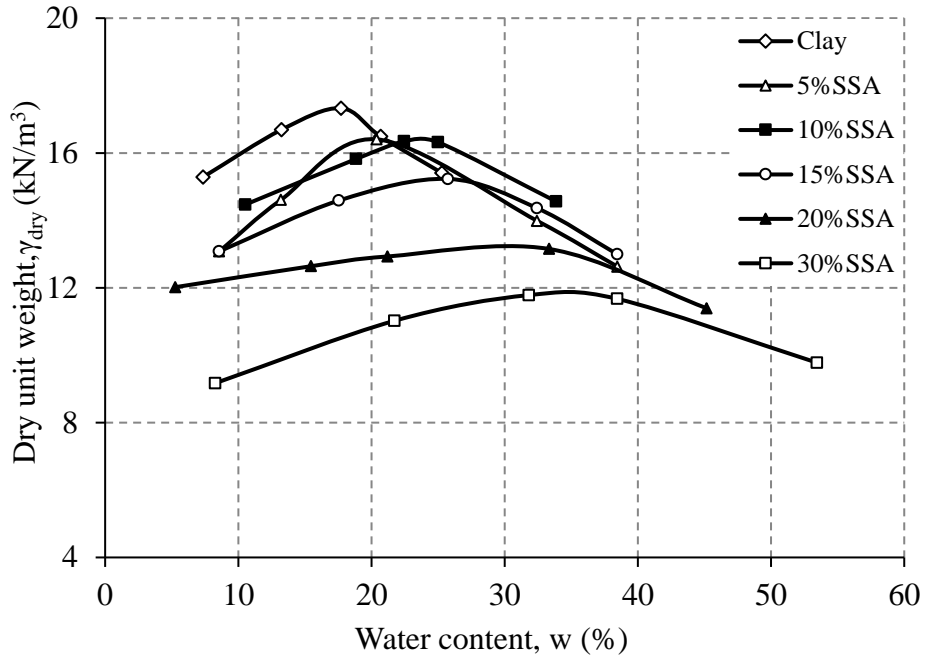


Figure 4.1 Plot of standard Proctor results for clay-SSA mixtures.

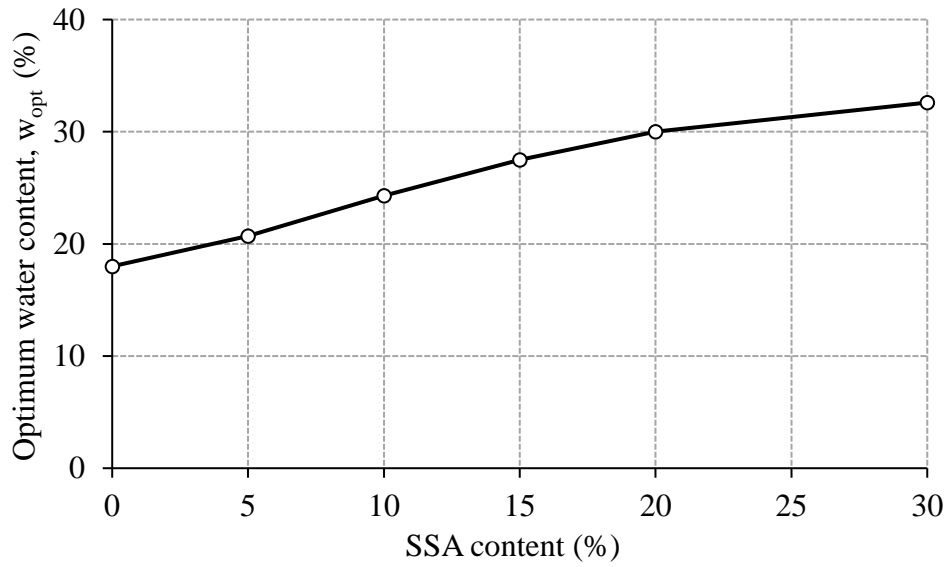


Figure 4.2 Effect of SSA on optimum moisture content.

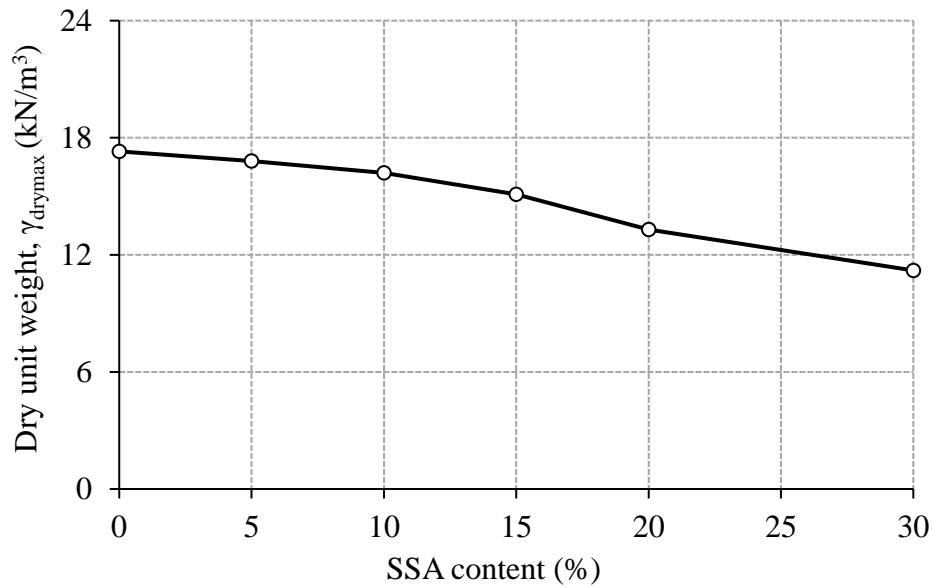


Figure 4.3 Effect of SSA on dry unit weight.

Table 4.1 Standard Proctor results of clay-SSA mixtures.

Mixtures	Optimum moisture content (%)	Maximum dry unit weight (kN/m ³)
Clay	18,0	17,30
5%SSA	20,7	16,80
10%SSA	24,3	16,20
15%SSA	27,5	15,10
20%SSA	30,0	13,30
30%SSA	32,6	11,20

In addition, the SSA particle does have a high ability to absorb water as compared with clay particles. Al-Sharif and Attom, (2014) expressed that soils with high plasticity index ($PI > 20$), SSA can lead to important decrease in the optimum moisture content (from 34% to 22%, with 12.5% SSA content). In this study, the tested clay was classified as low plasticity (CL) and will show a vice versa behavior that Al-Sharif and Attom, (2014) reported. Coarse-grained soils are affected more than the fine-grained soils. Coarse soil consists of larger voids which drainage is higher and more quickly than fine grained soil. In this study the main material (clay) and the additive (SSA), both have a fine-grained soil structure which is precise to have higher percentage of moisture contents. Moreover, the fine-grained soils have more water attraction with

the increase of SSA ratio due to chemical composition of SSA which absorbs more water (Deng et al., 2016).

4.2 Atterberg limits testing results

Plasticity characteristics and their deformation can be specified with index properties like liquid limit, plastic limit, plasticity index. The Atterberg's limits of clay and clay-SSA mixtures have been verified in Table 4.2. The results showed that the SSA mixes with clay that passing through sieve 0.425 mm in diameter. Also, the SSA has taken at various percentages from 0% to 30% by the weight of the mixture.

Table 4.2 Atterberg limits of clay-SSA mixtures.

Mixtures	Liquid Limit (%)	Plastic Limit (%)	Plasticity Index (%)	USCS
Clay	27	13	14	CL
5%SSA	31	15	15	CL
10%SSA	34	20	14	CL
15%SSA	36	23	13	CL
20%SSA	40	27	13	ML
30%SSA	43	28	15	ML

The liquid limit of clay increased to 27 from 43% with increasing percentage of SSA until 30%. In addition, the plastic limit of the clay-SSA mixtures also increase to 28% from 13, plasticity index fluctuated and do not have a trend. The results on the plasticity index (PI) of SSA have been somehow mixed. Scientist who has examined the plasticity index of SSA, without Atterberg limit results, have tended to classify this sustainable material as non-plastic to medium plasticity (Al-Sharif and Attom, 2014; Sato et al., 2012; Tempest and Pando, 2013; Wegman and Young, 1988 and Yusuf et al., 2012). SSA has been more commonly described as a non-plastic material (Sato et al., 2012; Wegman and Young, 1988; Yusuf et al., 2012), yet the specific values of plasticity index were not presented in these special cases. That study classified SSA as a medium plasticity material (Merino et al., 2005), an average plasticity index (PI) of 18% was expressed. Nevertheless, depending on the limited experimental results, it appears that SSA has plasticity characteristic like those of silts and organic soils. This offers that, in terms of strength, SSA may be somehow more sensitive to moisture changes, when used in geotechnical engineering applications. SSA may also have

dispersive feature (i.e., sensitivity to erosion), which would be significant to look at if SSA is used in such an environment where it is exposed to water pressure, such as water-retaining structures. (Dhir et al., 2017a)

4.3 Fall cone testing results

Variations of Fall Cone Test (FCT) penetrations and the water contents for each mixture are shown in Figure 4.4. As can be seen from Figure 4.4, there is almost a linear relationship between the cone penetration and the water content. As the water content increases the cone penetration values are also increasing for each mixture. Furthermore, at given water content as the SSA content increases, the penetration of mixtures decreased which means SSA increased the resistance of penetration. From FCT results liquid limit values generally obtained by water content corresponding 20 mm cone penetration (Cabalar and Mustafa, 2015).

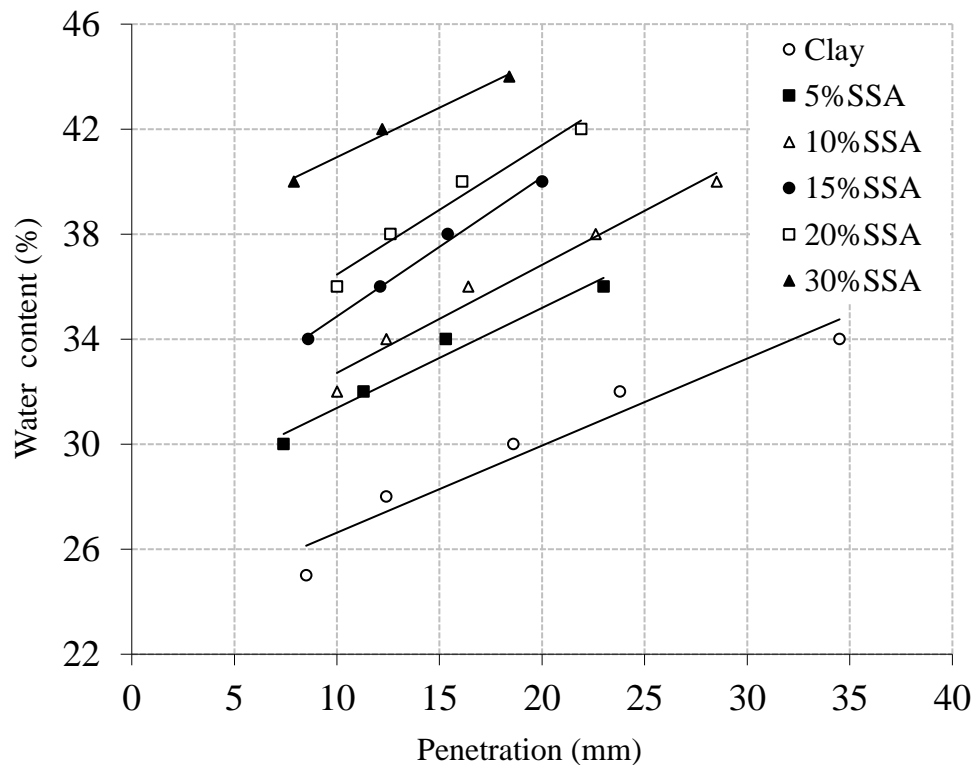


Figure 4.4 Effect of water content and SSA on penetration for clay-SSA mixtures.

The liquid limit results are shown in Figure 4.5. With the increase of the SSA liquid limit values were increased. While the liquid limit of clay was 30, with the addition of 10% and 20% SSA, the estimated value of liquid limit increased at a rate of 30%.

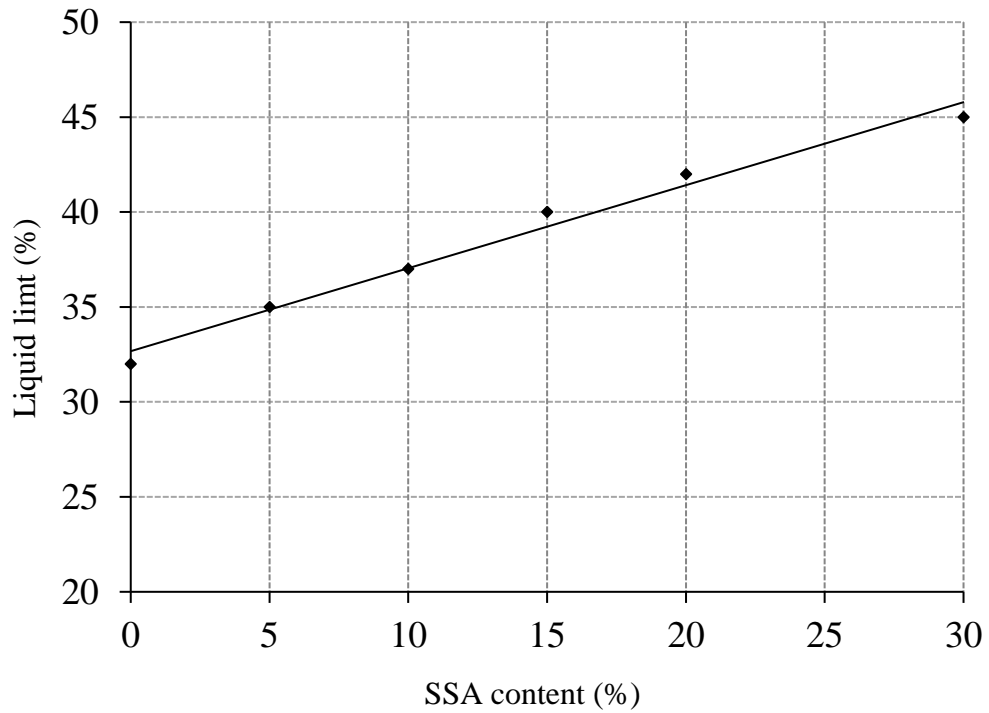


Figure 4.5 Liquid limit of clay with various SSA content.

Undrained shear strength (s_u) values are showed a relation with water content (see Figure 4.6). As can be seen from Figure 4.6 as increase water content for each mixing the s_u values are decrease. s_u values increase with the increase of SSA value at same water content. Comparable results were reported by Lin et al. (2005) who indicated that SSA increased triaxial shear strength. Veeresh et al., (2003), Likos and Jaafar, (2014) and Epstein, (1975) pointed out that stress could increase penetration resistance and undrained shear strength.

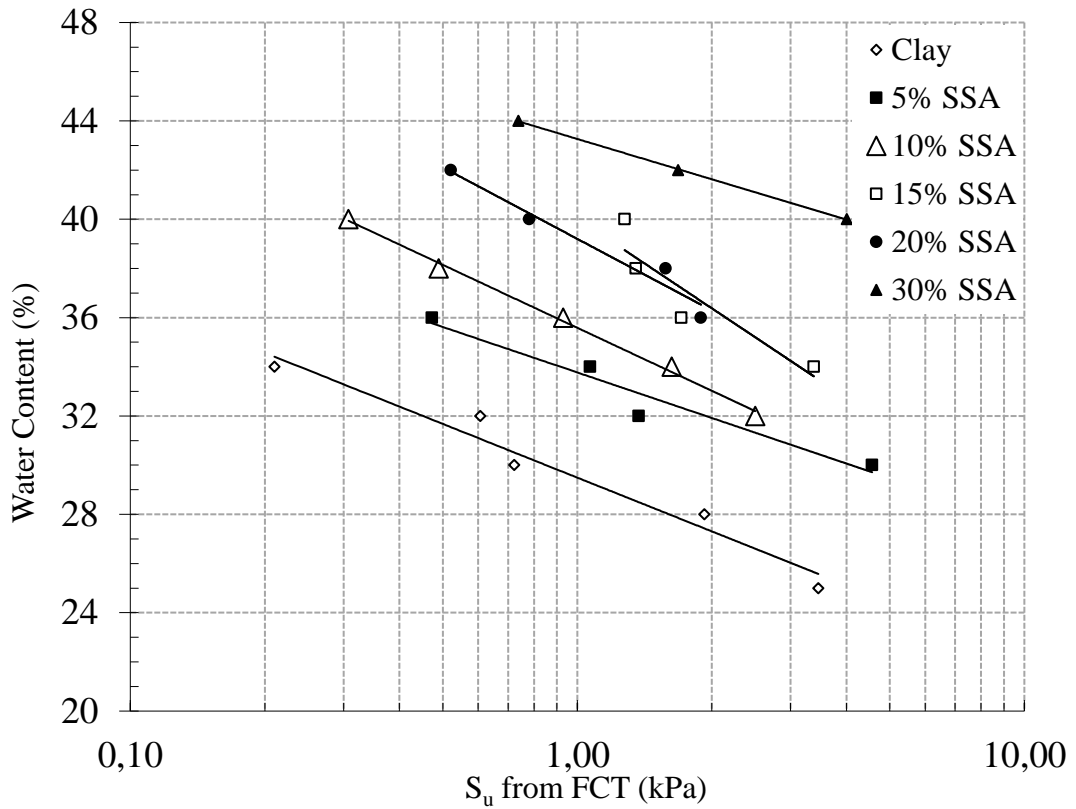


Figure 4.6 Effect of SSA on water content by fall cone test.

4.4 Vane Shear Testing Results

The laboratory vane shear tests (LVT) were also performed to compare and examine the relationship of s_u values for clay-SSA mixtures. To study the influence of the SSA content on the characteristics of clay, changes in undrained shear strength (s_u) with vane shear tests for each of the mixtures are shown in the Figure 4.7. As can be seen from Figure 4.7, it presents the changes in s_u estimated by vane shear testing equipment for clay with SSA at various contents. As SSA content increases, the penetration of mixtures decreased which means SSA increased the resistance of penetration.

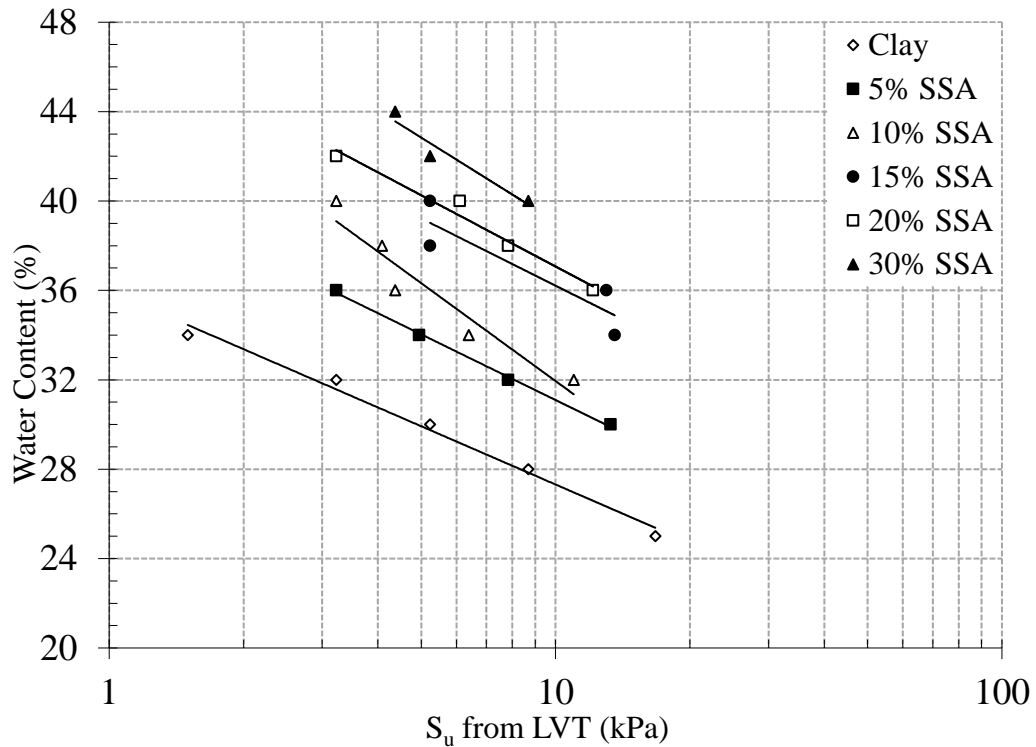


Figure 4.7 Effect of SSA on water content by laboratory vane shear test.

Figure 4.8 shows a summary of the LVT and FCT testing results for clay-SSA mixtures in terms of water content versus undrained shear strength. In the laboratory vane shear tests, the clay had a value of s_u ranging between 1.7 and 17 kPa, while the values for the fall cone tests were only between 0.20 and 3.50 kPa for the water contents from 34 to 25%. The fall cone tests predicted the s_u values of 10% SSA mixtures to be between 0.30 and 2.50 kPa, while the laboratory vane shear tests presented the s_u values of the same mixtures to be between 3.10 and 11.00 kPa for the water contents from 40 to 32% (Figure 4.8). Furthermore, the s_u parameters achieved from fall cone tests on 30% SSA ranged from 0.75 to 4.00 kPa, while the same parameter obtained from laboratory vane shear tests ranged from 4.30 to 8.80 kPa for the water contents from 44 to 40% (Figure 4.8). As can be seen from the testing results of both equipment's, it is confirmed the undrained shear strength decreases for increasing water content. To understand the relationship between two testing equipment's, a comparison between the results of fall cone and vane shear testing have been observed. The s_u by values predicted by the vane shear tests are plotted against that estimated by the fall cone test in Figure 4.8 for different SSA mixtures. It can be seen in Figure 4.8 that the vane shear tests estimated higher s_u values in comparison with the fall cone testing results.

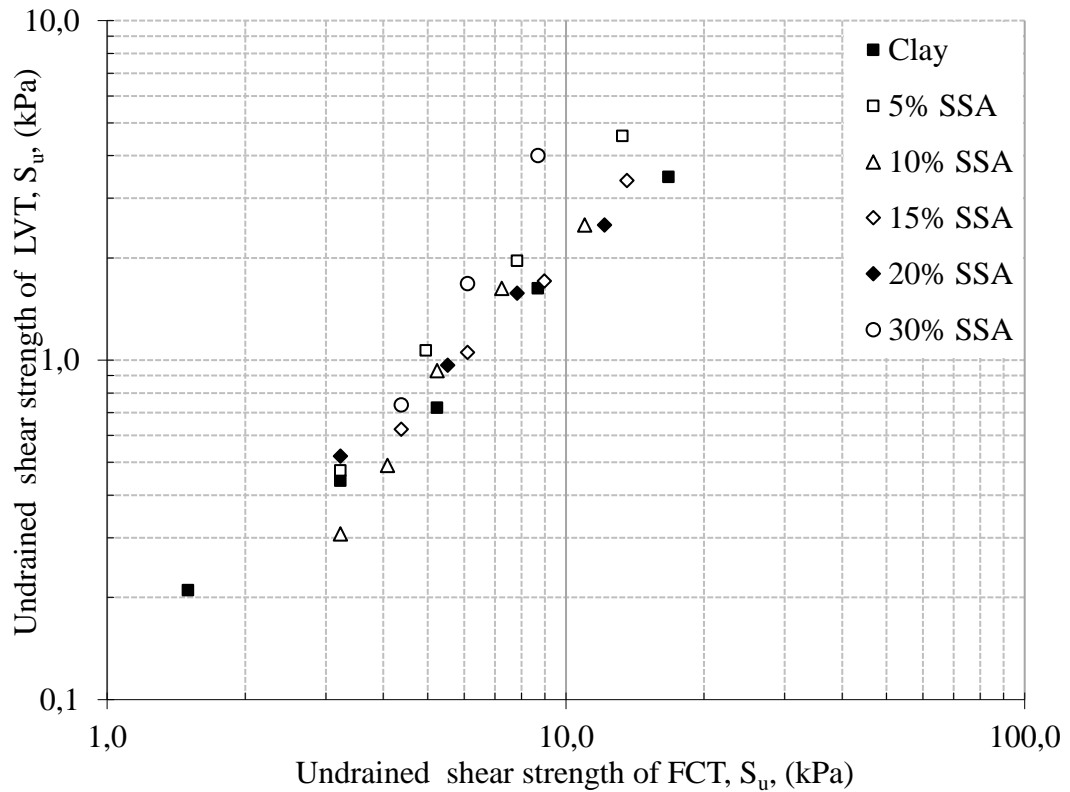


Figure 4.8 Undrained shear strength of SSA mixtures by FCT and LVT.

Figure 4.8 indicates the best fitting testing results for both vane shear and fall cone equipment's. In the few examples where testing results from the vane shear results could be compared with fall cone test, the vane shear always found to give higher values by a factor ranging from 2.2 to 10.3. This difference could be due to how the testing procedures are defined, what type of vane or cone is selected, the rate of rotation chosen, fall cone roughness and other characteristics. (Karlsson, 1961), (Matsui and Abe, 1981), (O'Kelly, 2014), (Farias abd Llano-Serna, 2016), (Cabalar et al., 2020). Even though, it can be concluded that there is a considerably relationship between these two testing methods, for a given water content.

4.5 California bearing ratio resting results

Table 4.3 summarizes the laboratory and field CBR experimental results. The strength and deformation behavior of SSA treated clay was determined at various ratios (0, 5, 10, 15, 20 and 30%) of SSA and curing time (4, 8, 16 and 32 days). Using these test results, compressive strength and bearing capacity were determined, which can be used for assessing the improvement based on the required stability. The evaluation of

strength behavior is most critical on the wet side of optimum moisture content. The optimum water content values of the specimens increased by an increase in the SSA content. Therefore, both soaked and unsoaked CBR tests were conducted on samples. CBR values increases with increasing SSA content and curing time for unsoaked tests. On the other hand, CBR values decreases with an increase in curing time for soaked condition.



Table 4.3 Experimental Results of CBR test (MPa)

Mixtures	Laboratory CBR Test Results								Field CBR Test Results (circular footing)			
	Unsoaked tests				Soaked tests				Location of Test Points			
	Curing				Curing				4 Days Cured			
	4 days	8 days	16 days	32 days	4 days	8 days	16 days	32 days	Left	Center	Right	Average
Clay	1,6	1,9	2,5	3,8	1,0	0,8	0,6	0,4	3,1	3,6	3,7	3,5
5%SSA	1,7	2,2	3,0	4,4	1,1	0,8	0,7	0,4	-	-	-	-
10%SSA	2,4	2,9	3,7	5,4	1,7	1,4	1,2	1,1	5,5	5,7	5,6	5,6
15%SSA	3,8	4,5	5,7	7,5	2,2	2,0	1,8	1,8	-	-	-	-
20%SSA	6,3	8,0	10,5	13,9	3,0	2,6	2,4	2,3	14,2	14,8	14,7	14,6
30%SSA	11,2	13,8	19,5	25,1	4,6	4,0	3,9	3,8	26,0	27,5	27,3	26,9

The tests on clay-SSA mixtures at various mix ratios were prepared at the optimum water content determined previously in standard compaction tests. Following the compaction of the specimens at five layers with 56 blows per layer, a surcharge plate of 2.44 kPa was placed on the specimen prior to testing and had been keeping waiting soaked and unsoaked. The loads were carefully recorded as a function of penetration up to a total penetration of 6.0 mm. Load penetration curves were illustrated for each case, and required corrections were applied based on the procedures identified in standards (see Figure 4.9-4.16). Then, CBR values obtained from the load-penetration curves were plotted in a column representation. (see Figure 4.17 and 4.18) CBR values expressed in this study are estimated using the stresses at 2.5 mm penetration. Some researchers reported that SSA treatment can significantly improve mechanical properties of a clay. The results presented by Lin et al. (2005), Chen and Lin (2009) and Lin et al. (2007a) reported that SSA on its own led to considerable increases in the soil CBR.

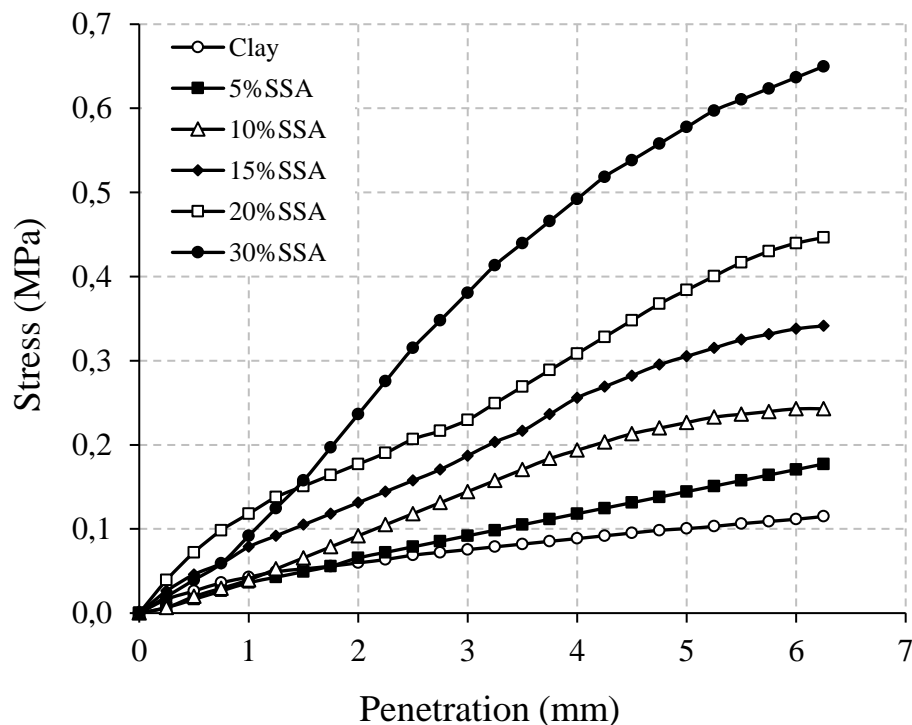


Figure 4.9 Stress vs. penetration for soaked samples under 4 days of curing time.

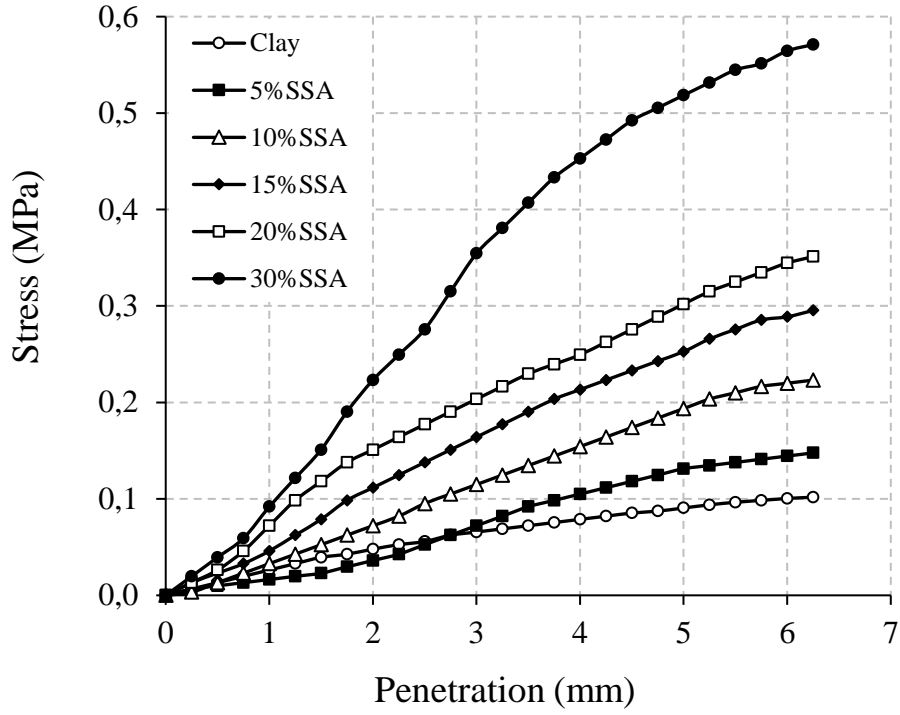


Figure 4.10 Stress vs. penetration for soaked samples under 8 days of curing time.

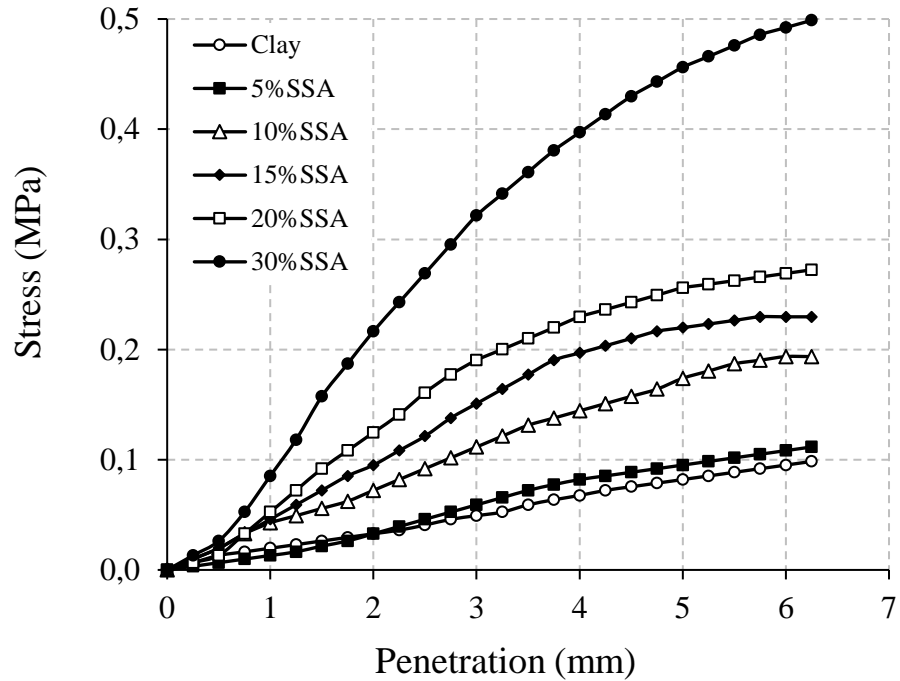


Figure 4.11 Stress vs. penetration for soaked samples under 16 days of curing time.

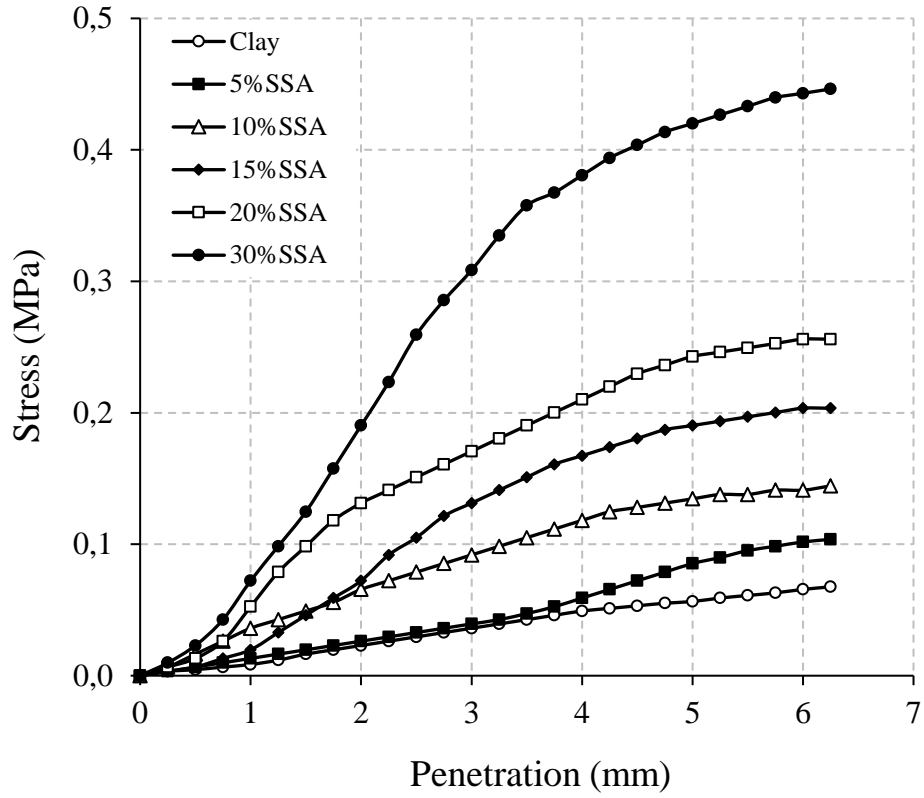


Figure 4.12 Stress vs. penetration for soaked samples under 32 days of curing time.

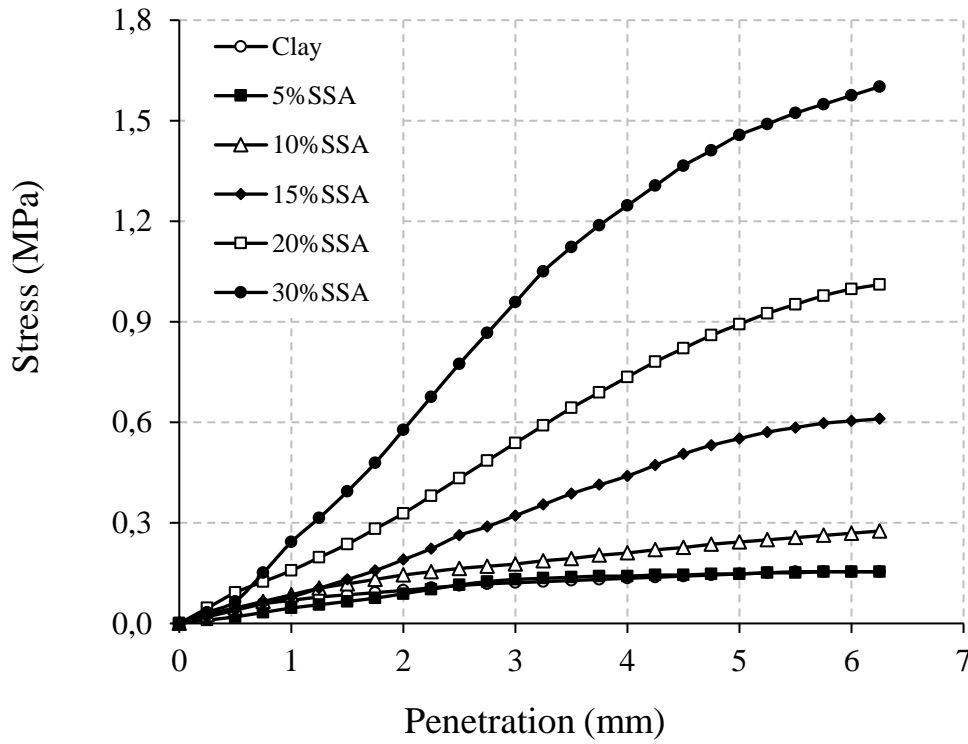


Figure 4.13 Stress vs. penetration for unsoaked samples under 4 days of curing time.

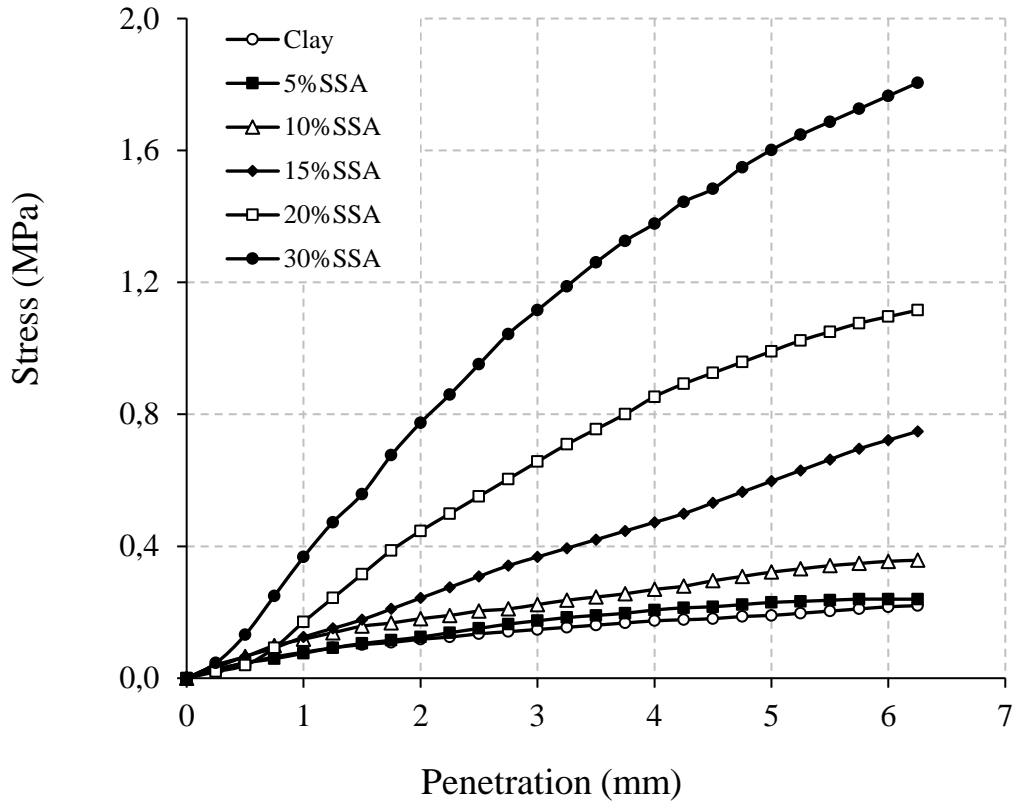


Figure 4.14 Stress vs. penetration for unsoaked samples under 8 days of curing time.

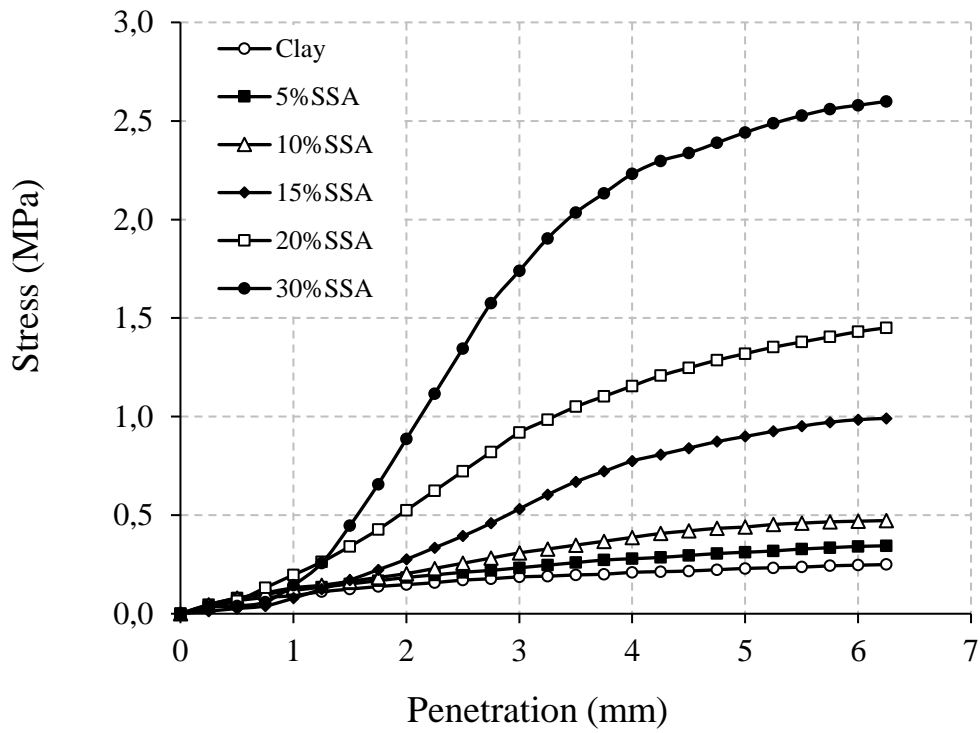


Figure 4.15 Stress vs. penetration for unsoaked samples under 16 days of curing time.

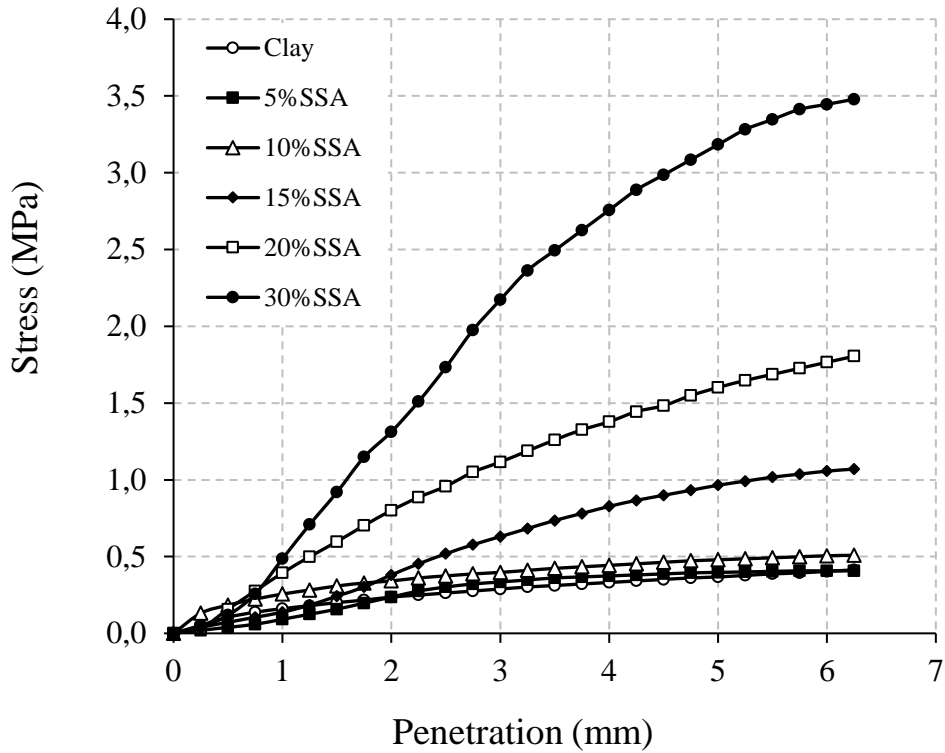


Figure 4.16 Stress vs. penetration for unsoaked samples under 32 days of curing time.

Figure 4.17 and Figure 4.18 shows the soaked and unsoaked CBR results in a column view.

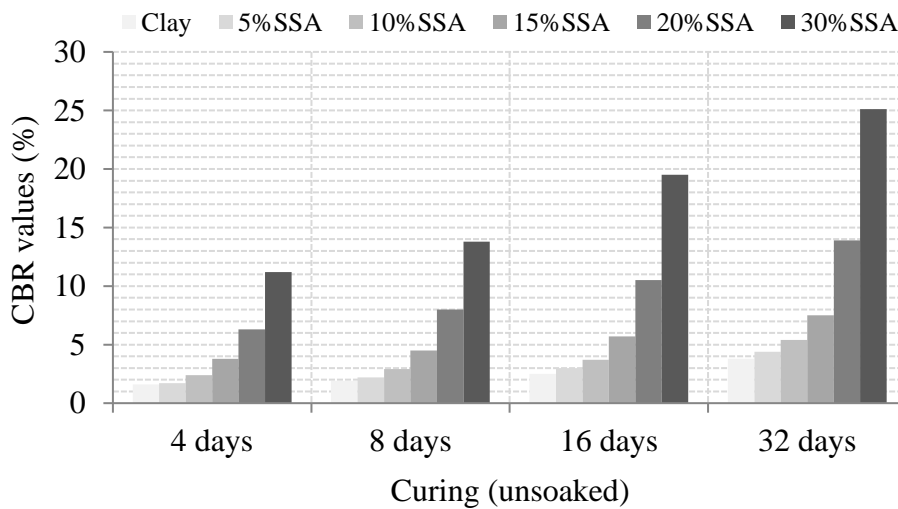


Figure 4.17 Effect of SSA on CBR values for unsoaked clay-SSA samples.

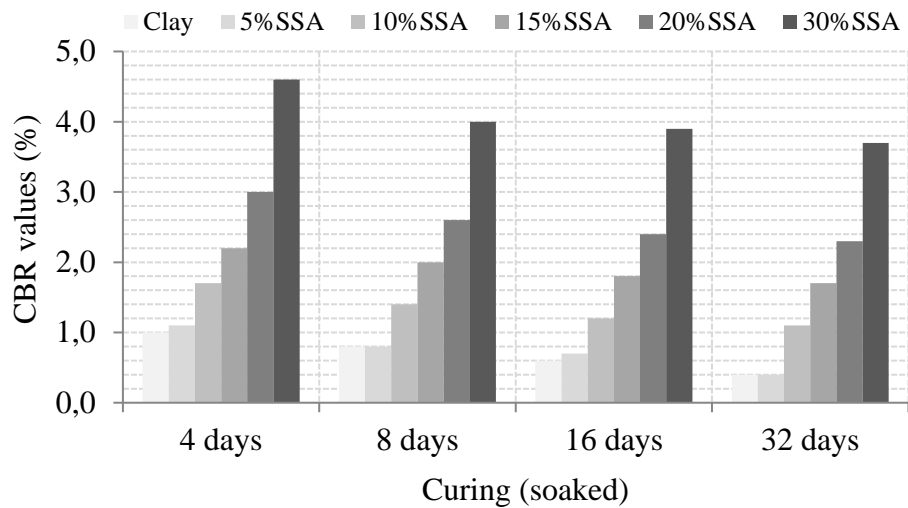


Figure 4.18 Effect of SSA on CBR values for soaked clay-SSA samples.

The field CBR values at in-situ condition were higher than the laboratory (4 days) unsoaked CBR values in the mould. Field CBR values are higher of 4 days soaked CBR values because natural moisture content of field was evaporated quicker than the moisture content at which the mould was prepared at unsoaked moisture content. Figures 4.19-4.22 highlights that the field CBR results which were prepared according to ASTM D4429 method. The field CBR results were 100% higher than in-situ laboratory CBR values.

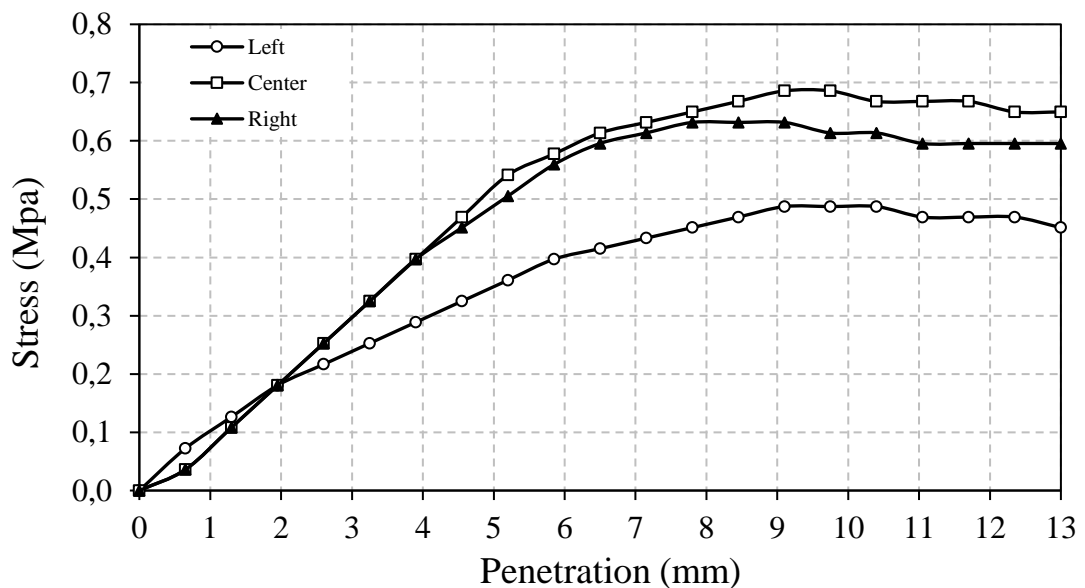


Figure 4.19 Plot of stress vs. penetration for clay field CBR samples under 4 days curing.

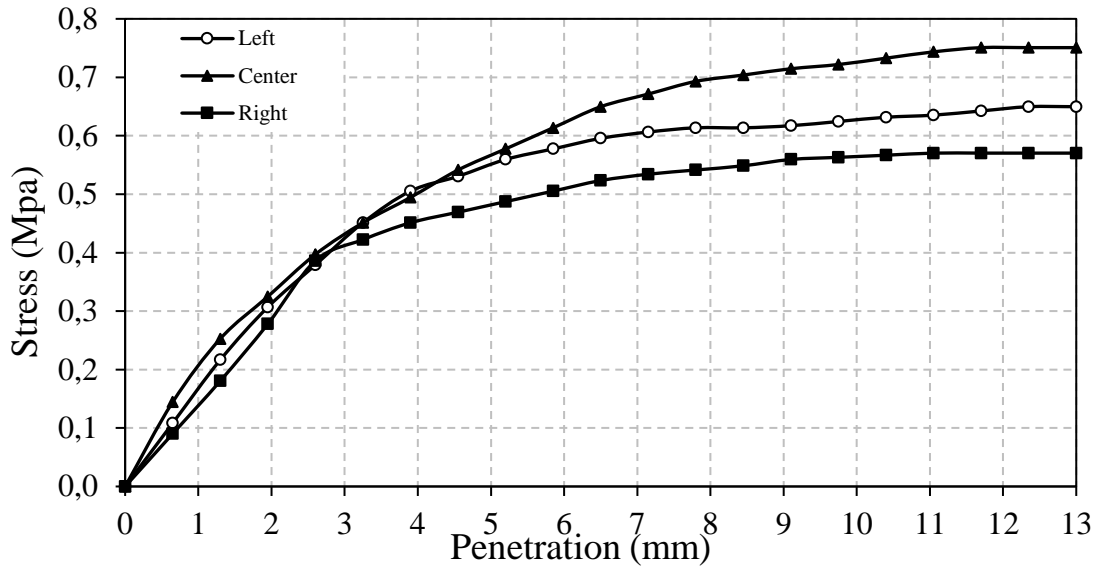


Figure 4.20 Plot of stress vs. penetration for 10% field CBR samples under 4 days curing.

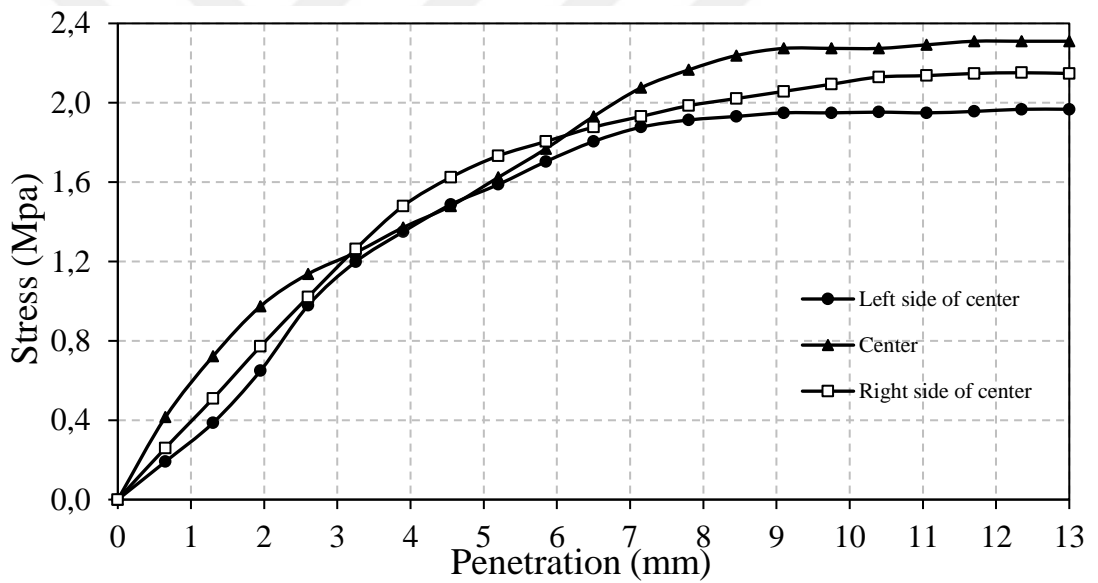


Figure 4.21 Plot of stress vs. penetration for 20% field CBR samples under 4 days curing.

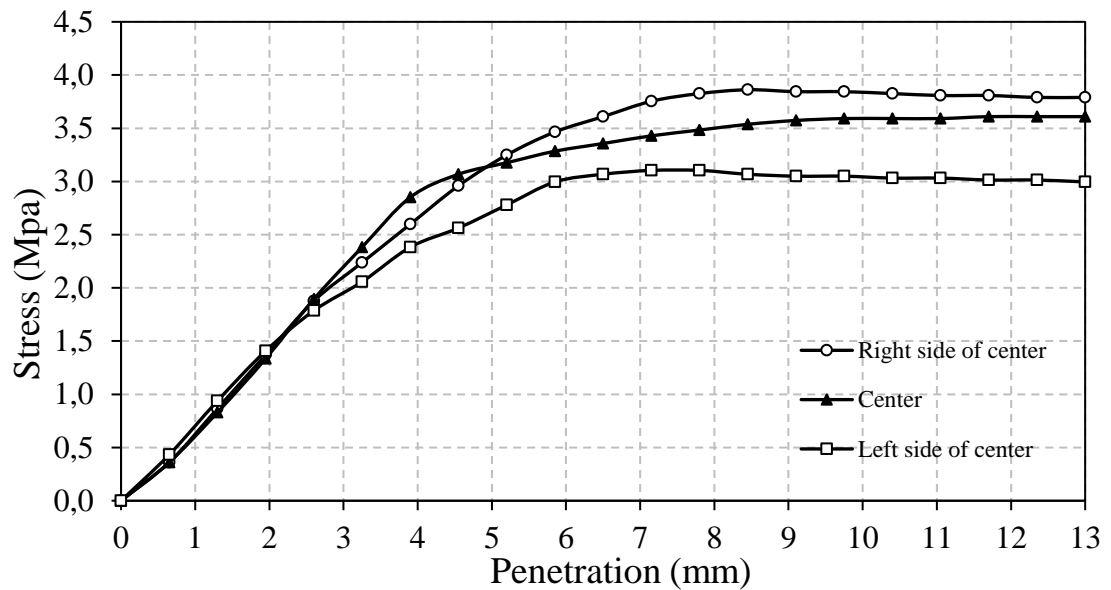


Figure 4.22 Plot of stress vs. penetration for 30% field CBR samples under 4 days curing.

4.6 Unconfined compression strength testing results

The unconfined compression strength testing results demonstrate that the strength behavior of the mixtures was greatly influenced by the addition of SSA (see Table 4.4). The unconfined compression strength tests were examined on the mixtures compacted at optimum water content. The peak compressive strength values of the mixtures increased regularly as the amount of SSA increased. Addition of SSA improves the strength of unconfined compression samples. This improvement is between 263.8-770.2 kPa for 4 days cured samples, 344.7-841 kPa for 8 days cured samples, 445.2-1150.3 kPa for 16 days cured samples and 514.8-1350.6 kPa for 32 days cured samples. Tempest and Pando (2013), Al Sharif et al. (2000), and Ingunza et al. (2014) reported similar results. As has been noted, observed UCS values occurred with different magnitudes, and with a similar increase in trend. Furthermore, the increments in strength observed in the clay with SSA were found to be higher clay. The stabilization additives have been found to be effective in upgrading the clay strength performance with curing time. It is also interesting to note that the soils treated with SSA only continued to see improvements in strength as the curing age progressed. This progress can be seen on the Figures 4.23-4.26 which were plots of stress versus axial strain for different curing periods.

Table 4.4 Effects of SSA on unconfined compressive strength samples.

Mixtures	Curing				Toughness			
	4 Days	8 Days	16 Days	32 Days	4 days	8 Days	16 Days	32 Days
	Max. Stress (kPa)				Energy Absorption (kJ/m ³)			
Clay	263,8	344,7	445,2	514,8	2,2	3,7	4,2	7,0
5% SSA	395,2	443,8	521,0	583,1	4,5	4,9	6,0	7,3
10% SSA	451,1	527,6	609,5	720,0	5,3	5,8	7,1	8,7
15% SSA	505,9	640,7	780,3	830,2	6,0	6,6	10,3	11,6
20% SSA	577,7	757,5	820,4	1150,3	6,9	8,8	11,7	14,4
30% SSA	770,2	841,0	1150,3	1350,6	9,7	11,8	12,9	18,3

The inclusion of SSA was also greatly beneficial to the higher-grade soils with UCS over 1000 kPa. Also, Figure 4.27 and Figure 4.28 showed that the maximum stress and energy absorption capacity increased with the increase percentage of SSA content, respectively. Energy absorption capacity in other words toughness increases the resistance of samples from fatigue failure. As the energy absorption capacity is higher, the samples get more ductile. Ingunza et al., (2014), demonstrate that the SSA material could have value for use in a wide range of applications.

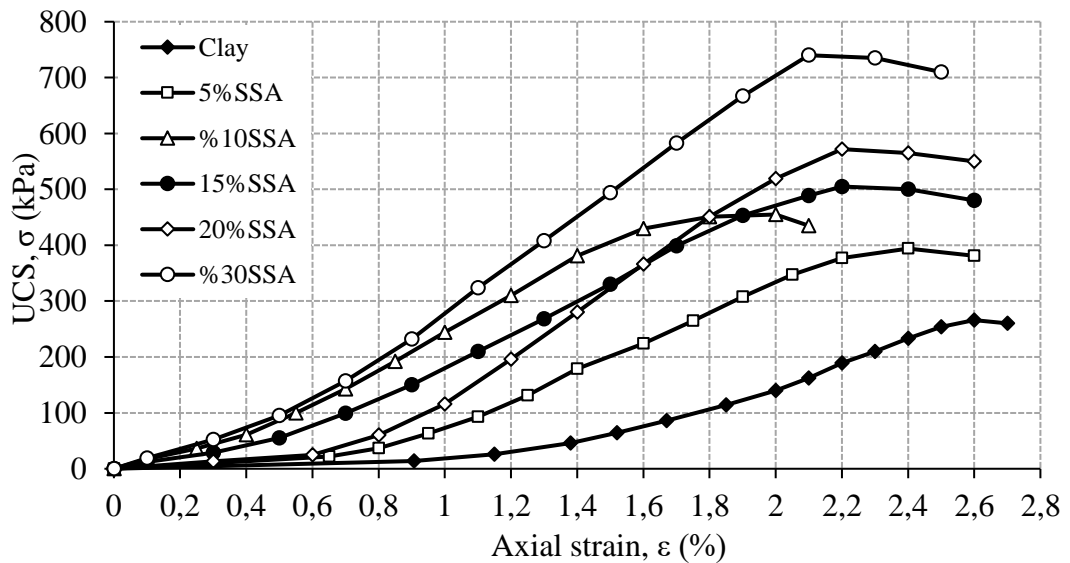


Figure 4.23 Plot of stress vs. axial strain for 4 days cured samples.

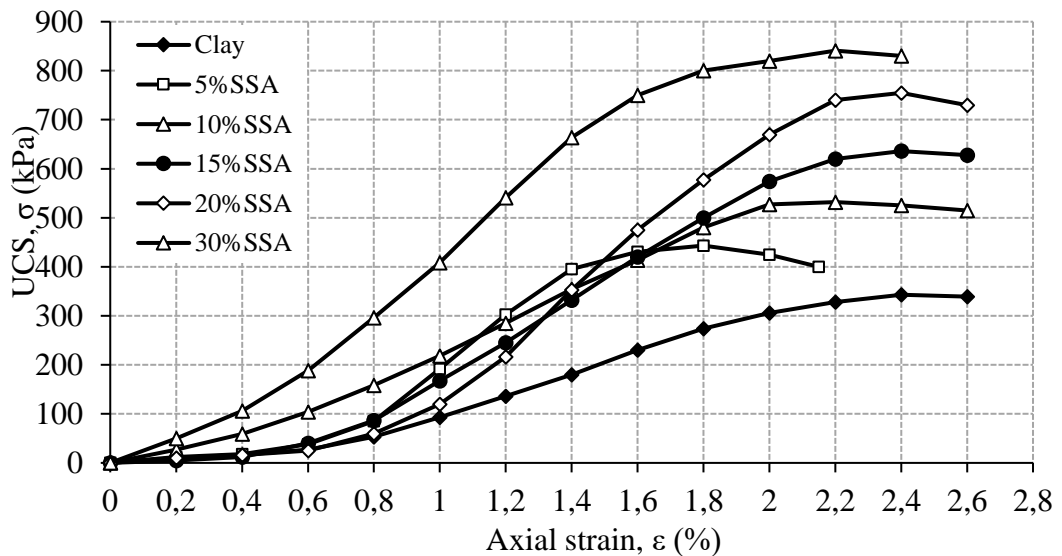


Figure 4.24 Plot of stress vs. axial strain for 8 days cured samples.

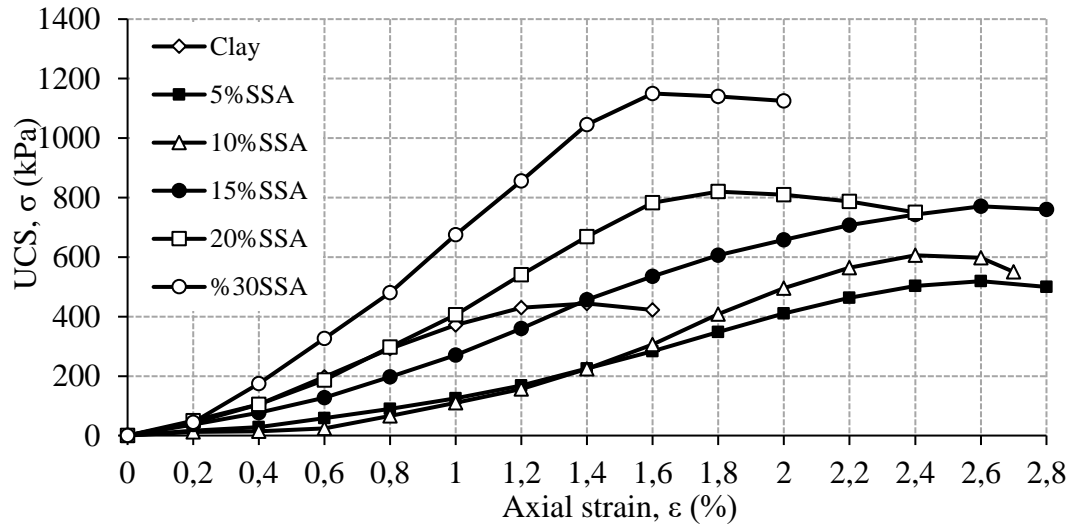


Figure 4.25 Plot of stress vs. axial strain for 16 days cured samples.

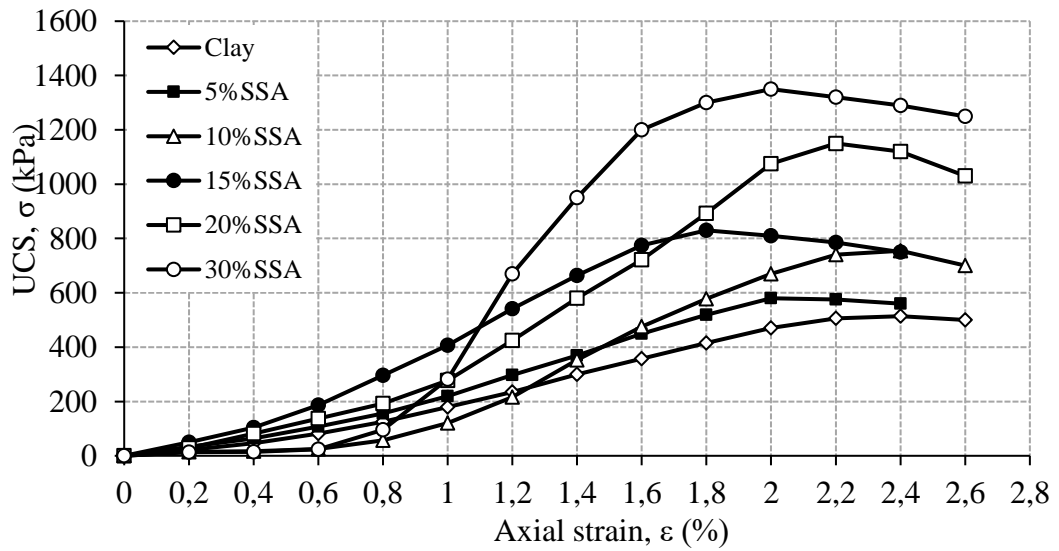


Figure 4.26 Plot of stress vs. axial strain for 32 days cured samples.

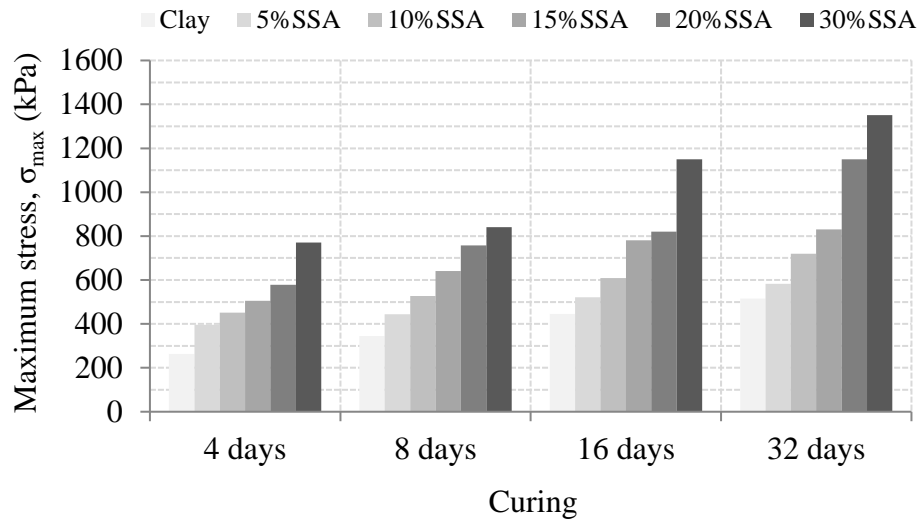


Figure 4.27 Variation of maximum stress with SSA content and curing time.

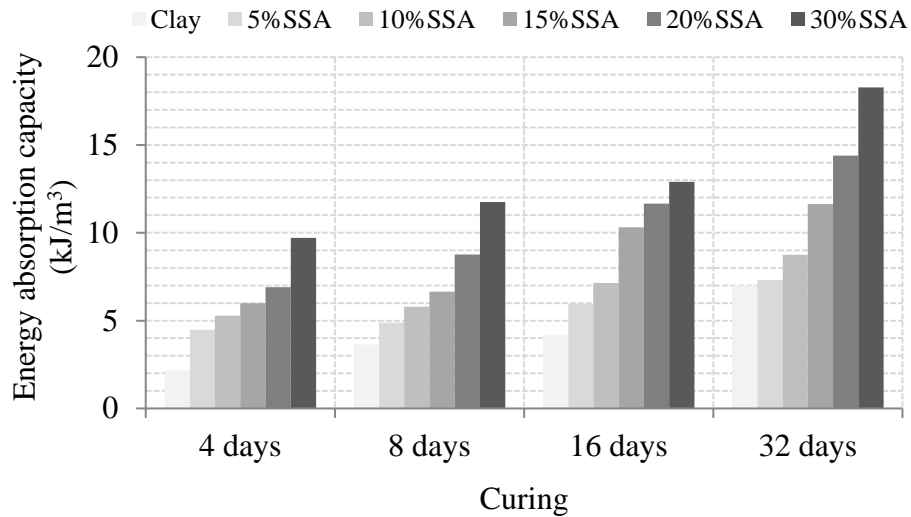


Figure 4.28 Variation of energy absorption capacity with SSA content and curing time.

4.7 Oedometer testing results

The oedometer test was examined with respect to ASTM D 2435. This test used to investigate the consolidation properties of clay with different percentages of SSA from 0% to 30% by the weight of the mixture. It is identified the effective stresses on clay with consolidation characteristics such as initial void ratio (e_0), void ratio (e), compression index (c_c), with SSA content, under different oedometer pressures as shown in Figures 4.29 to 4.32

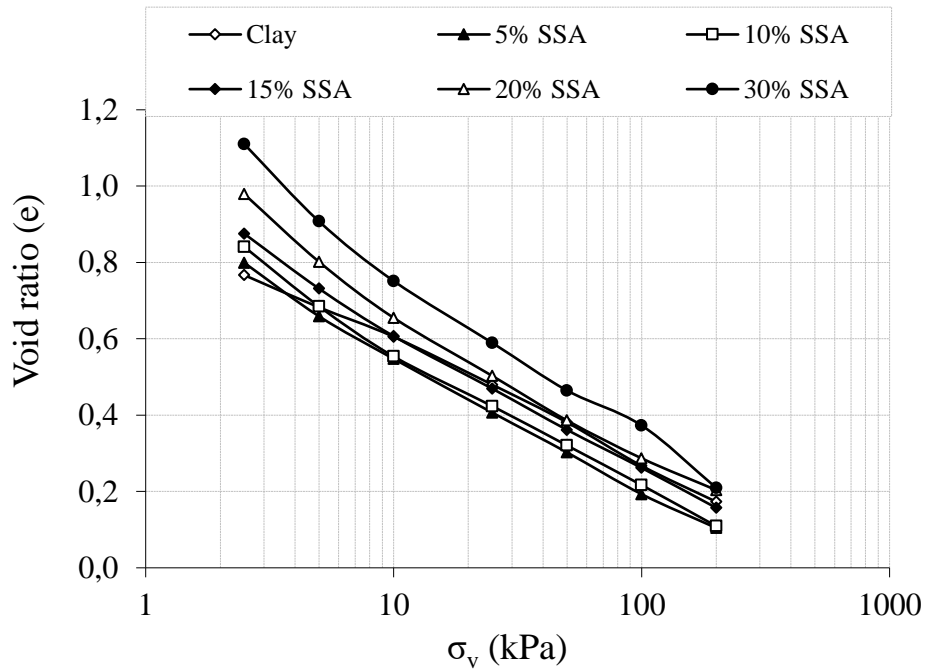


Figure 4.29 Variation of void ratio with different oedometer pressures.

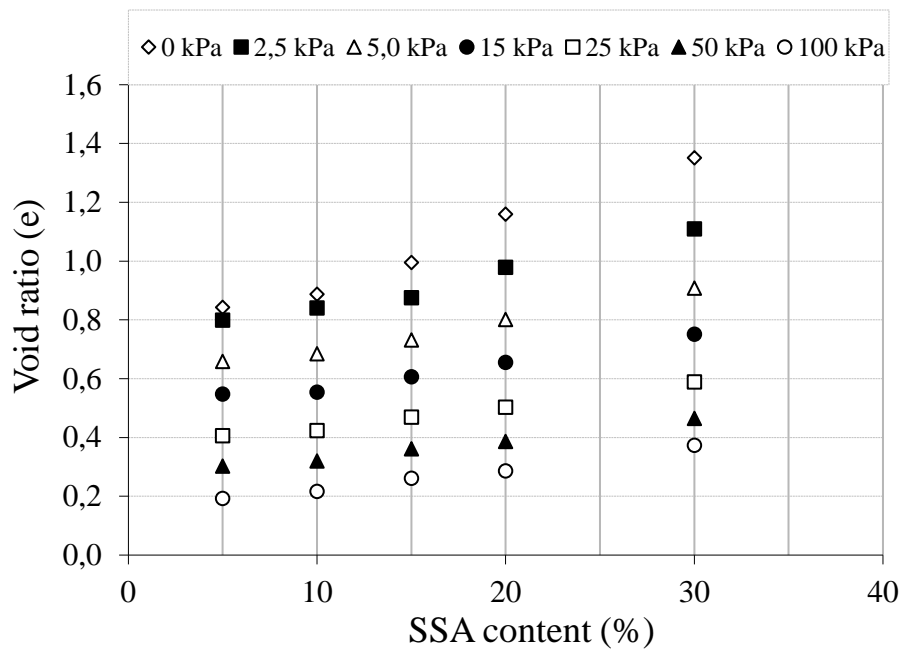


Figure 4.30 Variation of void ratio with different oedometer pressures.

4.7.1 Initial void ratio (e_0)

The initial void ratio (e_0) is one of the important characteristics of consolidation test. It is calculated by increasing percentage of SSA up to 30% to the clay. Also, the initial void ratio (e_0) was increased from 0.794 to 1.35 as shown in Figure 4.31. The increase

in e_0 may be due to increasing water content when the percentage of SSA, increased or may be due to fine particles of SSA material.

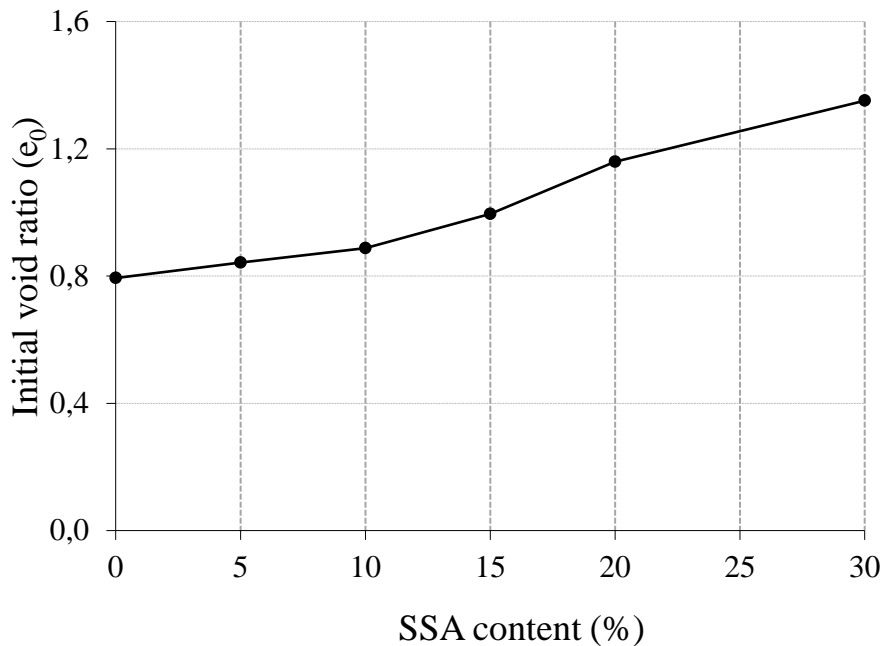


Figure 4.31 Relations between initial void ratio and SSA content.

4.7.2 Compression index (C_c)

Figure 4.32 illustrates the variation of compression index (C_c) with SSA contents. The compression index (C_c) is equal to the slope of the graph of pressure versus void ratio (log scale). Compression Index (C_c) for clay is in the range 0.258 to 0.968 (Srintharan and Gurtug, 2003). Values of compression index (C_c) is different between each type of soil; C_c usually for the grain course soil have a high permeability flow occurs very rapidly, while for finer grains soil that has low permeability, the flow process takes a longer time (Bujang et al., 1991). The C_c increased with addition percentage of SSA up to 30%. Hobbs, (1986) reported that there is relationship between compression index (C_c) and liquid limit (LL). Skempton and Petley (1970), (Al Raziqi et al., 2003). Based on the liquid limit results from Atterberg and Fall Cone test which were increasing with SSA content, the compression index (C_c) also increases.

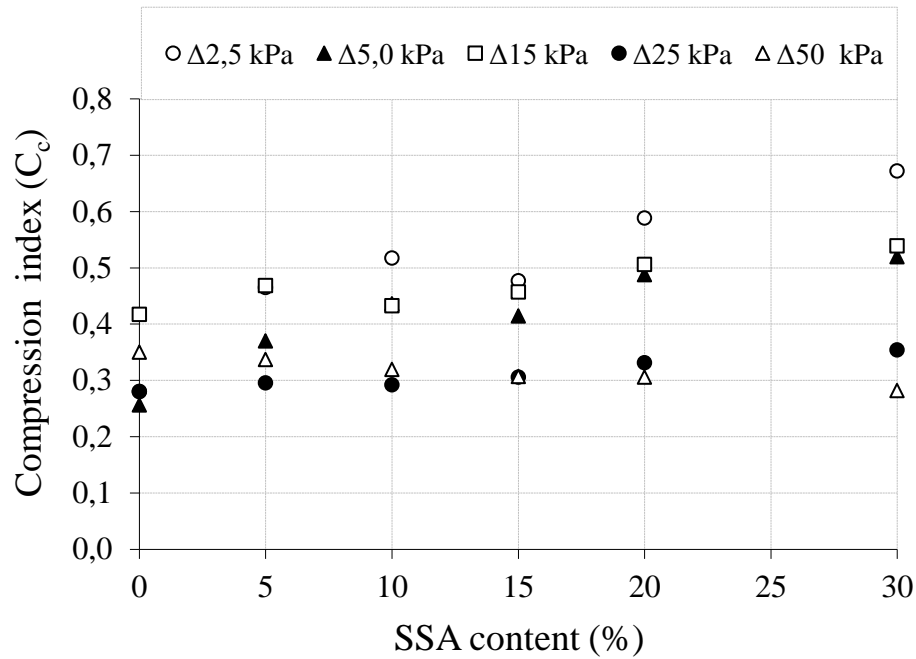


Figure 4.32 Compression index vs. SSA content under different stress changings.

4.8 Falling head permeability testing results

Table 4.5 and Figure 4.33 shows the values of hydraulic conductivity for compacted clay mixtures with 0 to 30% SSA. The measured values varied from 3.97×10^{-6} to 1.23×10^{-7} cm/sec, indicating a range like those of fine sand/silt mixtures or silt. As SSA mixtures increased from 0 to 30%, the values of hydraulic conductivity decreased gradually. The larger specific surface of SSA causes more resistance to flow of water through the voids. The coefficient of permeability of SSA has been found to range from 1×10^{-4} to 4×10^{-4} cm/sec (Al-Sharif and Attom, 2014; Federal Highway Administration, 1997; MPCT, 1980; NCHRP, 2013 and Yusuf et al., 2012). Permeability is highly based on void ratio, which is related to grain size distribution. It is obvious that the SSA contains widely fine silt and sand size particles. The effective size (D_{10}) and coefficient of uniformity of the SSA samples ranged from 0.003 to 0.7 and from 3 to 12, respectively. (Petavratzi, 2007; Koisor-Kazberuk, 2011; Maozhe et al., 2013; Ksepko, 2014; Krejcirikova, 2015 and Dhir et al., 2017a).

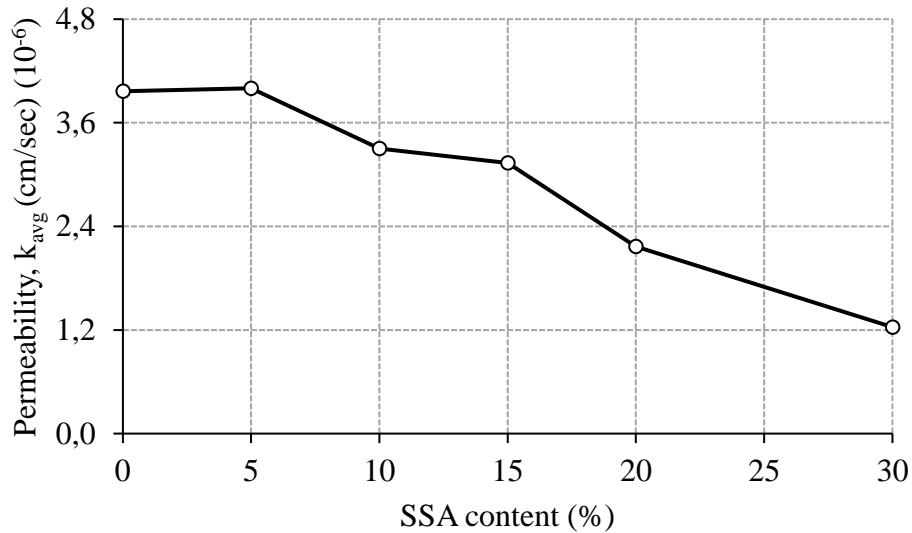


Figure 4.33 Coefficient of permeability (k) values for clay-SSA mixtures.

Table 4.5 Hydraulic conductivity values for clay-SSA mixtures.

Coefficient of Permeability (cm/sec)	Mixtures					
	Clay	5%SSA	10%SSA	15%SSA	20%SSA	30%SSA
k ($\times 10^{-6}$)	3,3	3,2	2,8	2,7	2	1,3
	4,9	4,5	3,5	3,2	2,1	1,2
	3,7	4,3	3,6	3,5	2,4	1,2
k_{avg} ($\times 10^{-6}$)	3,9	4,0	3,3	3,1	2,2	1,2

4.9 Plate load testing results

Plate load tests were done in circular model footing set-up for clay and clay-SSA mixtures. According to the laboratory tests and results 0, 10, 20 and 30% SSA were considered as a suitable percentage for using in the plate load test because of the heavy test conditions. Table 4.6 gives the settlements of clay and clay-SSA mixtures at different pressures applied at plate load test in the circular model footing set-up. Figure 4.34 to Figure 4.38 illustrates the pressure-settlements curve record by three strain gauges and their averages in plate load test for clay and clay-SSA. In the Figure 4.38, the loads-settlements curve obtains from the average of the three strain gauges, was shown to make a comparison between the results of plate load test of clay. It appears from Table 4.6 and Figures 4.34-4.38 that, the SSA improve the strength of clay representing by the increasing of bearing loads for clay-SSA mixtures. Also, the

specific settlement for SSA at any specific high load (larger than the 150 kN/m^2) was less than the settlement of clay for the same load. The addition of SSA, which considered as waste material changed the behavior of clay under the applied loads. Consistent with these findings, Figure 4.39 show time- settlement curve of 200 kN/m^2 pressure, for clay and clay-SSA mixtures. In this Figure, the clay indicates the highest settlement at any specific time than the clay-SSA mixtures. Figure 4.39 shows the time-settlement curve of 200 kN/m^2 pressure; the data in this Figure clearly show that the increase in SSA content cause lesser settlement at any specific time. 200 kN/m^2 have been chosen due to the failure point of clay. The clay will not appear in the other pressures because the failure happened at 200 kN/m^2 for clay. The rebound curve of loads-settlements curve for SSA mixtures could not be done because of cementation during the 4-day curing time. All the tests have been conducted after 4 days of curing time. As the SSA content increased the failure point have been increased and the settlement decreased. The same behavior of bearing failure (punching failure) was noted for clay and clay-SSA mixtures however, the most obvious failure was seen in clay. The possible improve in strength and stiffness of the SSA treated clay were assessed by analyzing the applied pressure versus plate settlement curves achieved from the plate load tests for each mixture. All tests were examined until a settlement of at least 25 mm was measured or until the failure happens. The settlement curves in Figure 4.38 presents an increase in bearing capacity and stiffness for 10, 20 and 30% SSA treated soil compared to the results obtained for the clay. For comparison purposes, this figure shows that for a plate settlement of 25 mm the applied pressures measured were 180, 250, 310 and 420 kPa for the clay, 10%, 20% and 30% SSA treated soils, respectively. These values represent relative bearing capacity improvements of 38% and 133 % when the clayey soil was treated with 10%, 20% and 30% of SSA by weight, respectively.

Table 4.6 Vertical settlements for clay-SSA mixtures in plate load test.

Applied Load (kN/m ²)	Average settlement (mm)			
	Clay	10%SSA	20%SSA	30%SSA
0	0,00	0,00	0,00	0,00
25	0,44	1,50	2,00	2,30
50	0,93	2,40	3,30	3,13
100	4,13	4,85	6,52	5,56
150	10,00	7,23	8,35	7,41
200	22,89	14,96	11,12	8,86
300		24,54	19,35	14,44
350		29,32	23,24	17,36
400			26,57	19,24
450			29,58	20,59
500				22,57
600				25,36

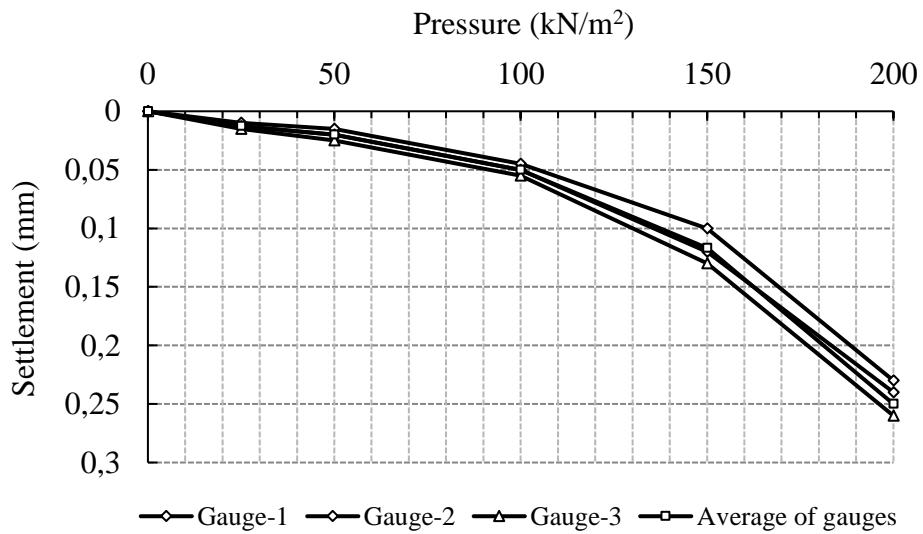


Figure 4.34 Pressure-settlement curves for clay in plate load test.

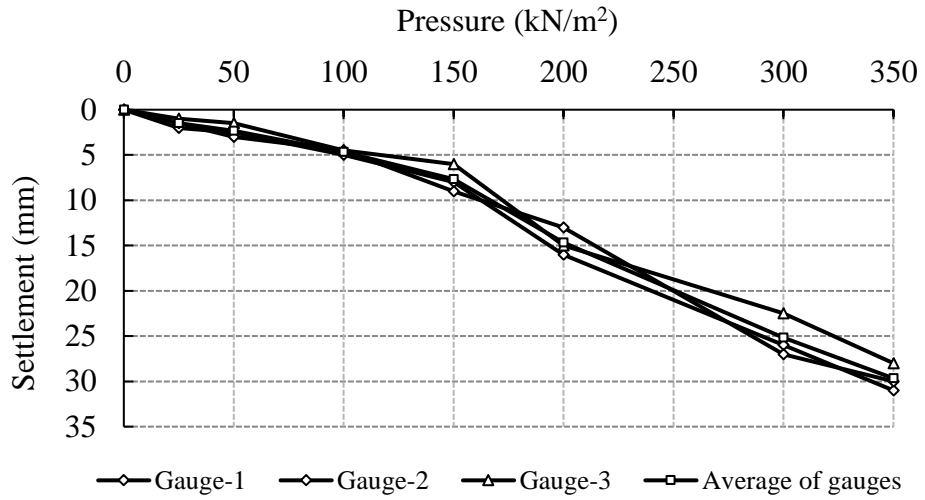


Figure 4.35 Pressure-settlement curves for 10% SSA in plate load test.

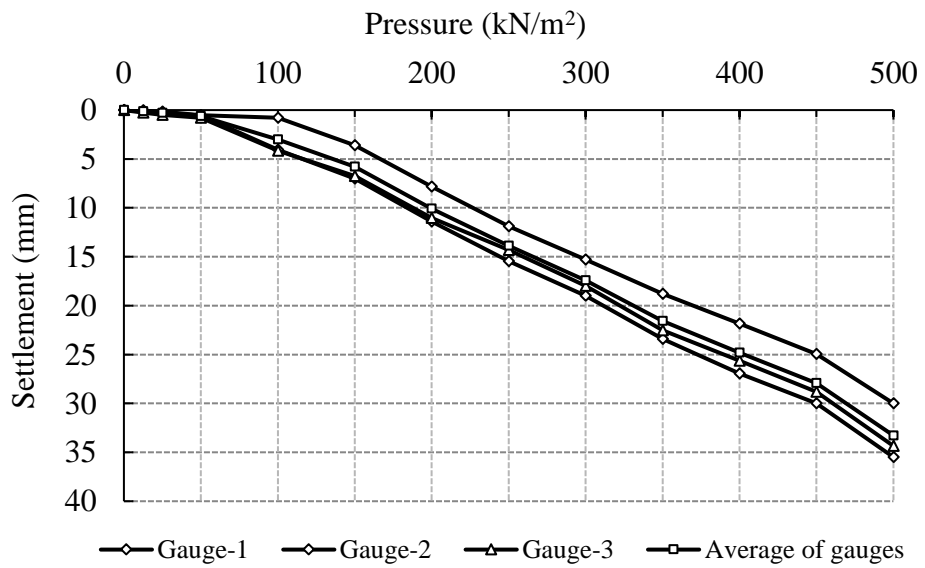


Figure 4.36 Pressure-settlement curves for 20% SSA in plate load test.

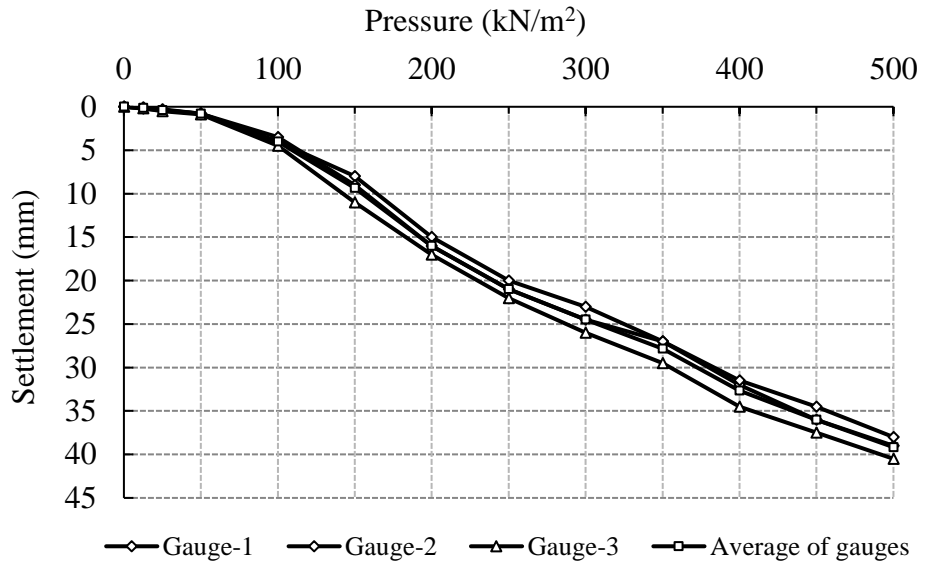


Figure 4.37 Pressure-settlement curves for 30% SSA in plate load test.

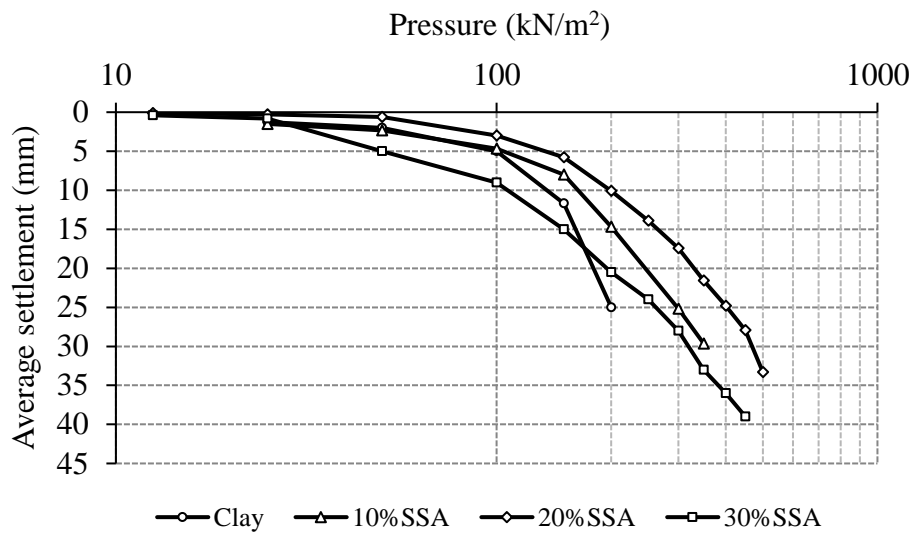


Figure 4.38 Plot of pressure-average settlement for all mixtures under different applied loads.

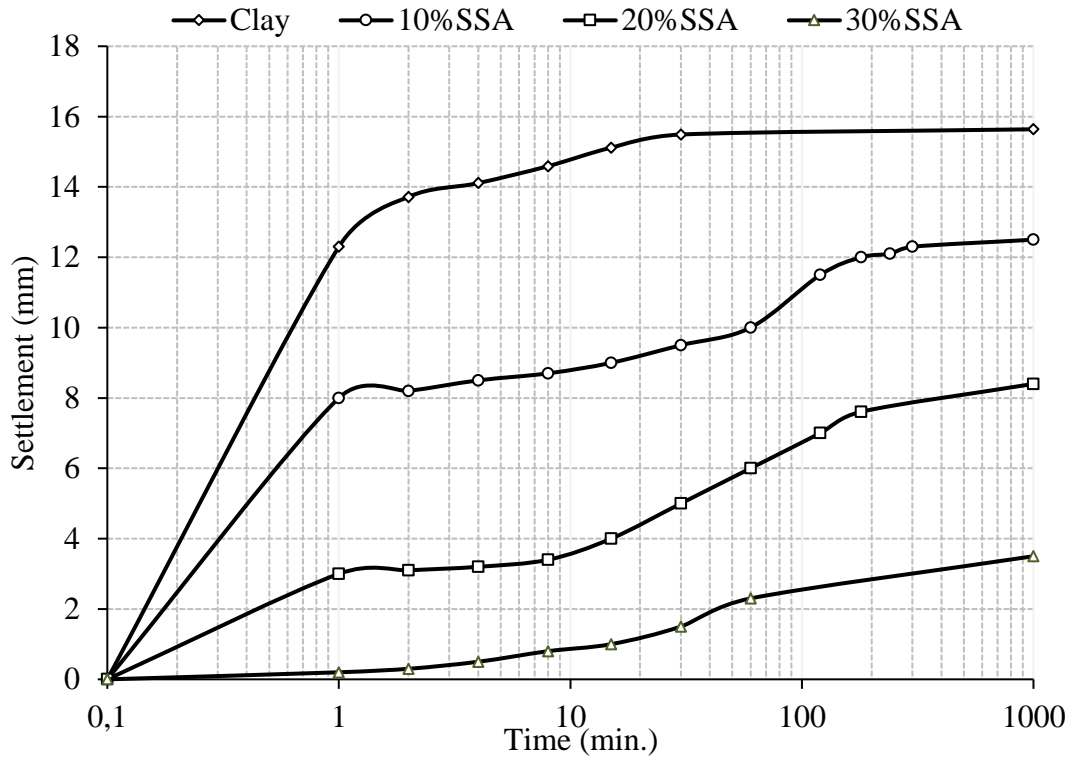


Figure 4.39 Time-settlement curves for 200 kN/m² pressure of clay-SSA mixtures in plate load test.

CHAPTER 5

CONCLUSIONS AND RECOMMENDATIONS

5.1 Conclusions

This thesis aimed to study the effect of SSA on some geotechnical properties experimentally; consistency, shear strength, compressive strength, compaction, settlement, bearing capacity, and permeability parameters of a clay treated with SSA. An extensive series of laboratory tests have been achieved to determine the soil improvement due to the addition of 0%, 5%, 10%, 15%, 20%, and 30% SSA by dry weight on clay. Also, a reinforced concrete circular model footing test equipment with inside dimensions of 2.0 -meter radius and 1.5 -meter depth has been constructed for the field tests. Moreover, a steel loading frame of 40 tons capacity has been designed to conduct the plate load and field CBR test inside this circular model footing set-up. The circular model set up tests were concerned with the settlement and bearing capacity of the plate load test of clay-SSA mixtures.

The primary objectives of this research can be summarized as:

- 1- To study the geotechnical characteristics (consistency, compaction, shear, and compressive strength, consolidation, permeability, bearing capacity) for clay and clay-SSA mixtures by different testing equipment's (Standard Proctor, vane shear, unconfined compression, fall cone, laboratory and field California bearing ratio, plate load, falling head),
- 2- To construct a concrete circular model footing for the large-scale field tests,
- 3- To investigate the effect of the curing time on the strength behavior of the clay-SSA mixtures by unconfined compression strength, California bearing ratio test, vane shear test and fall cone test.

This research has achieved all its objectives. In relation to the objectives of the study, an extensive laboratory and field investigation was carried out to determine the geotechnical properties of clay-SSA mixtures. The tests were divided into two parts as laboratory and field tests (circular model tests). In the laboratory part, the index properties including the consistency limits and sieve analysis were done to determine

the classification of clay and clay-SSA mixtures. After that, an extensive set of experiments were conducted to estimate the compaction, consolidation, permeability, bearing capacity, shear, and compressive strength characteristics. The strength of clay and clay-SSA were investigated using California Bearing Ratio test, Unconfined Compression Strength test, Vane shear test and fall cone test. Also Plate Load test was used in the circular model footing to obtain bearing capacity and shear strength properties. The conclusions taken from the experimental study are presented in four groups; (1) the general and index properties of clay and clay-SSA mixtures, (2) the strength characteristics from vane shear, unconfined compression, fall cone, plate load, laboratory CBR and field CBR tests, (3) the settlement characteristics from oedometer test and plate load test, (4) the permeability properties of clay and clay-SSA mixtures.

1- Conclusions from the index properties and compaction tests of clay and clay-SSA mixtures:

Consistency limits (liquid limit, plastic limit, and plasticity index), grain size distribution and the classification of clay and SSA have been carried out. As well as the SEM and EDX pictures for clay and SSA give extensive indications in the geotechnical properties of clay as a result of the SSA addition. The determination of the index characteristics offers a contribution on the explanation of clay-SSA behavior and the estimation of strength, compaction, bearing capacity, permeability compressibility parameters for clay-SSA mixtures. There are little-known efforts about the effect of SSA on the plasticity. The findings on the plasticity index of SSA have been somewhat mixed.

- a) The Energy Dispersive X-Ray (EDX) analysis of clay and SSA gives indication about the mineral composition of these materials. This information's produces an understanding of the mechanical properties of clay- SSA mixtures.
- b) The liquid limit of clay increased to 43 from 27% with increasing percentage of SSA until 30%. In addition, the plastic limit of the clay-SSA mixtures also increase to 28% from 13, plasticity index fluctuated and don't have a trend. This increasing was reflected on the geotechnical properties of clay-SSA mixtures such as the soil strength.
- c) The classification of clay according to USCS changes from CL to ML with SSA addition.

- d) Also, fall cone testing results indicated that the increase of the SSA content increased the liquid limit values. While the liquid limit of clay was 30, with the addition of 10% and 20% SSA, the estimated value of liquid limit increased at a rate of 30%.
- e) Addition of SSA showed that the MDD of clay-SSA mixtures decreased from 17.3 kN/m³ to 11.2 kN/m³ and the OMC increased from 18.0 to 32.6 as the percentage of SSA increases up to 30%.

2- Conclusions from the strength tests of clay and clay-SSA mixtures:

To understand the improvement of strength before the addition of SSA, the strength of untreated clay was tested firstly by CBR test. Then, the unconfined compression strength test was used as another parameter of strength. Moreover, fall cone and laboratory vane shear tests were examined to find out the undrained shear testing results. The behavior of clay and clay-SSA mixtures under plate load test was investigated using large scale circular model footing set-up. In addition to the laboratory CBR tests which have been examined in soaked and unsoaked condition, the field CBR test has also been investigated in the circular model footing set-up. All these tests have different test procedures and conditions. The previous little-known studies in the literature that have been conducted to determine the strength of SSA can be individually appeared.

- a) Generally, the strength of clay-SSA mixtures represented by CBR and UCS tests increased by increasing the SSA percentages. The strength enhancement depends on the type of testing (soaked unsoaked, etc), SSA ratio mixed with clay and curing time.
- b) The untreated clay sample in UCS and CBR which is not treated with SSA shows an increase with curing time. Therefore, it should be kept in mind that even without any mixing material that it could be expected to have different results at different curing times.
- c) Unconfined compression and CBR mixtures form an extensive cementation when have been cured without closing them in a plastic bag. This cementation induces the improvement that is seen in compressive strength and bearing capacity.

- d) Addition of SSA increases the strength of UCS samples. This increment is between 263.8-770.2 kPa for 4 days cured samples, 344.7-841 kPa for 8 days cured samples, 445.2-1150.3 kPa for 16 days cured samples and 514.8-1350.6 kPa for 32 days cured samples.
- e) CBR values increases as the SSA content and curing time increases. The CBR values reported in this research belong to 2.50 mm for all clay-SSA mixtures.
- f) The increment after 32 days for unsoaked samples is between 1.6-3.8 MPa for untreated clay samples, 1.7-4.4 MPa for 5%SSA samples, 2.4-5.4 MPa for 10%SSA samples, 3.8-7.5 MPa for 15%SSA samples, 6.3-13.9 MPa for 20%SSA samples and 11.2-25.1 MPa for 30%SSA samples
- g) On the other hand, there is a loss in bearing capacity for the soaked samples with curing time. The deduction after 32 days for soaked samples is between 1.0-0.4 MPa for untreated clay samples, 1.1-0.4 MPa for 5%SSA samples, 1.7-1.1 MPa for 10%SSA samples, 2.2-1.8 MPa for 15%SSA samples, 3.0-2.3 MPa for 20%SSA samples and 4.6-3.8 MPa for 30%SSA samples.
- h) Fall cone testing results showed that, at a given water content as the SSA content increases, the penetration of mixtures decreased which means SSA increased the resistance of penetration.
- i) The increases of water content for each mixture, the s_u values are decreasing. s_u values increase with the increase of SSA values at same water content.
- j) Vane shear testing results pointed out that the untreated clay had a value of s_u ranging between 1.7 and 17 kPa, while the values of fall cone tests were only between 0.20 and 3.50 kPa for the same water contents from 34 to 25%.
- k) The vane shear results were always found to give higher values by a factor ranging from 2.2 to 10.3. The author is thinking that this difference could be due to how the testing procedures are defined, what type of vane or cone is selected, the rate of rotation chosen, the cone roughness and other characteristics.
- l) The results of plate load test shown that the SSA addition improved the ultimate bearing capacity of clay.
- m) The results of plate load test also, showed that for any specific time, the SSA had the lesser settlement than the untreated clay.
- n) Generally, the results from the strength tests of clay and clay-SSA indicated the possibility of using SSA as a stabilizing agent.

3- Conclusions from oedometer and plate load tests of clay and clay-SSA mixtures:

Settlement is one of the biggest problems in the clayey soil. The large volume change happens in clay soil when the water content changes in this type of soil. The effect of SSA waste material mixing with the clayey soil was investigated. Previous studies on SSA only focused on the strength properties of this material. However, to the best of author's knowledge, no study has been found so far to examine the effect of SSA material on the compressibility of clayey soil. Although this study expressed many interesting results of SSA on the oedometer characteristics of the clayey soil.

- a) The presence of SSA in the mixtures tested had a significant effect on the compressibility of the material under load. Initial void ratio (e_0), and intergranular void ratio (e_s) values of the mixtures increase with the increasing SSA content at all oedometer pressure values conducted in the experimental study.
- b) Compression indices increase relatively linearly with SSA content. The C_c values for SSA tests varied between 0.2 and 1.0 for various SSA content. SSA ratios were increasing the amount of consolidation of clay-SSA mixtures by increasing the compression index C_c .
- c) Due to its high-water absorption, the increasing of SSA content gives the higher settlement on oedometer test.
- d) Generally, the increasing of SSA has a high effect on the compressibility features of consolidation.

4- Conclusions from permeability tests of clay and clay-SSA mixtures:

Permeability is highly dependent on pore size, which in turn is closely related to particle size distribution. It is evident that the SSA consists of predominantly fine silt and sand size fractions. An increase in permeability (k) coefficient with an increase in SSA content is observed. SSA is effective on the permeability results comparing to the results obtained from untreated clay. The values of hydraulic conductivity for compacted clay mixtures with 0 to 30% SSA varied from 3.97×10^{-6} to 1.23×10^{-7} cm/sec, indicating a range similar to those of fine sand/silt mixtures or silt. As SSA mixtures increased from 0 to 30%, the values of hydraulic conductivity decreased gradually. Addition of ash led to enhance the permeability properties of clay. The

author considers that this could be mainly due to the fineness and chemical reactions between clay and SSA.

5.2 Recommendations for future studies

These results are sufficiently positive to encourage further investigation. Due to the growing industry, new wastewater treatment plants are set up in Turkey and all over the world, stabilization of clayey soils is significantly attractive in geotechnical engineering. This research on the effects of SSA, may take a wide area in current and future research in geo-environmental engineering. For this aim, some suggestions can be taken from the conclusions of the current study to detect the geotechnical properties of soil-SSA mixtures more in-depth. Therefore, further investigations may be taken into consideration dealing the following items:

- These studies were carried out using a low plasticity clayey soil taken from one location of Gaziantep University campus, Turkey. The prospect use of SSA with other problematic soils like organic collapsible or high plasticity soils is recommended strongly.
- The current study may be extended using other types of field tests with different percentages of this material.
- The triaxial or cyclic triaxial test can be used to investigate the static and dynamic strength features of clay and clay -SSA mixtures, to understand the characteristics of this material when used as additive in clay or any other soil type.
- Adjustments of the circular model footing to study the shape and size effect of bearing plate may add significant information's about clay-SSA mixtures.
- The environmental applications can be carefully evaluated prior to expand alternative tests on a large scale. This should consist of determining the leaching behavior of the stabilized soils.
- The long-term durability of SSA treated soils should be evaluated. For the soil improvement, long-term monitoring of the tests should be observed to verify that the strength gains are permanent.
- The testing results of clay-SSA mixtures could be modeled with different geotechnical software's such as PLAXIS or ABAQUS for making a comparison between experimental and theoretical results.



REFERENCES

- AIIS-181, (1981). Asphalt Pavement Thickness Design. Information Series No. 181. Asphalt Institute, USA.
- Al Sayed M H, Madany I M and Buali A R M, (1995). Use of sewage sludge ash in asphaltic paving mixes in hot regions. *Construction and Building Materials* **9** (1), 19–23.
- Alcocel E G, Garcés P, Martínez J J, Payá J and Andión L G, (2006). Effect of sewage sludge ash (SSA) on the mechanical performance and corrosion levels of reinforced Portland cement mortars. *Construction Materials* **56** (282), 31–43.
- Al-Sharif M and Attom M F, (2000). The use of incinerated sludge as a new soil stabilizing agent. *Environmental and Pipeline Engineering*, 378–386.
- Al-Sharif M and Attom M F, (2014). A geoenvironmental application of incinerated wastewater sludge ash in soil stabilization. *Environmental Earth Sciences* **71**, 2453–2463.
- Anderson M and Skerratt R G, (2003). Variability study of incinerated sewage sludge ash in relation to future use in ceramic brick manufacture. *British Ceramic Transactions* **102** (3), 109–113.
- Anderson M, (2002). Encouraging prospects for recycling incinerated sewage sludge ash (ISSA) into clay-based building products. *Journal of Chemical Technology and Biotechnology* **77**, 352–360.
- Anderson M, Skerratt R G, Thomas J P and Clay S D, (1996). Case study involving using fluidised bed incinerator sludge ash as a partial substitute in brick manufacture. *Journal of Water Science and Technology*, **34**(3–4), 507–515
- Anderson M, Elliott M and Hickson C, (2002). Factory-scale proving trials using combined mixtures of three by-product wastes (including incinerated sewage sludge ash) in clay building bricks. *Journal of Chemical Technology and Biotechnology* **77**, 345–351.
- ASTM D1883, (1987). California Bearing Ratio (CBR) of Laboratory Compacted Soils. ASTM International, West Conshohocken, PA, USA.

ASTM D2850, (1987). Standard Test Method for Unconsolidated-Undrained Triaxial Compression Test on Cohesive Soils. ASTM International, West Conshohocken, PA, USA.

ASTM D1557, (2012). Standard Test Methods for Laboratory Compaction Characteristics of Soil Using Modified Effort. ASTM International, West Conshohocken, PA, USA.

ASTM D698, (2012). Standard Test Methods for Laboratory Compaction Characteristics of Soil Using Standard Effort. ASTM International, West Conshohocken, PA, USA.

ASTM C62, (2013). Standard Specification for Building Brick (Solid Masonry Units Made From Clay or Shale). ASTM International, West Conshohocken, PA, USA.

ASTM C311/C311M, (2013). Standard Test Methods for Sampling and Testing Fly Ash or Natural Pozzolans for Use in Portland-Cement Concrete. ASTM International, West Conshohocken, PA, USA.

ASTM D2166, (2013). Standard Test Method for Unconfined Compressive Strength of Cohesive Soil. ASTM International, West Conshohocken, PA, USA.

ASTM E303-93, (2013). Standard Test Method for Measuring Surface Frictional Properties Using the British Pendulum Tester. American Society for Testing and Materials.

ASTM C216, (2015). Standard Specification for Facing Brick (Solid Masonry Units Made From Clay or Shale). ASTM International, West Conshohocken, PA, USA.

ASTM C618, (2015). Standard Specification for Coal Fly Ash and Raw or Calcined Natural Pozzolan for Use in Concrete. ASTM International, West Conshohocken, PA, USA.

Baeza F, Paya J, Galao O, Saval J M and Garces P, (2014). Blending of industrial waste from different sources as partial substitution of Portland cement in pastes and mortars. *Construction and Building Materials* **66**, 645–653.

Baeza-Brotons F, Garces P, Paya J and Saval J M, (2014). Portland cement systems with addition of sewage sludge ash. Application in concretes for the manufacture of blocks. *Journal of Cleaner Production* **82**, 112–124.

Bhatty J I and Reid K J, (1989a), Lightweight aggregates from incinerated sludge ash, *Waste Management and Research* **7**, 363–376.

Bhatty J I and Reid K J, (1989b), Moderate strength concrete from lightweight sludge ash aggregates, *The International Journal of Cement Composites and Lightweight Concrete* **11 (3)**, 179–187.

Bhatty J I, Malisci A, Iwasaki I and Reid K J, (1992), Sludge ash pellets as coarse aggregate in concrete, *Journal of Cement, Concrete and Aggregates*, **14 (1)**, 55–61.

BS 598-3, (1985), Sampling and Examination of Bituminous Mixtures for Roads and Other Paved Areas, Methods for Design and Physical Testing. British Standards Institute, London.

BS 8004, (1986), Code of practice for foundations. British Standards Institute, London.

BS EN 196-1, (2005), Methods of testing cement and determination of strength. British Standards Institute, London.

BS EN 14411, (2012), Ceramic tiles, definitions, classification, characteristics, evaluation of conformity and marking. British Standards Institute, London.

BS EN 450-1, (2012), Fly ash for concrete, definition, specifications and conformity criteria. British Standards Institute, London.

BS EN 771-1, (2011), Specification for masonry units, clay masonry units, British Standards Institute, London.

Cheeseman C R and Viridi G S, (2005), Properties and microstructure of lightweight aggregate produced from sintered sewage sludge ash, *Resources, Conservation and Recycling*, **45**, 18–30.

Cheeseman C R, Sollars C J and Mcentee S, (2003), Properties, microstructure and leaching of sintered sewage sludge ash. *Resources, Conservation and Recycling*, **40**, 13–25.

Chen L and Lin D F, (2009a). Applications of sewage sludge ash and nano-SiO₂ to manufacture tile as construction material. *Construction and Building Materials* **23**, 3312–3320.

Chen L and Lin D F, (2009b). Stabilization treatment of soft subgrade soil by sewage sludge ash and cement. *Journal of Hazardous Materials* **162**, 321–327.

Chiou I J, Wang K S, Chen C H and Lin Y T, (2006). Lightweight aggregate made from sewage sludge and incinerated ash. *Waste Management* **26**, 1453–1461.

Clean Air Task Force, (2010). Black carbon from brick kilns, available from: http://www.catf.us/resources/presentations/files/Black_Carbon_from_Brick_Kilns.pdf.

China National Standard (CNS), (1999), Ceramic industry, pottery wares, bureau of standards, metrology and inspection; Ministry of Economic Affairs, Republic of China.

Coutand M, Cyr M and Clastres P, (2006), Use of sewage sludge ash as mineral admixture in mortars, *Construction Materials*, **159 (CM4)**, 153–162.

Cyr M, Coutand M and Clastres P, (2007a), Technological and environmental behaviour of sewage sludge ash (SSA) in cement based materials. *Cement and Concrete Research*, **37**, 1278–1289.

Dayalan J and Beulah M, (2014), Glazed sludge tile, *Journal of Engineering Research and Applications*, **4 (3)**, 201–204.

De Lima J F, Ingunza D and Del Pilar M, (2015), Effects of sewage sludge ash addition in Portland cement concretes, International Conference on Civil, Materials and Environmental Sciences (CMES 2015), London, 13–14th March, Atlantis Press, pp. 189–191.

Donatello S and Cheeseman C, (2013), Recycling and recovery routes for incinerated sewage sludge ash (ISSA): a review. *Waste Management* **33 (11)**, 2328–2340.

Donatello S, Tyrer M and Cheeseman C R, (2010), Comparison of test methods to assess pozzolanic activity, *Cement and Concrete Composites*, **32**, 121–127.

Durante Ingunza, M. P, Santos Junior O, and Andrade Medeiros S, (2014), “Sewage sludge as raw material in asphalt mixtures”, *Advandce Material Res.*, **664**, 638–643.

EN 197, (2011), Cement composition, specifications and conformity criteria for common cements. Comité Européen de Normalisation (CEN), Brussels, Belgium.

Endo H, Nagayoshi Y and Suzuki K, (1997), Production of glass ceramics from sewage sludge, *Journal of Water Science and Technology*, **36 (11)**, 235–241.

Environmental Protection Agency (EPA), (1990), Citizen's Guide to Radon, U.S. EPA, 402-K02-006, 11-16.

Federal Highway Administration, (1997), User guidelines for waste and by-product materials in pavement construction, 97-148, 736 pp.

Fontes C. M. A., Barbosa M. C., Filho R. D. and Gonçalves J. P., (2004), Potentiality of sewage sludge ash as mineral additive in cement mortar and high performance concrete, Proceedings of the International RILEM Conference on the Use of Recycled Materials in Buildings and Structures, November 8–11, 2004. RILEM Publications, pp. 797–806.

Franz M, (2008), Phosphate fertilizer from sewage sludge ash (SSA). *Waste Management*, **28**, 1809–1818.

GASKİ, (2018), Gaziantep su ve kanalizasyon idaresi performans programı.

Garcés P., Carrión M. P., Alcocel E. G., Payá J., Monzo J. and Borrachero M. V., (2008), Mechanical and physical properties of cement blended with sewage sludge ash *Journal of Waste Management*, **28**, 2495–2502.

Gunning P J, Antemir A, Hills C. D. and Carey P. J., (2011). Secondary aggregate from waste treated with carbon dioxide, *Construction Materials Proceedings of the Institute of Civil Engineers*, **164**, 231–239.

Head, K. H., (1994), Manual of soil laboratory testing, permeability, shear strength and compressibility tests, 2nd Ed., Vol. 2, Pentech Press, London.

Hnat J.G., Mathur A. and Simpson J. C., August 10, (1999). Manufacture of ceramic tiles from fly ash, Unites States Patent, 5935885, 12 pp.

Hu S.H., Hu S.C. and Fu Y.P., (2012). Recycling technology-artificial lightweight aggregates synthesized from sewage sludge and its ash at lowered comelting temperature, *Environmental Progress and Sustainable Energy*, **32 (3)**, 740–748.

Isa H., (2011), A review of glass-ceramics production from silicate wastes, *International Journal of the Physical Sciences* **6 (30)**, 6781–6790.

Jamshidi M., Jamshidi A., Mehrdadi N. and Pacheco-Torgal F., (2012), Mechanical performance and capillary water absorption of sewage sludge ash concrete (SSAC), *International Journal of Sustainable Engineering*, **5 (3)**, 228–234.

Johnson O.A., Napiah M. and Kamaruddin I., (2014), Potential uses of waste sludge in construction industry: a review, *Research Journal of Applied Sciences, Engineering and Technology*, **8 (4)**, 565–570.

Kadir A.A. and Mohajerani A., (2011), Bricks: an excellent building material for recycling wastes – a review, Proceedings of the IASTED International Conference July 4–6, 2011, Calgary, AB, Canada Environmental Management and Engineering (EME 2011), 108–115.

Kamon M., Katsumi T. and Inui T., (2001), Environmental suitability assessment of incinerator waste ashes in geotechnical applications, Yong R.N. and Thomas H.R., *Geoenvironmental Impact Management, Geoenvironmental Engineering*, Thomas Telford, pp. 21–26.

Khanbilvardi R. and Afshari-Tork S., (1995), Sludge ash as fine aggregate for concrete mix, *Journal of Environmental Engineering*, **121 (9)**, 633–638.

Khanbilvardi R. and Afshari-Tork S., (2002), Ash use from Suffolk county wastewater treatment plant sewer district No:3 Phase1, New York State Energy Research and Development Authority, 186 pp.

Kikuchi R., (2001), Recycling of municipal solid waste for cement production: pilot-scale test for transforming incineration ash of solid waste into cement clinker, *Resources, Conservation and Recycling*, **31**, 137–147.

Kingery W.D., Bowen H.K. and Uhlmann D.R., (1976), Introduction to ceramics, second edition, John Wiley and Sons, New York, 1032 pp.

Kosior-Kazberuk M., (2011), Application of SSA as partial replacement of aggregate in concrete, *Polish Journal of Environmental Studies*, **20 (2)**, 365–370.

Krejcirikova B, (2015). Zero Waste Materials. Presentation at Technical University of Denmark. Available from:

Ksepko E., (2014), Sewage sludge ash as an alternative low-cost oxygen carrier for chemical looping combustion, *Journal of Thermal Analysis and Calorimetry*, **116**, 1395–1407.

- Lam C.H.K., Barford J.P. and McKay G., (2010), Utilization of incineration waste ash residues in Portland cement clinker, *Chemical Engineering Transactions*, **21**, 757–762.
- Lin D.F. and Weng C.H., (2001), Use of sewage sludge ash as brick material, *Journal of Environmental Engineering*, **127** (10), 922–927.
- Lin K.L. and Lin C.Y., (2004), Hydration properties of eco-cement pastes from waste sludge ash clinkers, *Journal of the Air and Waste Management Association*, **54** (12), 1534–1542.
- Lin K.L. and Lin C.Y., (2005), Hydration characteristics of waste sludge ash utilized as raw cement material, *Cement and Concrete Research*, **35**, 1999–2007.
- Lin D.F., Luo H.L. and Sheen Y.N., (2005). Glazed tiles manufactured from incinerated sludge ash and clay. *Journal of the Air and Waste Management Association* **55** (2), 163–172.
- Lin K.L. and Tsai M.C., (2006), The effects of nanomaterials on microstructures of sludge ash cement paste, *Journal of the Air and Waste Management Association*, **56** (8), 1146–1154.
- Lin K.L. and Lin C.Y., (2006), Feasibility of using ash from sludge incineration as raw materials for eco-cement, *Journal of the Chinese Institute of Environmental Engineering*, **16** (1), 39–46.
- Lin K.L., (2006), Effects of the basicity on the comelting conditions of municipal solid waste incinerator fly ash and sewage sludge ash, *Journal of the Air and Waste Association*, **56** (12), 1743–1749.
- Lin K.L., Chiang K.Y. and Lin D.F., (2006), Effect of heating temperature on the sintering characteristics of sewage sludge ash, *Journal of Hazardous Materials*, **B128**, 175–181.
- Lin D.F., Luo H.L. and Zhang S.W., (2007). Effects on nano-SiO₂ on tiles manufactured with clay and incinerated sewage sludge ash, *Journal of Materials in Civil Engineering*, **19** (10), 801–808.
- Lin D.F., Chang W.C., Yuan C. and Luo H.L., (2008), Production and characterization of glazed tiles containing incinerated sewage sludge, *Waste Management*, **28**, 502–508.

- Lin K.L., Chang W.C., Lin D.F., Luo H.L. and Tsai M.C., (2008a), Effects of nano-SiO₂ on sludge ash-cement mortar, *Journal of Environmental Management*, **88**, 708–714.
- Lin K.L., Lin D.F. and Luo H.L., (2009), Influence of phosphate of the waste sludge on the hydration characteristics of eco-cement, *Journal of Hazardous Materials*, **168**, 1105–1110.
- Luo H.L. and Lin D.F., (2003), Evaluation of color changes in sewage sludge ash brick by using image analysis method, *Practice Periodical of Hazardous, Toxic and Radioactive Waste Management*, **7 (4)**, 214–223.
- Maozhe C., Denise B., Mathieu G., Jacques M. and Rémy G., (2013), Environmental and technical assessments of the potential utilization of sewage sludge ashes (SSA's) as secondary raw materials in construction, *Waste Management*, **33**, 1268–1275.
- McMillan P.W., (1979), *Glass ceramics*, second ed., Academic Press, London, 285 pp.
- Merino I., Arévalo L.F. and Romero F., (2005), Characterization and possible uses of ashes from wastewater treatment plants, *Waste Management*, **25**, 1046–1054.
- Merino I., Arévalo L.F. and Romero F., (2007), Preparation and characterization of ceramic products by thermal treatment of sewage sludge ashes mixed with different additives, *Waste Management*, **27**, 1829–1844.
- Monzo J., Payá J., Borrachero M.V. and Córcoles A., (1996), Use of sewage sludge ash (SSA) – cement admixtures in mortars, *Cement and Concrete Research*, **26 (9)**, 1389–1398.
- Monzo J., Payá J., Borrachero M.V. and Peris-Mora E., (1999), Mechanical behaviour of mortars containing sewage sludge ash (SSA) and Portland cements with different tricalcium aluminate content, *Cement and Concrete Research*, **29**, 87–94.
- Modern Pollution Control Technology (MPCT), (1980), vol. II. Research and Education Association, New York.
- National Cooperative Highway Research Program (NCHRP), (2013), Recycled materials and byproducts in highway applications, Non-coal combustion byproducts synthesis, vol. 3, p.435.
- Newport D.J., Wijeyesekara D.C. and Edwards K., (2004), Manufactured Aggregate as imported backfill material for plastic pipes, Plastic pipes XII, Italy.

Park J.P., Moon S.O. and Heo J., (2003), Crystalline phase control of glass ceramics obtained from sewage sludge fly ash, *Ceramics International*, **29**, 223–227.

Petavratzi E., (2007), Incinerated sewage sludge ash in facing bricks, Mineral Industry Research Organization, UK, (WRT 177/WR0115), 10 pp.

Pinarli V., (2000). Sustainable waste management – studies on the use of sewage sludge ash in construction industry as concrete material, Dhir R.K., Dyer T.D. and Paine K.A. (Eds.), *Sustainable Construction: Use of Incinerator Ash*, Thomas Telford, pp. 415–426.

Rawlings R.D., Wu J.P. and Boccaccini A.R., (2006), Glass-ceramics: their production from wastes: a review, *Journal of Materials Science*, **41**, 733–761.

Sato Y., Oyamada T., Hanehara S. and Sasaki T., (2012), The characteristics of ash of sewage sludge (SSA) in Iwate prefecture and application of SSA for asphalt mixture, *Journal of The Mining and Materials Processing Institute of Japan*, **128**, 519–525.

Smol M., Kulczycka J., Henclik A., Gorazda K. and Wzorek Z., (2015), The possible use of sewage sludge ash (SSA) in the construction industry as a way towards a circular economy, *Journal of Cleaner Production*, **95**, 45–54.

Stokes, G., (1891), *Mathematical and Physical Paper III*, Cambridge University Press, Cambridge, MA.

Suzuki S., Tanaka M. and Kaneko T., (1997), Glass-ceramic from sewage sludge ash, *Journal of Material Sciences*, **32**, 1775–1779.

Tay J.H., (1987), Bricks manufactured from sludge, *Journal of Environmental Engineering*, **113** (2), 278–284.

Tay J.H. and Yip W.K., (1989), Sludge ash as lightweight concrete material, *Journal of Environmental Engineering*, **115** (1), 56–64.

Tay J.H. and Show K.Y., (1992), The use of lime-blended sludge for production of cementitious material, *Water Environment Research*, **64** (1), 6–12.

Tempest B.Q. and Pando M.A., (2013), Characterization and demonstration of reuse applications of sewage sludge ash, *International Journal of Geomatics and Geosciences*, **4** (2), 552–559.

Tenza-Abril A.J., Saval J.M. and Cuenca A., (2014), Using sewage sludge ash as filler in bituminous mixes, *Journal of Materials in Civil Engineering*, 04014141, 9 pp.

Trauner E.J., (1993), Sludge ash bricks fired to above and below ash-vitrifying temperature, *Journal of Environmental Engineering*, **119** (3), 506–519.

Tsai C.C., Wang K.S. and Chiou I.J., (2006). Effect of $\text{SiO}_2 - \text{Al}_2\text{O}_3$ – flux ratio change on the bloating characteristics of lightweight aggregate material produced from recycled sewage sludge. *Journal of Hazardous Material* **B134**, 87–93.

Tseng D.H. and Pan S.C., (2000), Enhancement of pozzolanic activity and morphology of sewage sludge ash by calcinations, *Journal of the Chinese Institute of Environmental Engineering*, **10** (4), 261–270.

Uozumi M., et al., (1984). Incineration of sewage sludge with waste wood, *Journal of Japan Sewage Works Association*, **21** (236), 85.

Vouk D., Nakic D. and Stirmer N., (2015), Reuse of sewage sludge problems and possibilities – Reuse of sewage sludge in concrete industry from infrastructure to innovate construction products, Proceedings Industrial Waste, Wastewater Treatment and Valorisation. National Technical University of Athens, Athens, pp. 1–21.

Wegman D.E. and Young D.S., (1988), Testing and evaluating sewage sludge ash in asphalt paving mixtures, Presented at the 67th Annual Transportation Research Board Meeting, Washington, DC, January

Werther J. and Ogada T., (1999), Sewage sludge combustion, *Progress in Energy and Combustion Sciences*, **25**, 55–116.

Wienerberger Company, (2012), The use of materials from alternative, recycled and secondary sources in the manufacture of clay bricks, Available from: <http://www.wienerberger.co.uk/use-of-marss-in-manufacture-of-clay-bricks-full-version.html>.

Wystalska K., Sobik-Szolytysek J. and Bien J.B., (2013), Vitrification and devitrification of ash after sewage sludge combustion, *Annual Set the Environment Protection – Rocznik Ochrona Srodowiska*, **15**, 181–191.

Yoon S.D. and Yun Y.H., (2011), Preparation of glass ceramics from sludge bottom ash and waste glass, *Journal of Ceramic Processing Research*, **12** (4), 361–364.

Yusuf R.O., Noor Z.Z., Din M.F.M. and Abba A.H., (2012), Use of sewage sludge ash (SSA) in the production of cement and concrete – a review, *International Journal Global Environmental Issues*, **12** (2–4), 214–228.

Zhang Z., Li A., Yin Y. and Zhao L., (2013), Effect of crystallization time on behaviours of glass-ceramic produced from sludge incineration ash, *Procedia Environmental Sciences*, **18**, 788–793.

Zhang Z, Zhang L., Yin Y., Liang X. and Li A., (2015), The recycling of incinerated sewage sludge ash as a raw material for CaO-Al₂O₃-SiO₂-P₂O₅ glass ceramic production. *Environmental Technology*, **36** (9), 1098–1103.



CURRICULUM VITAE

PERSONAL INFORMATION

Name and Surname : Nurullah AKBULUT

EDUCATION

Degree	Graduate School	Year
MS	University of Gaziantep	2013
BS	University of Gaziantep	2011
High School	Hasan Suzer High School	2006

WORK EXPERIENCE

Year	Place	Enrollment
2012-2013	Hasan Kalyoncu University	Research Assistant
2013- present	Hasan Kalyoncu University	Lecturer

PUBLICATIONS

A. International Journals

1. Çabalar, A.F; **Akbulut, N.**, "Effects of the particle shape and size of sands on the hydraulic conductivity" *Acta Slovenica Geotechnica*, Vol:2, No:2016 (4), pp:83-93, December, 2016.
2. Çabalar, A.F; Uyan, R.S.; **Akbulut, N.**, "A Study of Foundation Design for Wind Turbines in Hasanbeyli, Turkey" *Soil Mechanics and Foundation Engineering*, Vol:53, No:5 pp:298-303, November, 2016.
3. Çabalar, A.F; **Akbulut, N.**, "Evaluation of actual and estimated hydraulic conductivity of sands with different gradation and shape" *SpringerPlus*, Vol:5, No:1, pp:820-830, June, 2016.
4. Cabalar, A.F.; Canbolat, A.; **Akbulut, N.**; Tercan, S.H. & Isik, H., "Soil liquefaction potential in Kahramanmaras, Turkey", *Geomatics, Natural Hazards and Risk*, 10:1, 1822-1838, June, 2019.

B. International/National Congress, Conference and Symposium

1. "Use of fly ash- lime mixtures in stabilization of a sand". *3rd International Conference on New Developments in Soil Mechanics and Geotechnical Engineering-* 28-30 June 2012, Nicosia/CYPRUS
2. "An investigation of the soil properties in Gaziantep". *With International Participation, Restructuring of Cities Symposium, Urban Regeneration.* 26-29 September 2012, Istanbul/TURKEY.

3. "Effects of clay content on the behaviour of various shaped sands". *ZM14, Turkish National Committee of Soil Mechanics and Geotechnical Engineering Conference*. 4- 5 October 2012, Isparta/ TURKEY
4. "A study of permeability on various sands and sand-waste tire mixtures". *ZM14, Turkish National Committee of Soil Mechanics and Geotechnical Engineering Conference*, 4- 5 October 2012, Isparta/TURKEY.
5. "A study on the improvement of clays in Gaziantep with crushed sands, and waste tires-crushed sands mixtures", *Journal of the Faculty of Engineering and Architecture of Cukurova University*, Vol: 28, No: 2, pp:1-14, December, 2013
6. "Applications of the oedometer and permeability tests to the study of waste tire inclusions-sand mixtures". *3rd International Conference on Geotechnical Engineering New Developments in Analysis, Modelling and Design*, 21-23 February 2013, Hammamet/TUNISIA.
7. "Hydraulic conductivity of various shapes of sands". *Asian Conference on Civil, Material and Environmental Sciences (ACCMES)*, Toshi Center Hotel, 15-17 March 2013, Tokyo/JAPAN.
8. "Applications of the oedometer, permeability, compaction, and CBR tests to the study of sand with fly ash- lime mixtures". *International Conference on Advances in Civil, Structural and Environmental Engineering, (ACSEE 2013)*, Zurich/SWITZERLAND.
9. "On the settlement of sand- clay mixtures". *5. Geotechnical Symposium*, 5-7 December 2013, Adana/TURKEY.
10. "Effects of bio-cementation on some geotechnical properties of a sand". *3rd GeoShanghai International Conference*, Shanghai/CHINA. (chosen for ASCE SPECIAL PUBLICATIONS)
11. "Improving Bearing Capacity of a Soil Using Biopolymers", *11th International Congress on Advances in Civil Engineering, (ACE2014)*, İstanbul/TURKEY
12. "Fall Cone Tests on Clay- Xanthan Gum Mixtures". *ZM15, Turkish National Committee of Soil Mechanics and Geotechnical Engineering Conference*, 16- 17 October 2014, Ankara/TURKEY.
13. "On the Transition Fines of Sand- Clay Mixtures", *International Symposium on Geomechanics from Micro to Macro, (IS- Cambridge 2014)*, Cambridge/UK
14. "Influences of Grain Shape and Size Distribution on Permeability", *International Symposium on Geomechanics from Micro to Macro, (IS- Cambridge 2014)*, Cambridge/UK
15. "The behaviour of clayey soil reinforced with waste aluminum pieces" *The World Multidisciplinary Earth Sciences Symposium, (WMESS2015)*, Prague/CZECH REPUBLIC (under review)
16. "Effect of Xanthan Gum on Liquefaction Potential of İzmir Sand" *The World Multidisciplinary Earth Sciences Symposium, (WMESS2015)*, Prague/CZECH REPUBLIC

17. "Stabilization of a Clay by Incinerated Sewage Sludge Ash", 5th International Conference On Computational And Experimental Science And Engineering (ICCESEN-2018), Antalya/TURKEY
18. "Some geotechnical properties of clay sand mixtures", Journal of the Faculty of Engineering of Dicle University, Vol: 9, No: 2, pp:871-879, May, 2018

